8-2019

Studies on Pathogenesis of the Diseases Caused by Macrophomina phaseolina and Phomopsis longicolla on Soybean

Marcio Leizer Zaccaron
University of Arkansas, Fayetteville

Studies on Pathogenesis of the Diseases Caused by *Macrophomina phaseolina* and *Phomopsis longicolla* on Soybean

A dissertation submitted in partial fulfillment
of the requirements for the degree of
Doctor of Philosophy in Plant Sciences

by

Marcio Zaccaron
Universidade Federal da Grande Dourados
Bachelor of Science in Agronomy, 2009
Iowa State University
Master of Science in Plant Pathology, 2013

August 2019
University of Arkansas

The dissertation is approved for recommendation to the Graduate Council.

_____
John Rupe, PhD
Dissertation Director

_____
Burt Bluhm, PhD
Committee Member

_____
Pengying Chen, PhD
Committee Member

_____
Edward Gbur, PhD
Committee Member

_____
Douglas Karcher, PhD
Committee Member

_____
Larry Purcell, PhD
Committee Member

Abstract

Soybean (*Glycine max*), a legume, is an economically important crop in many parts of the world, including the USA, Brazil, Argentina, China, and India, currently the top five producing countries. Soybean is primarily used as feed, with incising markets for food and biodiesel. Similar to most crops, soybean yield and quality are affected by a diverse group of plant pathogens. In particular, several species of filamentous fungi have been the cause of severe yield losses in most growing regions world-wide. The soil born fungus *Macrophomina phaseolina*, causal agent of charcoal rot, has been found to be endemic to several soybean production areas. Charcoal rot has been historically associated with severe yield reduction, particularly when coupled with drought stress. However, little is known about how irrigation-regimes change affect the relationship between disease severity and yield. A different soil and seed born fungus *Phomopsis longicolla*, causes severe seed decay under conducive environmental conditions, warm and wet weather during soybean senescence. Although both fungi co-inhabit soybean roots and stems for extended periods of times, little is known about their interactions. Recently, P. longicolla has been shown to be amenable to genetic manipulation via *Agrobacterium tumefaciens*. However, no study has yet taken advantage of this amenability to dissect potential mechanisms associated to Phomopsis seed decay. This study was designed to understand how different irrigation regimes may impact severity of charcoal rot and its relationship to soybean yield. Additionally, the interplay between *M. phaseolina* and *P. longicolla* in soybean tap roots via the formation of zone lines was investigated. Lastly, taking advantage of available genetic transformation methodology, experiments were implemented to elucidate putative molecular mechanisms of Phomopsis seed decay pathogenesis. Results indicated that drought stress significantly increases charcoal rot severity and decreased yield. However, no consistent

relationship was observed between these variables. Observations also showed that *P. longicolla* forms zone lines in soybean taproots thereby precluding *M. phaseolina* from colonizing these tissues. In this study, for the first time, forward and reverse genetic approaches and transcriptomics were employed on *P. longicolla* successfully. Multiple genes linked to decreased pathogenicity were identified in *P. longicolla*.

Table of contents

List of Published Papers

Chapter V published as:
Zaccaron, M., Sharma, S., and Bluhm, B. H. 2018. MoNSTR-seq, a restriction site-associated DNA sequencing technique to characterize *Agrobacterium*-mediated transfer-DNA insertions in *Phomopsis longicolla*. Lett. Appl. Microbiol. 66:19-24

Chapter VI submitted as:
Zaccaron, M., Zaccaron, A., Ridenour, J., Ramegowda, Y., Sharma, S., and Bluhm, B. H. 2019. *HAP3*, a component of the CCAAT-binding complex of *Phomopsis longicolla*, regulates pathogenesis during infection of soybean. Mol. Plant-Microbe Interact. ***under review***

Chapter I: General introduction

Biology of *M. phaseolina*

The Ascomycota fungi *Macrophomina phaseolina* and *Phomopsis longicolla* are economically important soybean pathogens worldwide (Wrather et al. 2010; Zorrilla et al. 1994; Bellaloui et al. 2008). Although these fungi cause very different diseases in soybean production systems, many similarities are noteworthy between these organisms and the diseases they cause. Both, *M. phaseolina* and *P. longicolla* are ubiquitous and endemic in many soybean production areas (Gacitua Arias et al. 2013; Short and Wyllie 1978; Roy and Abney 1988; Hartman, et al. 1999). Environmental conditions have been reported to play a very important role in the development of diseases caused by these filamentous fungal pathogens (Mengistu et al. 2011; Rupe and Ferriss 1986). While drought is associated with more severe epidemics of charcoal rot; caused my *M. phaseolina*, moist and warm conditions favor Phomopsis seed decay, caused by *P. longicolla* (Kendig et al. 2000; Baker et al. 1987). Additionally, chemical control has not been shown effective in the management of either charcoal rot or Phomopsis seed decay (Wrather et al. 2004; Jaiman et al. 2009). Furthermore, only limited sources of horizontal resistance are known for these diseases (Jackson et al. 2005; Bellaloui et al. 2008). Both organisms and the diseases caused by their association with soybean have been known and studied for nearly a century (Lehman 1923; Haigh 1930). However, to date little is known about the molecular mechanisms involved in their pathogenesis.

M. phaseolina is a soil borne fungus that infects soybean roots early in the season then systemically colonizes the root system and basal stem (Mengistu et al. 2011). Charcoal rot has been reported to cause severe yield losses in most soybean growing areas worldwide, including, but not limited to Brazil, Argentina, China, and the US (Wrather et al. 1997). *M. phaseolina* has

a wide host range, reportedly found to infect over 500 plant species within 100 families including several economically important crop species like cotton (*Gossypium hirsutum*) (Su et al. 2001), maize (*Zea mays*) (Livingston 1945), sorghum (*Sorghum bicolor*) (Tenkouano et al. 1993), tomatoes (*Solanum lycopersicum*) (Shaukat and Siddiqui 2003), strawberry (*Fragaria ananassa*) (Koike 2008), and common bean (*Phaseolus vulgaris*) (Songa et al. 1997). *M. phaseolina* is a ubiquitous agricultural soil inhabitant able to survive and remaining infectious in this environment for long intervals under adverse conditions (Gangopadhyay et al. 1982; Short et al. 1980; Sheikh and Ghaffar 1979). *M. phaseolina*'s wide host range coupled with its capability to persist in soil saprophytically on crop residue or via survival structures, i.e. microsclerotia, make disease control with chemical or cultural practices ineffective (Hartman, et al. 1999).

M. phaseolina asymptomatically infects soybean plants during vegetative developmental stages. *M. phaseolina* microsclerotia germinate early in the season when soil temperatures reach 20°C and is capable of infecting seedling or adult plants alike through their roots (Short et al. 1980; Bristow 1986; Collins et al. 1991). No signs or symptoms can be distinguished during infection (Cloud and Rupe 1994; Doubledee et al. 2018). However, *M. phaseolina* can be easily recovered from asymptomatic roots and stems of soybean plants under natural field inoculum (Mengistu et al. 2011; Kendig et al. 2000). In most epidemics, soybean plants remain symptomless and no signs of the pathogen are seen until beginning of plant senescence (Short et al. 1978; Wyllie and Calvert 1969). However, in some cases charcoal rot is reported to cause wilt and premature plant death, particularly when associated with drought stress (Hartman, et al. 1999; Navi and Yang 2008; Mengistu et al. 2011). Following the premature plant death or late senescence stages, *M. phaseolina* rapidly produces large numbers of microsclerotia in roots and stems of colonized plants (Short et al. 1978; Kendig et al. 2000). As a result, a distinct light

silvery-gray to blackish discoloration is observed in dead colonized plants. Even though multiple reports have described ubiquitous *M. phaseolina* colonization in dead soybean plants throughout the crop development stages (Hartman, et al. 1999; Romero Luna et al. 2017), no causal effect relationship has been experimentally demonstrated linking *M. phaseolina* colonization to plant death thus far (Doubledee et al. 2018).

During the onset of senescence, signs of *M. phaseolina* become visible. Colonized plants develop a silvery-gray aspect, root and stem tissues can present a dark-gray to blackish discoloration, and microsclerotia can be seen imbedded in most plant tissues, particularly the tap root and basal stem (Akhtar et al. 2011; Almeida et al. 2008; Azarmanesh et al. 2011; Hartman, et al. 1999). Disease assessments at or after soybean senescence have been the most common form of data gathering for epidemiological or resistance screening studies (Mengistu et al. 2013; Hartman, et al. 1999; Romero Luna et al. 2017). These disease quantifications are predicated upon the intensity of signs observed in the specimen tissues, particularly roots and stems (Mengistu et al. 2007).

Abiotic stresses, such as drought, heat, and mineral deficiency, have been shown to interact with plant disease resistance, at times exacerbating symptom development (Fujita et al. 2006; Xiong and Yang 2003; Atkinson and Urwin 2012). In particular, drought has been linked to increased severity of multiple row crop diseases including maize ear rot (Parsons and Munkvold 2010), sorghum stalk rot (Tesso et al. 2005), and crown rot of barley (*Hordeum vulgare*) (Liu and Liu 2016). Diseases caused by *M. phaseolina* have also been reported to increase in severity under drought stress in sorghum (Cloud and Rupe 1994; Pande et al. 1990; Diourte et al. 1995; Odvody and Dunkle 1979), sunflower (*Helianthus annuus*) (Blanco-López and Jiménez-Díaz 1983; Ijaz et al. 2013), and common bean (Garcia-Olivares et al. 2012;

Mayek-Pérez et al. 2002). In soybean, the amplifying effect of drought stress on charcoal rot has been described, including increased root colonization (Kendig et al. 2000; Mengistu et al. 2011). Root infection by *M. phaseolina* has been shown to reduce stomatal conductance in soybean plants while not affecting yield (Doubledee et al. 2018). As a result of climate change, drought events are projected to continue to increase in frequency and severity during this century in certain areas, including North America and northeast Brazil (Marvel et al. 2019; Cook et al. 2015). Thus, charcoal rot is likely to become a larger concern for soybean production, causing increased yield losses.

Vegetative indexes

Vegetative indexes have been used to remotely and non-destructively estimate soybean stress, including water deficit. The Normalized Difference Vegetative Index (NDVI) is a widely used vegetative index obtained by the difference of the reflectance of near-infrared (0.725 to 1.1µm) and visible spectrum (0.58 to 0.68µm) divided by the sum of these two quantities, thus yielding a ratio between -1 and 1 (Justice et al. 1985; Karnieli et al. 2010). NDVI takes advantage of unique plant features, such as the absorption of light in the visible spectrum, which includes photosynthetically active radiation, making them appear relatively dark in this wave-length band (Björkman and Demmig-Adams 1995). Meanwhile, plant canopies reflect most of near-infrared radiation received, which facilitates plant thermal regulation (Peñuelas and Filella 1998). Therefore, under conditions conducive to plant growth and development, healthy and vigorous plants will present an NDVI value closer to 1 and diseased or stressed plants close to 0 (Chenglin Liu et al. 2004; Moriondo et al. 2007; Bravo et al. 2003). NDVI is also consider a good estimator of photosynthesis activity (Gamon et al. 1995; Young and Harris 2005). More

recently, NDVI has been adopted as an indicator of drought stress. Drought conditions decrease plant greenness, thereby measurably decreasing their NDVI (Sims et al. 2006; Xu et al. 2011).

Biology of *P. longicolla*

Phomopsis longicolla is a soil and seed borne pathogen that causes pod and stem blight and seed decay in soybean (Hobbs et al. 1985; Sinclair 1993). *P. longicolla*, a ubiquitous and important seed pathogen of soybean, is a member of the *Diaporthe-Phomopsis* species complex that includes *D. phaseolorum* f. sp. *sojae*, *D. phaseolorum* f. sp. *caulivora*, and *D. aspalathi* (Gomes et al. 2013; Hobbs and Phillips 1985; Hobbs et al. 1985; Kmetz 1978; Mengistu et al. 2014; Nevena et al. 1997). *P. longicolla* is predominantly associated with Phomopsis seed decay (PSD) in the U.S. (Hobbs et al. 1985), although it has been reported to cause stem lesions in other regions of the world (Cui et al. 2009). Symptoms of PSD include shriveled and elongated seeds with chalky and cracked seed coats. These symptoms are easily discernable from other common soybean seed diseases, such as purple seed stain caused by *Cercospora kikuchii* (Hartman, et al. 1999). In addition to decreasing the nutritional quality of infected seeds (Hepperly and Sinclair 1978; Mayhew and Caviness 1994), *P. longicolla* can substantially impair seed germination and vigor, negatively affecting seedling emergence when infected seeds are planted in laboratory or field conditions (McGee et al. 1980; Mengistu and Heatherly 2006). Besides colonizing pods and seeds, *P. longicolla* can asymptomatically infect vegetative tissues as early as three weeks after seedling emergence only displaying signs upon senescence (Walcott et al. 1998; Impullitti and Malvick 2013).

P. longicolla can successfully overwinter in production areas in colonized plant debris and is capable of asymptomatically infecting soybean plants during vegetative and reproductive developmental stages (Roy and Abney 1988; Rupe and Ferriss 1987; Rupe 1990). Following

infection, *P. longicolla* maintains an endophytic-like lifestyle for most of crop development causing no apparent symptoms nor exhibiting any signs of colonization (Rupe and Ferriss 1987). At senescence, *P. longicolla* infects seeds and under conducive environmental condition can cause severe seed decay (Baker et al. 1987). Additionally, once plants mature, *P. longicolla* produces large numbers of pycnidia on the surfaces of aerial plant parts. In particular, characteristic vertical-row alignment pattern of pycnidia are distinctively observed on soybean plants main stem (Hartman, et al. 1999; Baker et al. 1987; Roy and Abney 1988).

PSD is endemic throughout North American soybean production areas, and has been described as one of the most common diseases affecting soybean seeds in the U.S. (Sinclair 1992). In recent years, PSD has increased in incidence and severity in Southeastern states, partly due to the prevalence of the early soybean production system (ESPS) in the region (TeKrony et al. 1996; Logan et al. 1998). The ESPS encourages early planting of short-season soybean cultivars to avoid late-summer stresses of heat and periodic droughts that occur throughout the region. Due to early planting, the reproductive stages of soybean development may occur during periods of high temperature and humidity, both of which favor PSD development (Shortt 1981). Delayed harvests also favor PSD, as the pathogen has an extended opportunity to colonize seeds before seed moisture can be adequately reduced by controlled drying (Wilcox et al. 1974). Beyond the Southeastern U.S., PSD occurs periodically in the Midwest when environmental conditions are favorable or harvests are substantially delayed (Kmetz 1978; Shortt 1981). The potential implications of climate change on PSD are difficult to project. However, several long-term forecasting models suggest the increased occurrence of extreme weather events, including heat waves, flooding, and storms (Pachauri et al. 2014), which could conceivably favor increased incidence of PSD across U.S. soybean producing regions.

The relationship between *P. longicolla* and soybean is complex and may involve more than one type of association. In addition to causing PSD, *P. longicolla* is commonly found as an asymptomatic endophyte in soybean vegetative tissues, including stems, leaves, and petioles (Kmetz 1978). Interestingly, *P. longicolla* is reported to endophytically associate with a range of taxonomically diverse plants, including *Euphorbia nutans* (Euphorbiaceae), *Abutilon theophrasti* (Malvaceae), *Ipomoea lacunosa* (Convolvulaceae), *Xanthium strumarium* (Asteraceae), and a tropical red seaweed *Bostrychia radicans* (Rhodomelaceae) (Erbert et al. 2012; Gomes et al. 2013; Udayanga et al. 2011), which suggests it has evolved broadly effective mechanisms of endophytism. *P. longicolla* produces a wide variety of anti-microbial compounds, such as 3-nitropropionic acid (Flores et al. 2013), 18-deoxy-cytochalasin H, mycophenolic acid, and dicerandrol C (Erbert et al. 2012). These observations suggest *P. longicolla* could function as a beneficial endophyte in soybean, although the exact nature of the relationship requires further elucidation.

Zone lines and *P. longicolla*

During colonization of soybean roots and stems, *P. longicolla* has been observed to form zone lines (Olson et al. 2015), structures that are postulated to be analogous to barrage zones on defined media (Brayford 1990). Zone lines are often seen in dead or senesced soybean taproots and lower stem and have been considered a sign of charcoal rot (Romero Luna et al. 2017). However, recent studies have shown that these typical black zone lines on soybean plants are caused by *P. longicolla* and not *M. phaseolina* (Olson et al. 2015; Vidić et al. 2013; Ghissi et al. 2014). Zone lines are macroscopic black lines seen in decaying woody plant tissues (Campbell 1933). They vary from a few millimeters to a several centimeters, straight or tortuous, in some cases they can be observed as stand-alone lines, but more often form an enclosed shape, e.g. an

ellipsoid (Olson et al. 2015; Li 1983). Zone lines are formed by intense colonization of plant material by pigmented fungal tissue and are often observed during wood decay (Lopez-Real 1975). Several species of filamentous fungi have been shown to cause zone lines including *Xylaria polymorpha* (Robinson and Laks 2010), *Polyporus* squamosus (Campbell and Munson 1936), *Armillaria melea* (Campbell 1934), and *Phellinus weirri* (Li 1981). However, *P. longicolla* is the first species observed to cause zone lines in soybean (Olson et al. 2015). *Phomopsis* spp. have been reported to cause zone lines in alfalfa (Nikandrow 1989, 1990) and elm trees (Webber and Gibbs 1984; Brayford 1990; Webber 1981). *Phomopsis* spp. isolated from elm trees have been shown to produce barrage zones in culture when colony margins of genetic distinct isolates meet or are in proximity to colonies from different fungal species (Webber 1981). Zone lines in plant debris have been considered a possible survival structure and demonstrably associated with long term viability of *Poria weirii* in soil environment (Nelson 1964).

The potential duality underlying the endophytic/pathogenic basis of the *P. longicolla*/soybean relationship has led to fundamental questions about how to dissect pathogenesis. A cut stem assay method is commonly used to assess *P. longicolla* virulence and soybean resistance (Li et al. 2010), in which soybean stems are cut and inoculated with an agar plug colonized by the pathogen. However, *P. longicolla* is reported to produce appressoria during infection of soybean pods (Baker et al. 1987), which suggests a degree of developmental specialization during plant infection. The cut stem assay is predicated on wounding, e.g., cutting the stem, which would presumably bypass specialized infectious development during pathogenesis. Additionally, soybean seeds and pods could express resistance responses not

observed in stems, and thus a cut stem assay may not fully capture the range of phenotypes associated with PSD.

Molecular genetics and *P. longicolla*

Despite its importance as the causal agent of PSD, few studies have explored the molecular basis of pathogenesis in *P. longicolla*. Recently, new molecular resources have become available, including a protocol for genetic transformation (Li et al. 2013) and draft genome sequences for two isolates of *P. longicolla*, including the type strain, TWH P74 (Li et al. 2015). However, functional genomics approaches have not yet been applied to the *P. longicolla*/soybean pathosystem. Forward genetic screens provide a powerful tool for the molecular dissection of pathogenesis in filamentous fungi. Forward genetic screens have been used effectively to discover novel genes and dissect pathogenesis in several filamentous fungi, including *Fusarium graminearum*, *Colletotrichum higginsianum*, *Magnaporthe grisea*, and *Leptosphaeria maculan* (Gupta and Chattoo 2007; Idnurm and Howlett 2002; Korn et al. 2015; Seong et al. 2005).

A key constraint with forward genetics is the ability to efficiently characterize genomic lesions in mutants. Numerous approaches have been developed to define insertion sites of mutagenesis cassettes, including plasmid rescue (Tam and Lefebvre 1993), thermal asymmetric interlaced PCR (TAIL PCR; Dent et al. 2005), restriction enzyme site directed amplification PCR (Gonzalez-Ballester et al. 2005), and 3'- rapid amplification of cDNA ends (Meslet-Cladiere and Vallon 2012). These methods, however, have distinct limitations, particularly regarding throughput. With the advent of next-generation DNA sequencing, whole-genome re-sequencing at varying depths of coverage has been utilized successfully to identify genomic lesions in some species of fungi (Esher et al. 2015). However, costs currently associated with

whole-genome resequencing often hinder the application of this approach to large collections of insertional mutants, and may be less effective for non-model organisms due to the limited availability of reference genome sequences.

Restriction Digestion Associated sequencing (RAD-seq) is a reduced representation sequencing strategy in which genomic regions flanking a specific restriction enzyme are selectively enriched for sequencing (Baird et al. 2008). The general workflow consists of digesting genomic DNA with a restriction enzyme, ligating oligonucleotide adapters to the digested DNA, enriching fragments containing the restriction site via PCR amplification, selecting fragments based on size, and sequencing fragments on a next-generation DNA sequencing platform. Distinct advantages of RAD-seq include flexibility regarding the selection of restriction enzymes, no requirement for a reference genome sequence *a priori*, and substantially higher throughput compared to whole-genome re-sequencing.

To date, the molecular basis of pathogenesis underlying PSD is poorly understood, in large part due to the unavailability of crucial genetic and genomic resources for *P. longicolla* or related species within the genus. In recent years, significant advancements have been made in support of molecular genetics and functional genomics approaches in *P. longicolla*, including protocols for genetic transformation (Li et al. 2013) and characterization of T-DNA insertions (Zaccaron et al. 2018), and draft genome sequences for two isolates of the pathogen, including the type strain (Li et al. 2015). In addition, draft genome sequences are available for *D. helianthi* (Baroncelli et al. 2016), two isolates of *D. ampelina* (Savitha et al. 2016), an unidentified *Diaporthe sp*. (de Sena Filho et al. 2016), and the causal agent of southern stem canker of soybean, *D. aspalathi* (Li et al. 2016). Recently, a targeted gene deletion approach utilizing *Agrobacterium tumefaciens*-mediated transformation was successfully employed to functionally

characterize *DhPKS1* in *D. helianthi* (Ruocco et al. 2018). However, the ability to perform functional genomics in *P. longicolla*, particularly reverse genetics via targeted gene deletion, has not been reported thus far.

The CCAAT-binding complex

The heterotrimeric CCAAT-binding complex (CBC) has recently been reported to control pathogenesis and mycotoxin production in Fusarium verticillioides in corn. CBC of eukaryotes is broadly conserved in animals, plants, and fungi (Becker et al. 1991; Edwards et al. 1998; McNabb and Pinto 2005). The fungal CBC was originally described in *Saccharomyces cerevisiae* as the Hap regulatory complex and found to consist of three core subunits: Hap2, Hap3, and Hap5 (McNabb et al. 1995; Olesen et al. 1987). More recently, a fourth subunit of the CBC exclusive to fungi, HapX, has been identified and characterized in filamentous Ascomycetes (Jung et al. 2010; Tanaka et al. 2002). In fungi, all three core components must be present for the functionality of the complex (McNabb et al. 1995; Ridenour and Bluhm 2014). The CBC is a key regulator of iron acquisition and homeostasis (Chakravarti et al. 2017) and the shift from fermentation to aerobic respiration in yeast (McNabb and Pinto 2005). In filamentous fungi, the CBC has been implicated as a regulator of responses to oxidative stress, secondary metabolism, and plant pathogenesis (Hong et al. 2013; Ridenour and Bluhm 2014; Thön et al. 2010; Yin and Keller 2011).

Dissertation scope

By reducing water deficit stress, irrigation could also decrease yield losses caused by charcoal rot. However, soybean yield response to charcoal rot under different water deficit stress levels is not well understood. Additionally, zone lines are now known not to be a sign of charcoal rot, but instead be caused by *P. longicolla* (Olson et al. 2015). However, there is no

current information on how these two soybean-root inhabitants interplay. Thus, in this dissertation the effect of charcoal rot on soybean yield under different water regimes was explored. Additionally, investigations were carried out on whether *P. longicolla* via zone lines alter root colonization by *M. phaseolina*. In addition to zone lines, *P. longicolla* is an endophyte with a wide host range, a seed pathogen of soybean, a soil inhabitant, and displays a distinct lifestyle switch from endophytism to saprophytism at the end of its host life cycle. The many interesting biological characteristics of *P. longicolla* coupled with its amenability to cultivation in vitro, DNA manipulation, and genetic transformation make this filamentous plant pathogenic fungi a particularly interesting model to better understand disease and biological mechanisms. Therefore, in this dissertation studies were carried out in an endeavor to generate tools and resources for future molecular genetics studies in this organism while simultaneously investigating mechanisms of its pathogenesis. Here are described a forward genetic study, a new method to identify T-DNA insertions in mutants created via *Agrobacterium*-mediated transformation, and a targeted gene knock-out experiment. These studies identified *P. longicolla* genes associated with its pathogenesis in soybean.

Literature cited

Akhtar, K. P., Sarwar, G., and Arshad, H. M. I. 2011. Temperature response, pathogenicity, seed infection and mutant evaluation against *Macrophomina phaseolina* causing charcoal rot disease of sesame. Archives of Phytopathology and Plant Protection 44:320-330

Almeida, Á. M., Amorim, L., Bergamin Filho, A., Torres, E., Farias, J. R., Benato, L. C., Pinto, M. C., and Valentim, N. 2003. Progress of soybean charcoal rot under tillage and no-tillage systems in Brazil. Fitopatologia Brasileira 28:131-135

Almeida, Á. M. R., Sosa-Gomez, D. R., Binneck, E., Marin, S. R. R., Zucchi, M. I., Abdelnoor, R. V., and Souto, E. R. 2008. Effect of crop rotation on specialization and genetic diversity of *Macrophomina phaseolina*. Tropical Plant Pathology 33:257-264

Atkinson, N. J., and Urwin, P. E. 2012. The interaction of plant biotic and abiotic stresses: from genes to the field. J Exp Bot. 63:3523-3543

Azarmanesh, N., Bond, J. P., Vick, A., Mengistu, A., and Fakhoury, A. M. 2011. A qPCR assay to detect and quantify *Macrophomina phaseolina* in soybean roots. Phytopathology 101:S11-S12

Baird, N.A., Etter, P.D., Atwood, T.S., Currey, M.C., Shiver, A.L., Lewis, Z.A., Selker, E.U., Cresko, W.A. and Johnson, E.A. 2008. Rapid SNP discovery and genetic mapping using sequenced RAD markers. PloS One 3:e3376

Baker, D. M., Minor, H. C., Brown, M. F., and Brown, E. A. 1987. Infection of immature soybean pods and seeds by *Phomopsis longicolla*. Can. J. Microbiol. 33:797-801

Baroncelli, R., Scala, F., Vergara, M., Thon, M. R., andRuocco, M. 2016. Draft whole-genome sequence of the *Diaporthe helianthi* 7/96 strain, causal agent of sunflower stem canker. *Genomics data 10*:151-152

Becker, D. M., Fikes, J. D., and Guarente, L. 1991. A cDNA encoding a human CCAAT-binding protein cloned by functional complementation in yeast. PNAS. 88:1968-1972

Bellaloui, N., Mengistu, A., and Paris, R. L. 2008. Soybean seed composition in cultivars differing in resistance to charcoal rot (*Macrophomina phaseolina*). Journal of Agricultural Science 146:667-675

Björkman, O., and Demmig-Adams, B. 1995. Regulation of Photosynthetic Light Energy Capture, Conversion, and Dissipation in Leaves of Higher Plants. In Ecophysiology of Photosynthesis. Springer, Berlin, Heidelberg 17-47

Blanco-López, M. A., and Jiménez-Díaz, R. M. 1983. Effect of irrigation on susceptibility of sunflower to *Macrophomina phaseolina*. Plant Disease 67:1214-1217

Bravo, C., Moshou, D., West, J., McCartney, A., and Ramon, H. 2003. Early Disease Detection in Wheat Fields using Spectral Reflectance. Biosystems Engineering. 84:137-145

Brayford, D. 1990. Vegetative incompatibility in *Phomopsis* from elm. Mycological Research. 94:745-752

Bristow, P. R. 1986. *Macrophomina phaseolina*, Another Cause of the Twin-Stem Abnormality Disease of Soybean. Plant Disease 70:1152-1153

Campbell, A. H. 1933. Zone lines in plant tissues I. The black lines formed by *Xylaria polymorpha* (Pers.) Grev. In hardwoods. Annals of Applied Biology 20:123-145

Campbell, A. H. 1934. Zone lines in plant tissues: II. The black lines formed by *Armillaria mellea* (Vahl) Quel. Annals of Applied Biology 21:1-22

Campbell, A. H., and Munson, R. G. 1936. Zone lines in plant tissues III. The black lines formed by *Polyporus squamosus* (Huds.) Fr. Annals of Applied Biology 23:453-464

Chakravarti, A., Camp, K., McNabb, D. S., and Pinto, I. 2017. The Iron-Dependent Regulation of the *Candida albicans* Oxidative Stress Response by the CCAAT-Binding Factor. PLOS ONE 12:e0170649

Chenglin Liu, Bingfang Wu, Yichen Tian, Wenbo Xu, and Jianxi Huang. 2004. Crop drought monitoring using serial NDVI amp; NDWI in Northern China. In: IGARSS 2004. IEEE International Geoscience and Remote Sensing Symposium 2264-2267

Cloud, G. L., and Rupe, J. C. 1994. Influence of nitrogen, plant growth stage, and environment on charcoal rot of grain sorghum caused by *Macrophomina phaseolina* (Tassi) Goid. Plant Soil 158:203-210

Collins, D. J., Wyllie, T. D., and Anderson, S. H. 1991. Biological activity of *Macrophomina phaseolina* in soil. Soil Biology and Biochemistry 23:495-496

Cook, B. I., Ault, T. R., and Smerdon, J. E. 2015. Unprecedented 21st century drought risk in the American Southwest and Central Plains. Science Advances 1:e1400082

Cui, Y.-L., Duan, C.-X., Wang, X.-M., Li, H.-J., and Zhu, Z.-D. 2009. First report of *Phomopsis longicolla* causing soybean stem blight in China. Plant Pathology 58:799

Dent, R. M., Haglund, C. M., Chin, B. L., Kobayashi, M. C., and Niyogi, K. K. 2005. Functional Genomics of Eukaryotic Photosynthesis Using Insertional Mutagenesis of *Chlamydomonas reinhardtii*. Plant Physiol. 137:545-556

Diourte, M., Starr, J. L., Jeger, M. J., Stack, J. P., and Rosenow, D. T. 1995. Charcoal rot (*Macrophomina phaseolina*) resistance and the effects of water stress on disease development in sorghum. Plant Pathology 44:196-202

Doubledee, M. D., Rupe, J. C., Rothrock, C. S., and Bajwa, S. G. 2018. Effect of root infection by *Macrophomina phaseolin*a on stomatal conductance, canopy temperature and yield of soybean. Canadian Journal of Plant Pathology 40:272-283

Edwards, D., Murray, J. A. H., and Smith, A. G. 1998. Multiple Genes Encoding the Conserved CCAAT-Box Transcription Factor Complex Are Expressed in *Arabidopsis*. Plant Physiology 117:1015-1022

Erbert, C., Lopes, A. A., Yokoya, N. S., Furtado, N. A. J. C., Conti, R., Pupo, M. T., Lopes, J. L. C., and Debonsi, H. M. 2012. Antibacterial compound from the endophytic fungus *Phomopsis longicolla* isolated from the tropical red seaweed Bostrychia radicans. Botm. 55:435-440

Esher, S.K., Granek, J.A. and Alspaugh, J.A. 2015. Rapid mapping of insertional mutations to probe cell wall regulation in *Cryptococcus neoformans*. Fungal Genet Biol. 82:9-21

Flores, A. C., Pamphile, J. A., Sarragiotto, M. H., and Clemente, E. 2013. Production of 3-nitropropionic acid by endophytic fungus Phomopsis longicolla isolated from *Trichilia elegans* A. JUSS ssp. elegans and evaluation of biological activity. World J Microbiol Biotechnol. 29:923-932

Fujita, M., Fujita, Y., Noutoshi, Y., Takahashi, F., Narusaka, Y., Yamaguchi-Shinozaki, K., and Shinozaki, K. 2006. Crosstalk between abiotic and biotic stress responses: a current view from the points of convergence in the stress signaling networks. Current Opinion in Plant Biology 9:436-442

Gacitua Arias, S., Rubilar Pons, R., and Sanfuentes Von Stowasser, E. 2013. Temporal analysis of charcoal root rot in forest nurseries under different pathogen inoculum densities and soil moisture content. Tropical Plant Pathology 38:179-187

Gamon, J. A., Field, C. B., Goulden, M. L., Griffin, K. L., Hartley, A. E., Joel, G., Penuelas, J., and Valentini, R. 1995. Relationships Between NDVI, Canopy Structure, and Photosynthesis in Three Californian Vegetation Types. Ecological Applications 5:28-41

Gangopadhyay, S., Wyllie, T. D., and Teague, W. R. 1982. Effect of bulk density and moisture content of soil on the survival of *Macrophomina phaseolina*. Plant and Soil 68:241-247

Garcia-Olivares, J. G., Lopez-Salinas, E., Cumpian-Gutierrez, J., Cantu-Almaguer, M. A., Zavala-Garcia, F., and Mayek-Pérez, N. 2012. Grain Yield and Charcoal Rot Resistance Stability in Common Beans under Terminal Drought Conditions. J. Phytopathol 160:98-105

Ghissi, V. C., Reis, E. M., and Deuner, C. C. 2014. Etiology of Phomopsis root rot in soybean. Summa Phytopathologica 40:270-272

Gomes, R. R., Glienke, C., Videira, S. I. R., Lombard, L., Groenewald, J. Z., and Crous, P. W. 2013. Diaporthe: a genus of endophytic, saprobic and plant pathogenic fungi. Persoonia 31:1-41

Gonzalez-Ballester, D., de Montaigu, A., Galván A., Fernández, E. 2005. Restriction enzyme site-directed amplification PCR: A tool to identify regions flanking a marker DNA. Analytical biochemistry 340:330-335

Gupta, A., and Chattoo, B. B. 2007. A novel gene MGA1 is required for appressorium formation in *Magnaporthe grisea*. Fungal Genetics and Biology 44:1157-1169

Haigh, J. C. 1930. *Macrophomina phaseoli* (Maubl.) Ashby and *Rhixoctonia bataticola* (Tanb.) Butler. Ann. Roy. Bot. Gard. 11:213-249

Hartman, G. L., Sinclair, J. B., and Rupe, J. C. 1999. Compendium of soybean diseases. American Phytopathological Society (APS Press), St. Paul.

Hepperly, P. R., and Sinclair, J. B. 1978. Quality losses in Phomopsis-infected soybean seeds. Phytopathology 68:1684-1687

Hobbs, T., and Phillips, D. 1985. Identification of *Diaporthe* and *Phomopsis* Isolates from Soybean. Phytopathology 75:500

Hobbs, T. W., Schmitthenner, A. F., and Kuter, G. A. 1985. A New *Phomopsis* species from soybean. Mycologia 77:535-545

Hong, S.-Y., Roze, L. V., and Linz, J. E. 2013. Oxidative Stress-Related Transcription Factors in the Regulation of Secondary Metabolism. Toxins 5:683-702

Idnurm, A., and Howlett, B. J. 2002. Isocitrate Lyase Is Essential for Pathogenicity of the Fungus *Leptosphaeria maculans* to Canola (*Brassica napus*). Eukaryot Cell 1:719-724

Ijaz, S., Sadaqat, H. A., and Khan, M. N. 2013. A review of the impact of charcoal rot (*Macrophomina phaseolina*) on sunflower. Journal of Agricultural Science 151:222-227

Impullitti, A. e., and Malvick, D. k. 2013. Fungal endophyte diversity in soybean. J Appl Microbiol. 114:1500–1506

Jackson, E. W., Fenn, P., and Chen, P. 2005. Inheritance of Resistance to Phomopsis Seed Decay in Soybean PI 80837 and MO/PSD-0259 (PI 562694). Crop Science 45:2400-2404

Jaiman, R. K., Jain, S. C., and Sharma, P. 2009. Field Evaluation of Fungicides, Bioagents and Soil Amendments Against Root Rot Caused by *Macrophomina phaseolina* in Cluster Bean. Journal of Mycology and Plant Pathology 39:74-76

Jung, W. H., Saikia, S., Hu, G., Wang, J., Fung, C. K.-Y., D'Souza, C., White, R., and Kronstad, J. W. 2010. HapX Positively and Negatively Regulates the Transcriptional Response to Iron Deprivation in *Cryptococcus neoformans*. PLOS Pathogens 6:e1001209

Justice, C. O., Townshend, J. R. G., Holben, B. N., and Tucker, C. J. 1985. Analysis of the phenology of global vegetation using meteorological satellite data. International Journal of Remote Sensing 6:1271-1318

Karnieli, A., Agam, N., Pinker, R. T., Anderson, M., Imhoff, M. L., Gutman, G. G., Panov, N., and Goldberg, A. 2010. Use of NDVI and land surface temperature for drought assessment: Merits and limitations. Journal of climate 23:618-633

Kendig, S. R., Rupe, J. C., and Scott, H. D. 2000. Effect of Irrigation and Soil Water Stress on Densities of *Macrophomina phaseolina* in Soil and Roots of Two Soybean Cultivars. Plant Disease 84:895-900

Kmetz, K. T. 1978. Soybean Seed Decay: Prevalence of Infection and Symptom Expression Caused by *Phomopsis* sp., *Diaporthe phaseolorum* var. *sojae*, and *D. phaseolorum* var. *caulivora*. Phytopathology 68:836-840

Koike, S. T. 2008. Crown rot of strawberry caused by *Macrophomina phaseolina* in California. Plant Disease 92:1253-1253

Korn, M., Schmidpeter, J., Dahl, M., Müller, S., Voll, L. M., and Koch, C. 2015. A Genetic Screen for Pathogenicity Genes in the Hemibiotrophic Fungus *Colletotrichum higginsianum* Identifies the Plasma Membrane Proton Pump Pma2 Required for Host Penetration. PLOS ONE 10:e0125960

Lehman, S. G. 1923. Pod and Stem Blight of Soybean. Annals of the Missouri Botanical Garden. 10:111-178

Li, C. Y. 1983. Melanin-like Pigment in Zone Lines of *Phellinus weirii*-Colonized Wood. Mycologia 75:562-566

Li, C. Y. 1981. Phenoloxidase and Peroxidase Activities in Zone Lines of *Phellinus weirii*. Mycologia. 73:811-821

Li, S., Hartman, G. L., and Boykin, D. L. 2010. Aggressiveness of *Phomopsis longicolla* and Other *Phomopsis* spp. on Soybean. Plant Disease 94:1035-1040

Li, S., Ridenour, J. B., Kim, H., Hirsch, R. L., Rupe, J. C., and Bluhm, B. H. 2013. *Agrobacterium tumefaciens*-mediated transformation of the soybean pathogen *Phomopsis longicolla*. Journal of Microbiological Methods 92:244-245

Li, S., Song, Q., Martins, A. M., and Cregan, P. 2016. Draft genome sequence of *Diaporthe aspalathi* isolate MS-SSC91, a fungus causing stem canker in soybean. Genomics Data 7:262-263

Li, S., Song, Q., Ji, P., and Cregan, P. 2015. Draft Genome Sequence of *Phomopsis longicolla* Type Strain TWH P74, a Fungus Causing Phomopsis Seed Decay in Soybean. Genome Announc. 3: e00010-15

Liu, X., and Liu, C. 2016. Effects of Drought-Stress on Fusarium Crown Rot Development in Barley. PLOS ONE 11:e0167304

Livingston, J. 1945. Charcoal Rot of Corn and Sorghum. Historical Research Bulletins of the Nebraska Agricultural Experiment Station.

Logan, J., Mueller, M. A., and Graves, C. R. 1998. A Comparison of Early and Recommended Soybean Production Systems in Tennessee. Journal of Production Agriculture 11:319-325

Lopez-Real, J. M. 1975. Formation of pseudosclerotia ('zone lines') in wood decayed by *Armillaria mellea* and *Stereum hirsutum*: I. Morphological aspects. Transactions of the British Mycological Society 64:465-471

Marvel, K., Cook, B. I., Bonfils, C. J. W., Durack, P. J., Smerdon, J. E., and Williams, A. P. 2019. Twentieth-century hydroclimate changes consistent with human influence. Nature 569:59-65

Mayek-Pérez, N., GarcÍa-Espinosa, R., LÓpez-CastaÑeda, Cá., Acosta-Gallegos, J. A., and Simpson, J. 2002. Water relations, histopathology and growth of common bean (*Phaseolus vulgaris* L.) during pathogenesis of *Macrophomina phaseolina* under drought stress. Physiological and Molecular Plant Pathology. 60:185-195

Mayhew, W. L., and Caviness, C. E. 1994. Seed Quality and Yield of Early-Planted, Short-Season Soybean Genotypes. Agronomy Journal. 86:16-19

McGee, D. C., Brandt, C. L., and Burris, J. S. 1980. Seed mycoflora of soybeans relative to fungal interactions, seedling emergence, and carry over of pathogens to subsequent crops. Phytopathology 70:615-617

McNabb, D. S., and Pinto, I. 2005. Assembly of the Hap2p/Hap3p/Hap4p/Hap5p-DNA Complex in *Saccharomyces cerevisiae*. Eukaryotic Cell 4:1829-1839

McNabb, D. S., Xing, Y., and Guarente, L. 1995. Cloning of yeast HAP5: a novel subunit of a heterotrimeric complex required for CCAAT binding. Genes Dev. 9:47-58

Mengistu, A., Arelli, P., Bond, J., Nelson, R., Rupe, J., Shannon, G., and Wrather, A. 2013. Identification of Soybean Accessions Resistant to *Macrophomina phaseolina* by Field

Screening and Laboratory Validation. Plant Health Progress DOI:10.1094/PHP-2013-0318-01-RS

Mengistu, A., Castlebury, L. A., Morel, W., Ray, J. D., and Smith, J. R. 2014. Pathogenicity of *Diaporthe* spp. isolates recovered from soybean (*Glycine max*) seeds in Paraguay. Canadian Journal of Plant Pathology 36:470-474

Mengistu, A., and Heatherly, L. G. 2006. Planting date, irrigation, maturity group, year, and environment effects on *Phomopsis longicolla*, seed germination, and seed health rating of soybean in the early soybean production system of the midsouthern USA. Crop Protection. 25:310–317

Mengistu, A., Ray, J. D., Smith, J. R., and Paris, R. L. 2007. Charcoal Rot Disease Assessment of Soybean Genotypes Using a Colony-Forming Unit Index. Crop Science. 47:2453-2461

Mengistu, A., Smith, J. R., Ray, J. D., and Bellaloui, N. 2011. Seasonal progress of charcoal rot and its impact on soybean productivity. Plant Disease 95:1159-1166

Meslet-Cladière, L., and Vallon, O. 2012. A new method to identify flanking sequence tags in *Chlamydomonas* using 3'-RACE. Plant Methods 8:21 DOI: 10.1186/1746-4811-8-21

Moriondo, M., Maselli, F., and Bindi, M. 2007. A simple model of regional wheat yield based on NDVI data. European Journal of Agronomy 26:266-274

Navi, S. S., and Yang, X. B. 2008. Foliar symptom expression in association with early infection and xylem colonization by *Fusarium virguliforme* (formerly *F. solani* f sp *glycines*), the causal agent of soybean sudden death syndrome. Plant Health Progress DOI:10.1094/PHP-2008-0222-01-RS

Nelson, E. E. 1964. Some probable relationships of soil fungi and zone lines to survival of *Poria weirii* in buried wood blocks. Phytopathology 54:120-121

Nevena, M., Jelena, V., and Franić-Mihajlović, D. 1997. A comparative study of *Diaporthe*/*Phomopsis* fungi on soybean from two different regions of the world. Mycopathologia 139:107-113

Nikandrow, A. 1990. *Acrocalymma medicaginis* and *Phomopsis* sp. as Causal Agents of Crown Rot of Lucerne in Australia. Journal of Phytopathology 130:24-36

Nikandrow, A. 1989. Zone lines diagnostic of *Phomopsis* sp. in lucerne crown rot. Australasian Plant Pathology 18:86-89

Odvody, G. N., and Dunkle, L. D. 1979. Charcoal stalk rot of sorghum: effect of environment on host-parasite relations. Phytopathology 69:250-254

Olesen, J., Hahn, S., and Guarente, L. 1987. Yeast HAP2 and HAP3 activators both bind to the CYC1 upstream activation site, UAS2, in an interdependent manner. Cell 51:953-961

Olson, T. R., Gebreil, A., Micijevic, A., Wise, K. A., Mueller, D. S., Chilvers, M. I., and Mathew, F. M. 2015. Association of Diaporthe longicolla with Black Zone Lines on Mature Soybean Plants. Plant Health Progress DOI:10.1094/PHP-RS-15-0020

Pachauri, R. K., Allen, M. R., Barros, V. R., Broome, J., Cramer, W., Christ, R., Church, J. A., Clarke, L., Dahe, Q., Dasgupta, P., and others. 2014. Climate change 2014: synthesis report. Contribution of Working Groups I, II and III to the fifth assessment report of the Intergovernmental Panel on Climate Change. IPCC.

Pande, S., Mughogho, L. K., and Karunakar, R. I. 1990. Effect of moisture stress, plant population density and pathogen inoculation on charcoal stalk rot of sorghum. Annals of Applied Biology 116:221-232

Parsons, M. W., and Munkvold, G. P. 2010. Associations of planting date, drought stress, and insects with Fusarium ear rot and fumonisin B1 contamination in California maize. Food Addit Contam Part A Chem Anal Control Expo Risk Assess. 27:591-607

Peñuelas, J., and Filella, I. 1998. Visible and near-infrared reflectance techniques for diagnosing plant physiological status. Trends in Plant Science 3:151-156

Ridenour, J. B., and Bluhm, B. H. 2014. The HAP complex in *Fusarium verticillioides* is a key regulator of growth, morphogenesis, secondary metabolism, and pathogenesis. Fungal Genetics and Biology 69:52-64

Robinson, S. C., and Laks, P. E. 2010. Wood Species and Culture Age Affect Zone Line Production of *Xylaria polymorpha*. Open Mycology Journal 4:18-21

Romero Luna, M. P., Mueller, D., Mengistu, A., Singh, A. K., Hartman, G. L., and Wise, K. A. 2017. Advancing Our Understanding of Charcoal Rot in Soybeans. J Integr Pest Manag. 8:DOI10.1093/jipm/pmw020

Roy, K. W., and Abney, T. S. 1988. Colonization of pods and infection of seeds by *Phomopsis longicolla* in susceptible and resistant soybean lines inoculated in the greenhouse. Canadian Journal of Plant Pathology 10:317-320

Ruocco, M., Baroncelli, R., Cacciola, S. O., Pane, C., Monti, M. M., Firrao, G., Vergara, M., Magnano, S. L. G., Vannacci, G., Scala, F. 2018. Polyketide synthases of *Diaporthe helianthi* and involvement of DhPKS1 in virulence on sunflower. BMC genomics 27 DOI:10.1186/s12864-017-4405-z

Rupe, J. C., and Ferriss, R. S. 1986. Effects of pod moisture on soybean seed infection by *Phomopsis* sp. Phytopathology 76:273-277

Rupe, J. C. 1990. Effect of temperature on the rate of infection of soybean seedlings by *Phomopsis longicolla*. Canadian Journal of Plant Pathology. 12:43-47

Rupe, J., and Ferriss, R. 1987. A Model for Predicting the Effects of Microclimate on Infection of Soybean by *Phomopsis longicolla*. Phytopathology 77:1162-1166

Savitha, J., Bhargavi, S. D., & Praveen, V. K. 2016. Complete Genome Sequence of the Endophytic Fungus *Diaporthe* (*Phomopsis*) *ampelina*. *Genome announcements* 4:e00477-16

de Sena Filho, J. G., Quin, M. B., Spakowicz D. J., Shaw, J. J., Kucera, K., Dunican, B., Strobel, S. A., Schmidt-Dannert, C. 2016. Genome of *Diaporthe* sp. provides insights into the potential inter-phylum transfer of a fungal sesquiterpenoid biosynthetic pathway. Fungal biology 120: 1050-1063

Seong, K., Hou, Z., Tracy, M., Kistler, H. C., and Xu, J.-R. 2005. Random Insertional Mutagenesis Identifies Genes Associated with Virulence in the Wheat Scab Fungus *Fusarium graminearum*. Phytopathology 95:744-750

Shaukat, S. S., and Siddiqui, I. A. 2003. The influence of mineral and carbon sources on biological control of charcoal rot fungus, *Macrophomina phaseolina* by fluorescent pseudomonads in tomato. Letters in Applied Microbiology 36:392-398

Sheikh, A. H., and Ghaffar, A. 1979. Relation of sclerotial inoculum density and soil moisture to infection of field crops by *Macrophomina phaseolina*. Pakistan Journal of Botany 11:185-189

Short, G. E., Wyllie, T. D., and Ammon, V. D. 1978. Quantitative enumeration of *Macrophomina phaseolina* in soybean tissues. Phytopathology 68:736-741

Short, G. E., Wyllie, T. D., and Bristow, P. R. 1980. Survival of *Macrophomina phaseolina* in soil and in residue of soybean. Phytopathology 70:13-17

Shortt, B. J. 1981. Epidemiology of Phomopsis Seed Decay of Soybean in Illinois. Plant Disease 65:62-64

Sims, D. A., Luo, H., Hastings, S., Oechel, W. C., Rahman, A. F., and Gamon, J. A. 2006. Parallel adjustments in vegetation greenness and ecosystem CO_2 exchange in response to drought in a Southern California chaparral ecosystem. Remote Sensing of Environment 103:289-303

Sinclair, J. B. 1992. Discoloration of Soybean Seeds - An Indicator of Quality. Plant Disease 76:1087-1091

Sinclair, J. B. 1993. Phomopsis Seed Decay of Soybeans- A Prototype for Studying Seed Disease. Plant Disease 77:329-334

Songa, W., Hillocks, R. J., Mwango'mbe, A. W., Buruchara, R., and Ronno, W. K. 1997. Screening common bean accessions for resistance to charcoal rot (*Macrophomina phaseolina*) in Eastern Kenya. Experimental Agriculture 33:459-468

Su, G., Suh, S.-O., Schneider, R. W., and Russin, J. S. 2001. Host Specialization in the Charcoal Rot Fungus, *Macrophomina phaseolina*. Phytopathology 91:120-126

Tam, L. W., and Lefebvre, P. A. 1993. Cloning of flagellar genes in *Chlamydomonas reinhardtii* by DNA insertional mutagenesis. Genetics 135:375-384

Tanaka, A., Kato, M., Nagase, T., Kobayashi, T., and Tsukagoshi, N. 2002. Isolation of genes encoding novel transcription factors which interact with the Hap complex from *Aspergillus* species. Biochimica et Biophysica Acta - Gene Structure and Expression 1576:176-182

TeKrony, D. M., Grabau, L. J., DeLacy, M., and Kane, M. 1996. Early Planting of Early-Maturing Soybean: Effects on Seed Germination and Phomopsis Infection. Agronomy Journal 88:428-433

Tenkouano, A., Miller, F. R., Frederiksen, R. A., and Rosenow, D. T. 1993. Genetics of nonsenescence and charcoal rot resistance in sorghum. Theoret. Appl. Genetics 85:644-648

Tesso, T. T., Claflin, L. E., and Tuinstra, M. R. 2005. Analysis of Stalk Rot Resistance and Genetic Diversity among Drought Tolerant Sorghum Genotypes. Crop Science 45:645-652

Thön, M., Al Abdallah, Q., Hortschansky, P., Scharf, D. H., Eisendle, M., Haas, H., and Brakhage, A. A. 2010. The CCAAT-binding complex coordinates the oxidative stress response in eukaryotes. Nucleic Acids Res. 38:1098-1113

Udayanga, D., Liu, X., McKenzie, E. H. C., Chukeatirote, E., Bahkali, A. H. A., and Hyde, K. D. 2011. The genus *Phomopsis*: biology, applications, species concepts and names of common phytopathogens. Fungal Diversity 50:189-225

Vidić, M., Petrović, K., Đorđević, V., and Riccioni, L. 2013. Occurrence of *Phomopsis longicolla* β Conidia in Naturally Infected Soybean. J Phytopathol. 161:470-477

Yin, W., and Keller, N. P. 2011. Transcriptional regulatory elements in fungal secondary metabolism. J Microbiol. 49:329-339

Walcott, R. R., McGee, D. C., and Misra, M. K. 1998. Detection of Asymptomatic Fungal Infections of Soybean Seeds by Ultrasound Analysis. Plant Disease 82:584-589

Webber, J. 1981. A natural biological control of Dutch elm disease. Nature 292:449-451

Webber, J. F., and Gibbs, J. N. 1984. Colonization of elm bark by *Phomopsis oblonga*. Transactions of the British Mycological Society 82:348-352

Wilcox, J. R., Laviolette, F. A., Athow, K. L., and others. 1974. Deterioration of soybean seed quality associated with delayed harvest. Plant Disease Reporter 58:130-133

Wrather, J. A., Shannon, J. G., Stevens, W. E., Sleper, D. A., and Arelli, A. P. 2004. Soybean cultivar and foliar fungicide effects on *Phomopsis* sp. seed infection. Plant disease 88:721-723

Wrather, A., Shannon, G., Balardin, R., Carregal, L., Escobar, R., Gupta, G. K., Ma, Z., Morel, W., Ploper, D., and Tenuta, A. 2010. Effect of diseases on soybean yield in the top eight producing countries in 2006. Plant Health Progress DOI:10.1094/PHP-2010-0125-01-RS.

Wrather, J. A., Anderson, T. R., Arsyad, D. M., Gai, J., Ploper, L. D., Porta-Puglia, A., Ram, H. H., and Yorinori, J. T. 1997. Soybean disease loss estimates for the top 10 soybean producing countries in 1994. Plant Disease 81:107-110

Wyllie, T. D., and Calvert, O. H. 1969. Effect of flower removal and pod set on formation of sclerotia and infection of Glycine max by *Macrophomina phaseoli*. Phytopathology 59:1243-1245

Xiong, L., and Yang, Y. 2003. Disease Resistance and Abiotic Stress Tolerance in Rice Are Inversely Modulated by an Abscisic Acid–Inducible Mitogen-Activated Protein Kinase. The Plant Cell 15:745-759

Xu, L., Samanta, A., Costa, M. H., Ganguly, S., Nemani, R. R., and Myneni, R. B. 2011. Widespread decline in greenness of Amazonian vegetation due to the 2010 drought. Geophysical Research Letters 38: L07402

Young, S. S., and Harris, R. 2005. Changing patterns of global-scale vegetation photosynthesis, 1982–1999. International Journal of Remote Sensing 26:4537-4563

Zaccaron, M., Sharma, S., and Bluhm, B. H. 2018. MoNSTR-seq, a restriction site-associated DNA sequencing technique to characterize *Agrobacterium*-mediated transfer-DNA insertions in *Phomopsis longicolla*. Lett. Appl. Microbiol. 66:19-24

Zorrilla, G., Knapp, A. D., and McGee, D. C. 1994. Severity of Phomopsis Seed Decay, Seed Quality Evaluation, and Field Performance of Soybean. Crop Science 34:172-177

Chapter II: Drought stress and its effects on charcoal rot and yield of soybean

Abstract

Charcoal rot, caused by the soil-borne fungal pathogen *Macrophomina phaseolina*, is associated with drought stress. The primary controls for charcoal rot in soybean are to avoid drought stress and, if possible, plant a moderately resistant cultivar. To determine the effect of irrigation and cultivar on charcoal rot in soybean, a study was conducted in 2011 and 2013 with four soybean cultivars, with and without *M. phaseolina* inoculation, and with three irrigation regimes: full season irrigation, irrigation terminated (cut) at R5, and no irrigation. Canopy reflectance as measured by the normalized difference vegetative index (NDVI) was greater in irrigated than non-irrigated plots, in non-inoculated than inoculated plots, and with 'Ozark' than the other cultivars. At R6, NDVI was not different among the cultivars in 2011, but was significantly lower in 'R01581F' than in 'Osage' or 'Hutcheson'. With most cultivars at R6, NDVI were significantly lower for the no irrigation and the irrigation cut at R5 treatments than the full season irrigation. There were no significant differences in NDVI with the no irrigation or irrigation cut at R5 treatments. Full season irrigation yielded significantly more than no irrigation or irrigation cut at R5 plots in 2012 with most cultivars, but only for R01581F in 2013. Non-inoculated plots yielded significantly more than inoculated plots across cultivar and irrigation treatments. In 2011, stem colonization by *M. phaseolina* was significantly less in full season irrigation than in no irrigation plots. In 2013, colonization was significantly greater in full season irrigation plots than in plot where irrigation was cut at R5. There was a significant three-way interaction of inoculation, cultivar and irrigation in root colonization measured visually using a 1 to 5 index. When there were significant differences among cultivars, Osage had lower RSS ratings than the other cultivars. Hutcheson and R01581F generally had higher RSS ratings

than the other cultivars in the different inoculation and irrigation treatments and Ozark usually had lower ratings than Hutcheson and R01581F, but higher than Osage. Comparing irrigation treatments within cultivars and inoculations, in general full-season irrigation had the lowest distribution of RSS ratings followed by no irrigation and then irrigation cut at R5. Regressions of yield to NDVI at R3 and at R6 were significant in both years with positive slopes. Regression analysis relating charcoal rot to yield within a year and irrigation treatment were not significant for CFU's in 2013, proportion stem colonization in either year, or RSS except for irrigation cut at R5 in 2011 where the regression was significant with a positive slope and an R^2 of 0.355. Overall, irrigation significantly affected yield and there were significant effects of irrigation, cultivar, and inoculation on RSS, but RSS did not negatively affect yield.

Introduction

Macrophomina phaseolina, the causal agent of charcoal rot, is an important soil-borne pathogen of soybean (Almeida et al. 2003; Wrather et al. 1997; Hartman, et al. 1999). Charcoal rot has been reported to cause severe yield losses in most soybean growing areas worldwide, including, but not limited to Brazil, Argentina, China, and the US (Wrather et al. 1997). *M. phaseolina* has a wide host range, reportedly found to infect over 500 plant species within 100 families including several economically important crop species like cotton (Su et al. 2001), maize (Livingston 1945), sorghum (Tenkouano et al. 1993), tomatoes (Shaukat and Siddiqui 2003), strawberry (Koike 2008), and common bean (Songa et al. 1997). *M. phaseolina* is a ubiquitous agricultural soil-inhabitant able to survive and remaining infectious in this environment for long periods under adverse conditions (Gangopadhyay et al. 1982; Short et al. 1980; Sheikh and Ghaffar 1979). *M. phaseolina* wide host range coupled with its capability to

persist in soil saprophytically on crop residue or via survival structures, i.e. microsclerotia, make disease control with chemical or cultural practices ineffective (Hartman, et al. 1999).

M. phaseolina asymptomatically infects soybean plants during vegetative developmental stages. *M. phaseolina* microsclerotia germinate early in the season when soil temperatures reach 20°C and are capable of infecting seedling or adult plants alike through their roots (Short et al. 1980; Bristow 1986; Collins et al. 1991). No signs or symptoms are visually apparent until soybean late reproductive stages (Cloud and Rupe 1994; Doubledee et al. 2018; Mengistu et al. 2011b). However, *M. phaseolina* can be easily recovered from asymptomatic roots and stems of soybean plants under natural field inoculum (Mengistu et al. 2011b; Kendig et al. 2000). Multiple reports have described ubiquitous signs of *M. phaseolina* in dead soybean plants throughout the crop development stages (Hartman, et al. 1999; Romero Luna et al. 2017). However, thus far no causal effect relationship has been experimentally demonstrated linking *M. phaseolina* colonization to plant death (Doubledee et al. 2018). During the onset of senescence, signs of *M. phaseolina* become visible. Colonized plants develop a silvery-gray aspect, root and stem tissues can present a dark-gray to blackish discoloration, and microsclerotia can be seen imbedded in most plant tissues, particularly taproot and basal stem (Akhtar et al. 2011; Almeida et al. 2008; Azarmanesh et al. 2011; Hartman, et al. 1999). Disease assessments at or after soybean senescence have been the most common form of evaluating for epidemiological or resistance screening studies (Mengistu et al. 2013; Hartman, et al. 1999; Romero Luna et al. 2017). These disease quantifications are predicated upon the intensity of signs observed in the root and stem tissues (Mengistu et al. 2007).

Abiotic stresses, such as drought, heat, and mineral deficiency interacts with plant disease resistance, at times exacerbating symptom development (Fujita et al. 2006; Xiong and Yang

2003; Atkinson and Urwin 2012). In particular, drought has been linked to increased severity of multiple row crop diseases including maize ear rot (Parsons and Munkvold 2010), sorghum stalk rot (Tesso et al. 2005), and crown rot of barley (Liu and Liu 2016). Diseases caused by *M. phaseolina* have also been reported to increase in severity under drought stress in sorghum (Cloud and Rupe 1994; Pande et al. 1990; Diourte et al. 1995; Odvody and Dunkle 1979), sunflower (Blanco-López and Jiménez-Díaz 1983; Ijaz et al. 2013), and common bean (Garcia-Olivares et al. 2012; Mayek-Pérez et al. 2002). In soybean, the amplifying effect of drought stress on charcoal rot has been described, including increased root colonization (Kendig et al. 2000; Mengistu et al. 2011b). Root infection by *M. phaseolina* reduces stomatal conductance in soybean plants while having inconsistent effects on yield (Doubledee et al. 2018). As a result of climate change, drought events are projected to continue to increase in frequency and severity during this century in certain areas, including North America and northeast Brazil (Marvel et al. 2019; Cook et al. 2015). Thus, charcoal rot is likely to become a larger concern for soybean production, causing increased yield losses.

Vegetative indexes based on canopy reflectance have been used to remotely and non-destructively estimate soybean stress, including water deficit. The Normalized Difference Vegetative Index (NDVI) is a widely used vegetative index obtained by the difference of the reflectance of near-infrared (0.725 to 1.1µm) and visible spectrum (0.58 to 0.68µm) divided by the sum of these two quantities, thus yielding a ratio between -1 to 1 (Justice et al. 1985; Karnieli et al. 2010). NDVI takes advantage of unique plant features, such as the absorption of light in the visible spectrum, which includes photosynthetically active radiation, making them appear relatively dark in this wave-length band (Björkman and Demmig-Adams 1995). Meanwhile, plant canopies reflect most of near-infrared radiation received, which facilitates plant thermal

regulation (Peñuelas and Filella 1998). Therefore, under conditions conducive to plant growth and development, healthy and vigorous plants will present an NDVI value closer to 1 and diseased or stressed plants close to 0 (Chenglin Liu et al. 2004; Moriondo et al. 2007; Bravo et al. 2003). NDVI is also consider a good estimator of photosynthesis activity (Gamon et al. 1995; Young and Harris 2005). More recently, NDVI has been adopted as an indicator of drought stress. Drought conditions decrease plant greenness, thereby measurably decreasing their NDVI (Sims et al. 2006; Xu et al. 2011).

When available and economically viable, irrigation is used in soybean production to curtail yield losses due to drought stress. By reducing water deficit stress, irrigation could also decrease yield losses caused by charcoal rot. However, soybean yield response to charcoal rot under different water deficit stress levels is not well understood. Thus, the objectives of the present study were to elucidate: (1) the effect of charcoal rot on soybean yield under field conditions, (2) the result of drought stress on charcoal rot severity, and (3) the change in yield in response to charcoal rot under different irrigation regimes.

Materials and methods

Experimental design and implementation. A field experiment was designed and implemented at Lon Mann Cotton research station, Marianna, AR to examine how drought stress modulates the effect of charcoal rot on soybean yield. The experiment had a full-factorial design with three irrigation regimes, four cultivars, and two inoculation treatments. A split-plot design was implemented in the field with irrigation being the main plot and the combination of cultivar x inoculation the split-plot level. Each treatment combination was replicated six times. The experiment was executed during the growing season of 2011 and repeated in 2013.

Experimental units were represented by six-row plots, 6.1 meters in length, with approximately 81 cm between rows planted in-furrow. Plots were sown at a rate of 32 seeds m^{-1}.

Three irrigation regimes were established to induce different levels of water deficit stress on plants. Plots were irrigated according to crop recommendations throughout the growing season (full-season), or the irrigation was stopped at the R5 developmental stage (irrigation cut at R5), or no irrigation was applied at any moment. Four cultivars, with maturity within 5 days of each other, were used in this experiment, 'Osage', 'Ozark', 'Hutcheson', and 'RO1581F'. Preliminary results indicated that the cultivar Osage had moderate resistance to charcoal rot, and cultivar RO1581F had moderate tolerance to drought stress. Additionally, reports also indicate cultivars Ozark and Hutcheson to be susceptible to charcoal rot (da Silva et al. 2019; Mengistu et al. 2012, 2011a). To ensure disease development, each combination of cultivar and irrigation regime had an inoculated and a non-inoculated treatment. Plots were mechanically harvested and yield adjusted to 13% moisture content.

Inoculum preparation. The isolate Conway (Twizeyimana et al. 2012) collected from disease soybean plants at Conway, AR was the source for inoculum production used in the field inoculation. The isolate was first grown on potato dextrose agar. After five days, the colonized growth medium was fragmented and used to inoculate sterile sorghum seeds. After three weeks, colonized sorghum seeds were transferred to a metal screen and allowed to air dry in a fume hood for approximately five days. After drying, any large clump of colonized seeds was broken by hand. The inoculum was mixed with soybean seeds in the planting envelope at the rate of 5 grams per 200 seeds.

NDVI. The normalized vegetative index (NDVI) was obtained directly from a hand held GreenSeeker® sensor (Trimble®, Sunnyvale, CA, USA) employed in the field. Between 15 and

20 measurements were taken on each of the two central rows of every plot. Measurements were made at the R3 and R6 developmental stages during the growing seasons of 2011 and 2013. The sensor was kept approximately 50 cm above the top of plant canopies. Measurements were made between 10am and 3pm. For each assessment, readings from each plot were averaged yielding a single data point per plot that was used for statistical analysis.

Disease measurements. Charcoal rot was assessed by root colonization severity, length of stem colonization, and by estimating *M. phaseolina* CFUs per gram of root. At physiological maturity, ten plants were collected from the outer two rows of every plot. All disease measurements were performed on the same plants. Soil was removed with running tap water and plants were allowed to air dry on a greenhouse bench. Charcoal rot severity on soybean roots was estimated as previously described (Mengistu et al. 2013). In short, tap roots from ten plats were excised from the main stem and split along the vertical axis. Each root was given a 1 to 5 severity rating based on the level of colonization observed in the interior tissues, where 1 signifies the absence of charcoal rot signs and 5 was given to roots with severe charcoal rot. The level of colonization was primarily assessed based on the presence and abundance of *M. phaseolina* microsclerotia and discoloration of root tissue, typical signs of charcoal rot. Charcoal rot was also measured in regards to how much of the main stem was colonized by *M. phaseolina*. The main stems of ten plants were split along its vertical axis and assessed for the presence of microsclerotia. Then, the length between the soil line and the upper-most charcoal rot sign and the plant height from the soil line to the tip of the main stem were measured to determine the percent the stem colonization. In 2013, the colony forming unities per gram of root (CFU) were enumerated as previously described (Mengistu et al. 2011a). In short, after split and rated for severity, taproots collected from each plot were pooled and dried at 30°C for 15 days and ground

with a Wiley ® mill (Model 4; Thomas Scientific, Swedesboro, NJ, USA) with a 28-mesh screen. The mill was cleaned with compressed air and disinfested with 70% ethanol between samples. A subsample of 5mg was taken from ground roots of every plot and mixed in a blender for one minute with 100 ml of 0.5% sodium hypochlorite aqueous solution. Root grounds were recovered and rinsed with sterile distilled water on a 45μm sieve. Root grounds were mixed with molten PDA kept at 60°C. The medium was amended with tergitol (100 μl L^{-1}; Sigma-Aldrich, St. Louis, MO, USA) and rifampicin (100mg L^{-1}; RPI, Mount Prospect, IL, USA). The medium with the root grounds was dispensed evenly on five Petri dishes and incubated at 28°C for five days. *M. phaseolina* colonies were morphologically identified on each plate and counted and CFU's calculated.

Zone lines. The incidence of root zone lines (Olson et al. 2015) was recorded on roots sampled for charcoal rot assessments. In split soybean tap roots, zone lines were distinguishable as continuous black lines or curves often tracing an elliptical or circular shape, or a segment thereof. The presence of these zone lines was scored as present or absent on every root and the incidence of zone lines calculated for each plot.

Soil initial inoculum. To estimate the initial inoculum *M. phaseolina* colony forming units were enumerated per gram of soil in the area where the experimental was conducted. At planting, three soil cores were collected at depth of 0-10 cm from each of the two central rows of every plot. Soil was kept refrigerated at 4°C till processing. Soil from each sample was thoroughly homogenized and CFU's were enumerated as previously described (Mengistu et al. 2008). A subsample of approximately 5 grams was taken, weighed and oven-dried for the estimation of moisture content. A second 5g subsample was used for plating. To estimate *M. phaseolina* CFUs, soil was disinfested, rinsed and plated as described above. After 5 days plates

were read and CFUs were expressed per unit of dry soil. Enumeration of *M. phaseolina* CFU was normalized for 1 gram of dry soil.

Environmental data. Soil temperature and moisture were recorded in full season irrigation and no irrigation treatments. A soil moisture and temperature sensor (Grainger, Lake Forest, IL, USA) was buried 10 cm bellow the soil surface in two plots in the central area of the experiment in the field. One sensor was placed in a plot under the full-season irrigation regime and another sensor in a plot without any irrigation. The sensors were deployed at planting, placed approximately 5 cm from the row. Each sensor was equipped with a data logger recovered at the end of the season for data retrieval.

Statistical analysis. Analysis of variance for all variables was performed with the GLIMMIX procedure in SAS version 9.4 (SAS Institute, Cary, NC, USA). Charcoal rot root severity (RSS) was analyzed as an ordered categorical variable. For RSS, statistical analysis was carried out with the Multinomial distribution and cumulative logit link function options in the GLIMMIX procedure in SAS. The variables NDVI, colonization proportion, and zone line incidence were analyzed with a Beta distribution option in the GLIMMIX procedure in SAS. The Variables yield and root CFU were analyzed with the Gamma distribution option in the GLIMMIX procedure in SAS. Before Analysis, the variable root CFU was transformed to $\log_2$ of x. Linear regression analysis was performed with the lm function in R version 3.5.1 (R. Core Team 2018).

Results

Charcoal rot severity. Root rot severity (RRS) was affected by a 3-way interaction of irrigation x cultivar x inoculation ($P<0.05$; **Table 1**). The distribution of ratings for each treatment are presented in Figure 1A. The significant contrasts between all treatments is

presented in Figure 2. Inoculation did not always significantly affect RRS, but when it did ratings were more severe in inoculated than non-inoculated plots. This occurred for Osage in the cut at R5 irrigation, Hutcheson and Osage in the full season irrigation and Ozark and R01581F in the no irrigation treatment. Figure 1B shows the significant differences between cultivars under different irrigation and inoculation treatments. In the inoculated plots, Hutcheson had significantly greater RRS ratings than Osage and R01581F with full season irrigation. With no irrigation Osage had lower RRS ratings than all the other cultivars and Hutcheson had significantly lower ratings than R01581F. There were no cultivar differences in RSS ratings with the cut at R5 irrigation. With the non-inoculated plots, Osage had significantly lower RSS ratings than all of the other cultivars with the cut at R5 and the full season irrigation treatments and Ozark had significantly lower RSS ratings than Hutcheson under with irrigation. Figure 1C presents the significant differences between irrigation treatments with each cultivar in inoculated and non-inoculated plots. With Hutcheson, RSS ratings were significantly greater in the full season than the no irrigation inoculated plots, Osage had significantly greater RSS ratings with the cut at R5 than the other irrigation treatments in inoculated plots. R01581F had significantly lower RSS ratings with full season irrigation than the other irrigation treatments in inoculated plots. With Hutcheson, Osage and R01581F in non-inoculated plots, RSS ratings were significantly higher with cut at R5 than full season irrigation. With Osage RSS ratings were also higher for no irrigation than full season irrigation in non-inoculated plots. RSS ratings for Ozark in inoculated or in non-inoculated plots were not significantly different between irrigation treatments.

Soybean main stem colonization was affected by the interactions of cultivar x year and irrigation x year ($P<0.05$; **Table 1**). In 2011, the greatest stem colonization was in the no

irrigation plots and that was significantly greater than the full season irrigation **(Fig. 3)**. However, in 2013, stem colonization was greatest with full season irrigation and least with irrigation cut at R5. Stem colonization in 2011 was significantly lower with Osage than all of the other cultivars **(Fig. 3B)**. There were no significant differences in stem colonization between cultivars in 2013. There were no significant effects on root colonization by *M. phaseolina* (CFU; Table 1). Root colonization levels ranged from 825 to 68,455 colony forming unities per gram of dried root tissue.

NDVI. At R3, there were significant cultivar and inoculation main effects and a significant year by irrigation interaction (Table 1). Osage had a significantly greater NDVI than the other cultivars **(Fig. 4a)**. Non-inoculated plots had a significantly greater NDVI than inoculated plots **(Fig. 4b)**. In both years, plots with full irrigation had significantly greater NDVI's than plots with no irrigation **(Fig. 4c)** NDVI's were greater in 2013 than 2011.

At R6, there were significant year by cultivar and irrigation by cultivar interactions (Table 1). The lowest NDVI occurred with R01581F in 2013 at R6 **(Fig. 5A)**. All other cultivars in 2013 and all cultivars in 2011 were not significantly different. NDVI's were significantly greater for full season irrigation than the no irrigation or the cut at R6 irrigation treatments with all cultivars except Osage **(Fig. 6B)**.

Yield. There was a significant main effect of inoculation and a significant year x irrigation x cultivar interaction on yield **(Table 1)**. Yields were significantly greater in the non-inoculated than the inoculated plots, 1857 vs 1722 kg ha^{-1}, respectively. In 2011, Yields were significantly greater for the irrigated than the cut at R5 or the no irrigation treatments for all cultivars except Osage (Fig. 7). With Osage, full season and cut at R5 had significantly greater yields than no irrigation. In 2013, yields were lower, but not significantly lower for the no

irrigation and the cut at R5 irrigation than the full season irrigation plots for all cultivars except R01581F. R01581F had significantly greater yields in the full season than the other irrigation treatments. Analyzed across year, cultivar and inoculation, there were significant positive correlations between NDVI at both R3 and R6 with yield **(Table 2).** There were no significant correlations between yield and stem colonization.

Zone line incidence. There was a significant year and cultivar interaction for zone line incidence **(Table 1)**. Osage and R01581F had the greatest incidences of zone lines in 2011 and Hutcheson and Osage had the greatest incidence in 2013. Ozark had the lowest incidence in 2011 and the Ozark and R01581F had the lowest in 2013. **(Table 3)**.

Environmental conditions. Average soil temperatures were above 30^{o}C from July 1 through August 8 in 2011, but was at or below 30^{o}C throughout 2013 **(Fig. 7)**. Soil moisture in the non-irrigated plots reached -200 kPa from July 20-29, August 5-8, and September 1-20 in 2011. In 2013, non-irrigated plots reached -200 kPa from September 1-20.

Discussion

Irrigation strongly impacted soybean yield. As expected, treatments under full-season irrigation had much higher yields, indicating that there was a significant water deficit stress on plots under no irrigation, or when irrigation was cut at the developmental stage R5. Water deficit stress, consequence of the different irrigation regimes, was also illustrated by canopy greenness levels measured by NDVI. Together, yield and NDVI differences among the irrigation treatments support considerable differences in stress levels the different treatments underwent during the growing seasons. NDVI has been previously identified not only as a good estimator for drought stress but also a good predictor of yield in multiple crops (Moriondo et al. 2007; Crusiol et al. 2017). A significant relationship between NDVI and yield was also identified in

both years of this study further supporting considerable water deficit stress differences among the treatments. Surprisingly, yield and NDVI at R6 indicated very little differences between irrigating soybean thru R5 and no irrigation. Although, the critical importance of irrigation scheduled during reproductive stages of soybean, in particular during pod fill, has been amply reported in the literature (Francis et al. 2018; Doss et al. 1974; Ashley and Ethridge 1978).

Charcoal rot root symptoms were affected by irrigation. Higher root disease severity was observed in treatments where irrigation was cut at R5, particularly in artificially inoculated plots. This was the only treatment combination where no cultivar effect was observed; all cultivars presented high severity levels. Additionally, when irrigation was cut at R5, artificial inoculation only affected charcoal rot symptoms for the cultivar Osage, increasing it. Together, these data indicate the water deficit stress may have provided a more conducive environment for disease development, overwhelming any horizontal resistance in this cultivar. Meanwhile, in treatments not irrigated or irrigated full season, where disease severity was lower, cultivar had a more significant effect. In particular, Hutcheson consistently presented higher disease severity while Osage presented lower disease. Thus, the present work further implicates drought stress as an important factor in charcoal rot severity. Furthermore, under extreme environmental conditions and abundance of inoculum, differences due to quantitative genetic resistance may not be detectable wish RSS assessment. Therefore, some level of water deficit stress management may be advisable in field-based resistance screening for charcoal rot. Our results indicate that inoculation coupled with full season irrigation were the best circumstances to observe charcoal rot severity differences among cultivars.

Charcoal rot severity poorly explained variations in yield although non-inoculated plots yielded significantly better than inoculated plots. *M. phaseolina* is considered to be a major

soybean pathogen. Charcoal rot has been reported to cause severe yield loss throughout soybean growing regions world-wide, particularly when coupled with drought. Even though irrigation had an observable effect on charcoal rot severity, the variation in disease due to irrigation was not significantly correlated to yield, even in treatments with increased drought stress levels. This study found little relationship between charcoal rot severity and yield responses. These results were not replicated in 2013. Meanwhile, root CFU and stem colonization could not explain yield in any circumstance. This poor relationship between disease measurements and yield response could be the result of cultivar tolerance. Tolerance is the host genetic-controlled phenomenon where the presence of disease does not impact yield. However, significant levels of tolerance to charcoal rot have not been described. Alternatively, the poor relationship between charcoal rot and yield could be the result of non-representative disease assessments. The measurements used to assess disease might not appropriately describe damage done to soybean by charcoal rot. This would indicate that disease measurements done at or after the onset of senescence, as it is commonly done for over five decades, may not hold great value for genetic resistance screening or epidemiological studies. In this case, disease assessments done during developmental stages critical for yield components might provide a more reliable estimation of yield loss due to charcoal rot.

No charcoal rot symptoms were observed before plant senescence. When severe, charcoal rot has been reported to kill soybean plants, causing discoloration on dead tissues, particularly under drought stress. Even though severe tap root symptoms were observed in most taproots of plants under no irrigation, no premature dead plants were observed before harvest maturity. Furthermore, there are no reports of charcoal rot causing death of soybean plants under controlled experimental conditions. However, the ready production of abundant microsclerotia

at the onset of senescence or premature plant death caused by extraneous factors, could make apparent a correlation relationship between plant death and signs of charcoal rot despite the lack of cause-effect.

Literature cited

Akhtar, K. P., Sarwar, G., and Arshad, H. M. I. 2011. Temperature response, pathogenicity, seed infection and mutant evaluation against *Macrophomina phaseolina* causing charcoal rot disease of sesame. Arch. Phytopathol. Plant Prot. 44:320–330

Almeida, Á. M., Amorim, L., Bergamin Filho, A., Torres, E., Farias, J. R., Benato, L. C., Pinto, M. C., and Valentim, N. 2003. Progress of soybean charcoal rot under tillage and no-tillage systems in Brazil. Fitopatol. Bras. 28:131–135

Almeida, Á. M. R., Sosa-Gomez, D. R., Binneck, E., Marin, S. R. R., Zucchi, M. I., Abdelnoor, R. V., and Souto, E. R. 2008. Effect of crop rotation on specialization and genetic diversity of *Macrophomina phaseolina.* Trop. Plant Pathol. 33:257–264

Ashley, D. A., and Ethridge, W. J. 1978. Irrigation Effects on Vegetative and Reproductive Development of Three Soybean Cultivars 1. Agron. J. 70:467–471

Atkinson, N. J., and Urwin, P. E. 2012. The interaction of plant biotic and abiotic stresses: from genes to the field. J. Exp. Bot. 63:3523–3543

Azarmanesh, N., Bond, J. P., Vick, A., Mengistu, A., and Fakhoury, A. M. 2011. A qPCR assay to detect and quantify *Macrophomina phaseolina* in soybean roots. Phytopathology. 101:S11–S12

Björkman, O., and Demmig-Adams, B. 1995. Regulation of Photosynthetic Light Energy Capture, Conversion, and Dissipation in Leaves of Higher Plants. Pages 17–47 in: Ecophysiology of Photosynthesis, Springer Study Edition. E.-D. Schulze and M.M. Caldwell, eds. Springer Berlin Heidelberg, Berlin, Heidelberg.

Blanco-López, M. A., and Jiménez-Díaz, R. M. 1983. Effect of irrigation on susceptibility of sunflower to *Macrophomina phaseoli*. Plant Dis. 67:1214–1217

Bravo, C., Moshou, D., West, J., McCartney, A., and Ramon, H. 2003. Early Disease Detection in Wheat Fields using Spectral Reflectance. Biosyst. Eng. 84:137–145

Bristow, P. R. 1986. *Macrophomina phaseolina,* Another Cause of the Twin-Stem Abnormality Disease of Soybean. Plant Dis. 70:1152

Chenglin Liu, Bingfang Wu, Yichen Tian, Wenbo Xu, and Jianxi Huang. 2004. Crop drought monitoring using serial NDVI and NDWI in Northern China. Pages 2264–2267 vol.4 in: IGARSS 2004. 2004 IEEE International Geoscience and Remote Sensing Symposium

Cloud, G. L., and Rupe, J. C. 1994. Influence of nitrogen, plant growth stage, and environment on charcoal rot of grain sorghum caused by *Macrophomina phaseolina* (Tassi) Goid. Plant Soil. 158:203–210

Collins, D. J., Wyllie, T. D., and Anderson, S. H. (Department of P. P. 1991. Biological activity of *Macrophomina phaseolina* in soil. Soil Biol. Biochem. U. K.

Cook, B. I., Ault, T. R., and Smerdon, J. E. 2015. Unprecedented 21st century drought risk in the American Southwest and Central Plains. Sci. Adv. 1:e1400082

Crusiol, L. G. T., Carvalho, J. de F. C., Sibaldelli, R. N. R., Neiverth, W., do Rio, A., Ferreira, L. C., Procópio, S. de O., Mertz-Henning, L. M., Nepomuceno, A. L., Neumaier, N., and Farias, J. R. B. 2017. NDVI variation according to the time of measurement, sampling size, positioning of sensor and water regime in different soybean cultivars. Precis. Agric. 18:470–490

Diourte, M., Starr, J. L., Jeger, M. J., Stack, J. P., and Rosenow, D. T. 1995. Charcoal rot (*Macrophomina phaseolina*) resistance and the effects of water stress on disease development in sorghum. Plant Pathol. 44:196–202

Doss, B. D., Pearson, R. W., and Rogers, H. T. 1974. Effect of Soil Water Stress at Various Growth Stages on Soybean Yield 1. Agron. J. 66:297–299

Doubledee, M. D., Rupe, J. C., Rothrock, C. S., and Bajwa, S. G. 2018. Effect of root infection by *Macrophomina phaseolina* on stomatal conductance, canopy temperature and yield of soybean. Can. J. Plant Pathol. 40:272–283

Francis, P. B., Stark, C. R., Henry, C. G., Espinoza, L., Ismanov, M., Hayes, S., and Earnest, L. 2018. Scheduling of Furrow Irrigation Initiation on Soybean Yield and Net Returns. Crop Forage Turfgrass Manag. 4

Fujita, M., Fujita, Y., Noutoshi, Y., Takahashi, F., Narusaka, Y., Yamaguchi-Shinozaki, K., and Shinozaki, K. 2006. Crosstalk between abiotic and biotic stress responses: a current view from the points of convergence in the stress signaling networks. Curr. Opin. Plant Biol. 9:436–442

Gamon, J. A., Field, C. B., Goulden, M. L., Griffin, K. L., Hartley, A. E., Joel, G., Penuelas, J., and Valentini, R. 1995. Relationships Between NDVI, Canopy Structure, and Photosynthesis in Three Californian Vegetation Types. Ecol. Appl. 5:28–41

Gangopadhyay, S., Wyllie, T. D., and Teague, W. R. 1982. Effect of bulk density and moisture content of soil on the survival of *Macrophomina phaseolina*. Plant Soil. 68:241–247

Garcia-Olivares, J. G., Lopez-Salinas, E., Cumpian-Gutierrez, J., Cantu-Almaguer, M. A., Zavala-Garcia, F., and Mayek-Perez, N. 2012. Grain Yield and Charcoal Rot Resistance Stability in Common Beans under Terminal Drought Conditions. J. Phytopathol. 160:98–105

Hartman, G. L., Sinclair, J. B., and Rupe, J. C., eds. 1999. *Compendium of soybean diseases*. Fourth Edition. American Phytopathological Society (APS Press), St. Paul.

Ijaz, S., Sadaqat, H. A., and Khan, M. N. 2013. A review of the impact of charcoal rot (*Macrophomina phaseolina*) on sunflower. J. Agric. Sci. 151:222–227

Justice, C. O., TOWNSHEND, J. R. G., HOLBEN, B. N., and TUCKER, C. J. 1985. Analysis of the phenology of global vegetation using meteorological satellite data. Int. J. Remote Sens. 6:1271–1318

Karnieli, A., Agam, N., Pinker, R. T., Anderson, M., Imhoff, M. L., Gutman, G. G., Panov, N., and Goldberg, A. 2010. Use of NDVI and land surface temperature for drought assessment: Merits and limitations. J. Clim. 23:618–633

Kendig, S. R., Rupe, J. C., and Scott, H. D. 2000. Effect of Irrigation and Soil Water Stress on Densities of *Macrophomina phaseol*ina in Soil and Roots of Two Soybean Cultivars. Plant Dis. 84:895–900

Koike, S. T. 2008. Crown rot of strawberry caused by *Macrophomina phaseolina* in California. Plant Dis. 92:1253–1253

Liu, X., and Liu, C. 2016. Effects of Drought-Stress on Fusarium Crown Rot Development in Barley. PLOS ONE. 11:e0167304

Livingston, J. 1945. Charcoal Rot of Corn and Sorghum. Hist. Res. Bull. Neb. Agric. Exp. Stn.

Marvel, K., Cook, B. I., Bonfils, C. J. W., Durack, P. J., Smerdon, J. E., and Williams, A. P. 2019. Twentieth-century hydroclimate changes consistent with human influence. Nature. 569:59

Mayek-Pérez, N., GarcÍa-Espinosa, R., LÓpez-CastaÑeda, Cá., Acosta-Gallegos, J. A., and Simpson, J. 2002. Water relations, histopathology and growth of common bean (*Phaseolus vulgaris* L.) during pathogenesis of *Macrophomina phaseolina* under drought stress. Physiol. Mol. Plant Pathol. 60:185–195

Mengistu, A., Arelli, P. A., Bellaloui, N., Bond, J. P., Shannon, G. J., Wrather, A. J., Rupe, J. C., Chen, P., Little, C. R., Canaday, C. H., Newman, M. A., and Pantalone, V. R. 2012. Evaluation of Soybean Genotypes for Resistance to Three Seed-borne Diseases. Plant Health Prog.

Mengistu, A., Arelli, P. A., Bond, J. P., Shannon, G. J., Wrather, A. J., Rupe, J. B., Chen, P., Little, C. R., Canaday, C. H., Newman, M. A., and Pantalone, V. R. 2011a. Evaluation of Soybean Genotypes for Resistance to Charcoal Rot. Plant Health Prog.

Mengistu, A., Arelli, P., Bond, J., Nelson, R., Rupe, J., Shannon, G., and Wrather, A. 2013. Identification of Soybean Accessions Resistant to *Macrophomina phaseolina* by Field Screening and Laboratory Validation. Plant Health Prog.

Mengistu, A., Ray, J. D., Smith, J. R., and Paris, R. L. 2007. Charcoal Rot Disease Assessment of Soybean Genotypes Using a Colony-Forming Unit Index. Crop Sci. 47:2453

Mengistu, A., Reddy, K. N., Zablotowicz, R. M., and Wrather, A. J. 2008. Propagule Densities of *Macrophomina phaseolina* in Soybean Tissue and Soil as Affected by Tillage, Cover Crop, and Herbicide. Plant Health Prog.

Mengistu, A., Smith, J. R., Ray, J. D., and Bellaloui, N. 2011b. Seasonal progress of charcoal rot and its impact on soybean productivity. Plant Dis. 95:1159–1166

Moriondo, M., Maselli, F., and Bindi, M. 2007. A simple model of regional wheat yield based on NDVI data. Eur. J. Agron. 26:266–274

Odvody, G. N., and Dunkle, L. D. 1979. Charcoal stalk rot of sorghum: effect of environment on host-parasite relations. Phytopathology. 69:250–254

Olson, T. R., Gebreil, A., Micijevic, A., Wise, K. A., Mueller, D. S., Chilvers, M. I., and Mathew, F. M. 2015. Association of *Diaporthe longicolla* with Black Zone Lines on Mature Soybean Plants. Plant Health Prog.

Pande, S., Mughogho, L. K., and Karunakar, R. I. 1990. Effect of moisture stress, plant population density and pathogen inoculation on charcoal stalk rot of sorghum. Ann. Appl. Biol. 116:221–232

Parsons, M. W., and Munkvold, G. P. 2010. Associations of planting date, drought stress, and insects with Fusarium ear rot and fumonisin B1 contamination in California maize. Food Addit. Contam. Part Chem. Anal. Control Expo. Risk Assess. 27:591–607

Peñuelas, J., and Filella, I. 1998. Visible and near-infrared reflectance techniques for diagnosing plant physiological status. Trends Plant Sci. 3:151–156

R. Core Team. 2018. R: A Language and Environment for Statistical Computing.

Romero Luna, M. P., Mueller, D., Mengistu, A., Singh, A. K., Hartman, G. L., and Wise, K. A. 2017. Advancing Our Understanding of Charcoal Rot in Soybeans. J. Integr. Pest Manag. 8

Shaukat, S. S., and Siddiqui, I. A. 2003. The influence of mineral and carbon sources on biological control of charcoal rot fungus, *Macrophomina phaseolina* by fluorescent pseudomonas in tomato. Lett. Appl. Microbiol. 36:392–398

Sheikh, A. H., and Ghaffar, A. 1979. Relation of sclerotial inoculum density and soil moisture to infection of field crops by *Macrophomina phaseolina*. Pak. J. Bot. 11:185–189

Short, G. E., Wyllie, T. D., and Bristow, P. R. 1980. Survival of *Macrophomina phaseolina* in soil and in residue of soybean. Phytopathology. 70:13–17

da Silva, M. P., Pereira, A., Rupe, J. C., Bluhm, B. H., Gbur, E. E., Wood, L., Mozzoni, L. A., and Chen, P. 2019. Effectiveness of a Seed Plate Assay for Evaluating Charcoal Rot Resistance in Soybean and the Relationship to Field Performance. Plant Dis. :PDIS-10-18-1908-RE

Sims, D. A., Luo, H., Hastings, S., Oechel, W. C., Rahman, A. F., and Gamon, J. A. 2006. Parallel adjustments in vegetation greenness and ecosystem CO2 exchange in response to drought in a Southern California chaparral ecosystem. Remote Sens. Environ. 103:289–303

Songa, W., Hillocks, R. J., Mwango'mbe, A. W., Buruchara, R., and Ronno, W. K. 1997. Screening common bean accessions for resistance to charcoal rot (*macrophomina phaseolina*) in eastern Kenya. Exp. Agric. 33:459–468

Su, G., Suh, S.-O., Schneider, R. W., and Russin, J. S. 2001. Host Specialization in the Charcoal Rot Fungus, *Macrophomina phaseolina*. Phytopathology. 91:120–126

Tenkouano, A., Miller, F. R., Frederiksen, R. A., and Rosenow, D. T. 1993. Genetics of nonsenescence and charcoal rot resistance in sorghum. Theor. Appl. Genet. 85:644–648

Tesso, T. T., Claflin, L. E., and Tuinstra, M. R. 2005. Analysis of Stalk Rot Resistance and Genetic Diversity among Drought Tolerant Sorghum Genotypes. Crop Sci. 45:645–652

Twizeyimana, M., Hill, C. B., Pawlowski, M., Paul, C., and Hartman, G. L. 2012. A Cut-Stem Inoculation Technique to Evaluate Soybean for Resistance to *Macrophomina phaseolina*. Plant Dis. 96:1210–1215

Wrather, J. A., Anderson, T. R., Arsyad, D. M., Gai, J., Ploper, L. D., Porta-Puglia, A., Ram, H. H., and Yorinori, J. T. 1997. Soybean disease loss estimates for the top 10 soybean producing countries in 1994. Plant Dis. 81:107–110

Xiong, L., and Yang, Y. 2003. Disease Resistance and Abiotic Stress Tolerance in Rice Are Inversely Modulated by an Abscisic Acid–Inducible Mitogen-Activated Protein Kinase. Plant Cell. 15:745–759

Xu, L., Samanta, A., Costa, M. H., Ganguly, S., Nemani, R. R., and Myneni, R. B. 2011. Widespread decline in greenness of Amazonian vegetation due to the 2010 drought. Geophys. Res. Lett. 38

Young, S. S., and Harris, R. 2005. Changing patterns of global-scale vegetation photosynthesis, 1982–1999. Int. J. Remote Sens. 26:4537–456

Tables

Table 1. Analysis of variance for fixed effects. The *p* values of each fixed effect are shown for each dependent variable studied. The analyze of variance was performed with the GLIMMIX procedure of SAS 9.4 system.

Effect	NDVI at R3[1]	NDVI at R6[2]	Yield[3]	Colonization proportion[4]	Zone line incidence[5]	Root CFU[6]	RSS[7]
year	<.0001	0.096	0.3263	0.9955	0.4841	-	0.0951
irrigation	<.0001	<.0001	<.0001	0.0079	0.2791	0.6071	0.0009
cultivar	<.0001	<.0001	0.7188	<.0001	0.0100	0.2533	<.0001
inoculation	0.0233	0.2221	0.0185	0.1355	0.4077	0.6903	<.0001
year*irrigation	0.0002	0.1891	0.0387	0.0016	0.5727	-	0.0584
year*cultivar	0.1710	0.0049	0.0639	0.0010	0.0261	-	0.2027
year*inoculation	0.5698	0.6776	0.7432	0.9403	0.4520	-	0.2745
irrigation*cultivar	0.2933	<.0001	0.0639	0.3797	0.6726	0.4176	0.3837
irrigation*inoculation	0.7355	0.7741	0.9347	0.4175	0.6761	0.2658	0.366
cultivar*inoculation	0.0736	0.8509	0.5576	0.654	0.7595	0.7425	0.9546
year*irrigation*cultivar	0.8590	0.5087	0.0363	0.5938	0.8373	-	0.0509
year*irrigation*inoculation	0.6637	0.8978	0.4886	0.7417	0.4265	-	0.4967
year*cultivar*inoculation	0.0682	0.8415	0.7931	0.5252	0.4073	-	0.2179
irrigation*cultivar*inoculation	0.9947	0.9686	0.9151	0.8495	0.9790	0.8952	0.0139
year*irrigation*cultivar*inoculation	0.5524	0.8376	0.2933	0.1390	0.6147	-	0.5403

[1]NDVI measure at the pod stage, before seed filling. [2]NDVI measured at the completion of seed filling stage. [3]grain yield adjusted to 13% moisture content. [4]Mean proportion of main stem with signs of charcoal rot. [5]Incidence of zone lines caused by *P. longicolla* visually assessed in ten taproots for every plot. [6]Colony forming unities of *M. phaseolina* per gram of dry soybean tap root evaluated from plants collected in 2013. [7]Severity of charcoal rot on soybean taproots measured from 1, no disease, to 5 severe signs of charcoal rot.

Table 2. Relationship between NDVI and soybean yield.

Stage	Year	Intercept			Slope			R^2
		P value[1]	Estimate	Standard error	*P* value[2]	Estimate	Standard error	
R3	2011	0.000481	-1221.5	341.8	3.60E-16	6213	673.5	0.3747
	2013	5.80e-11	-8771	1236	1.72E-15	12851	1477	0.3629
R6	2011	<2e-16	-3226.9	317.2	<2E-16	7764.1	477.1	0.6509
	2013	0.0495	-673.4	339.9	2.16E-13	4226.6	538.2	0.3184

Statistics generated from linear regression where yield is modelled as a function of NDVI measured at wither the pod stage before seed filling (R3) and the completion of seed filling stage (R6). [1]*P* value for the null hypothesis of intercept = 0. [2]*P* value for the null hypothesis of regression slope = zero.

Table 3. Incidence of zone lines in soybean roots.

Year	Cultivar	Mean[1]	SE
2011	Hutchens	17.19 B	0.0306
2011	Osage	25.86 A	0.0408
2011	Ozark	7.78 C	0.0165
2011	RO1581F	21.86 AB	0.0422
2013	Hutchens	28.98 A	0.0413
2013	Osage	26.59 A	0.0403
2013	Ozark	19.17 B	0.0335
2013	RO1581F	18.39 B	0.0321

[1]Means incidence of zone lines caused by P. longicolla in soybean tap roots. Zone lines were visually assessed in ten taproots for every plot. Roots were collected after the onset of senescence. Means followed by different letters are significantly different from each other ($P<0.05$) according to Tukey's range test.

Figures

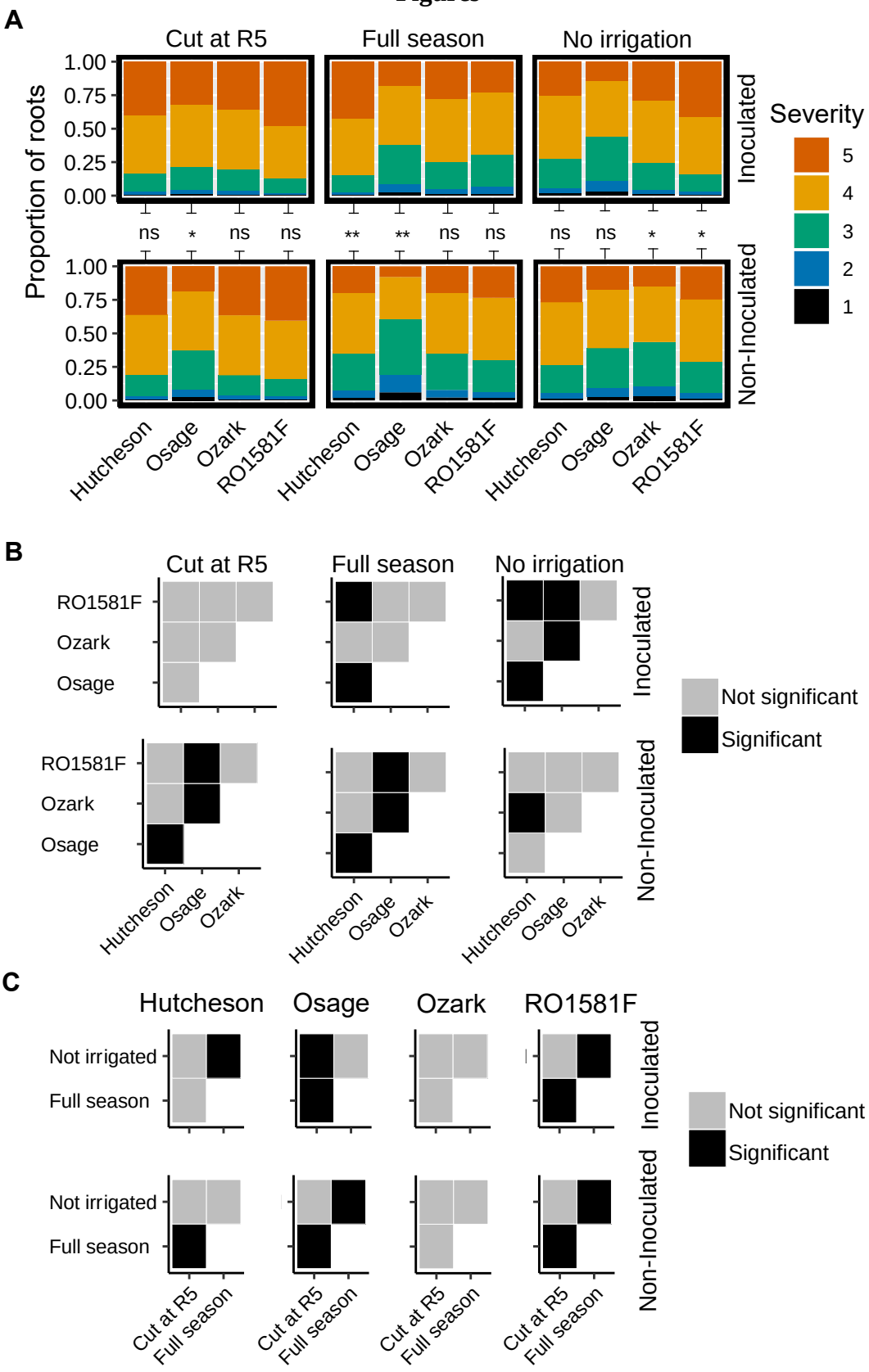
A
Cut at R5
Full season
No irrigation
Proportion of roots
1.00
0.75
0.50
0.25
0.00
ns * ns ns ** ** ns ns ns ns * *
Inoculated
Non-Inoculated
Severity
5
4
3
2
1
Hutcheson
Osage
Ozark
RO1581F
B
Cut at R5
Full season
No irrigation
RO1581F
Ozark
Osage
Inoculated
Non-Inoculated
Not significant
Significant
C
Hutcheson
Osage
Ozark
RO1581F
Not irrigated
Full season
Inoculated
Non-Inoculated
Not significant
Significant
Cut at R5
Full season

Figure 1. Irrigation interacted with cultivar and inoculation and significantly impacted charcoal rot severity in soybean roots as measured with the RSS severity scale. **(A)** Bars of different colors indicate the proportion of roots rated for within each severity scale, 1- absence of signs to 5- severe charcoal rot. Significance levels are shown for inoculation comparisons within cultivar and irrigation, not significant (ns), $P<0.05$ (*), and $P<0.01$ (**). **(B)** significance for contrasts of cultivars within inoculation and irrigation. **(C)** significance for contrasts of irrigation within inoculation and cultivars. Contrasts were considered significant when $P<0.05$. Analysis of variance, least square means, and contrasts were obtained with the GLIMMIX procedure in SAS 9.4. RSS severity scale was treated as ordered categorical with Multinomial distribution.

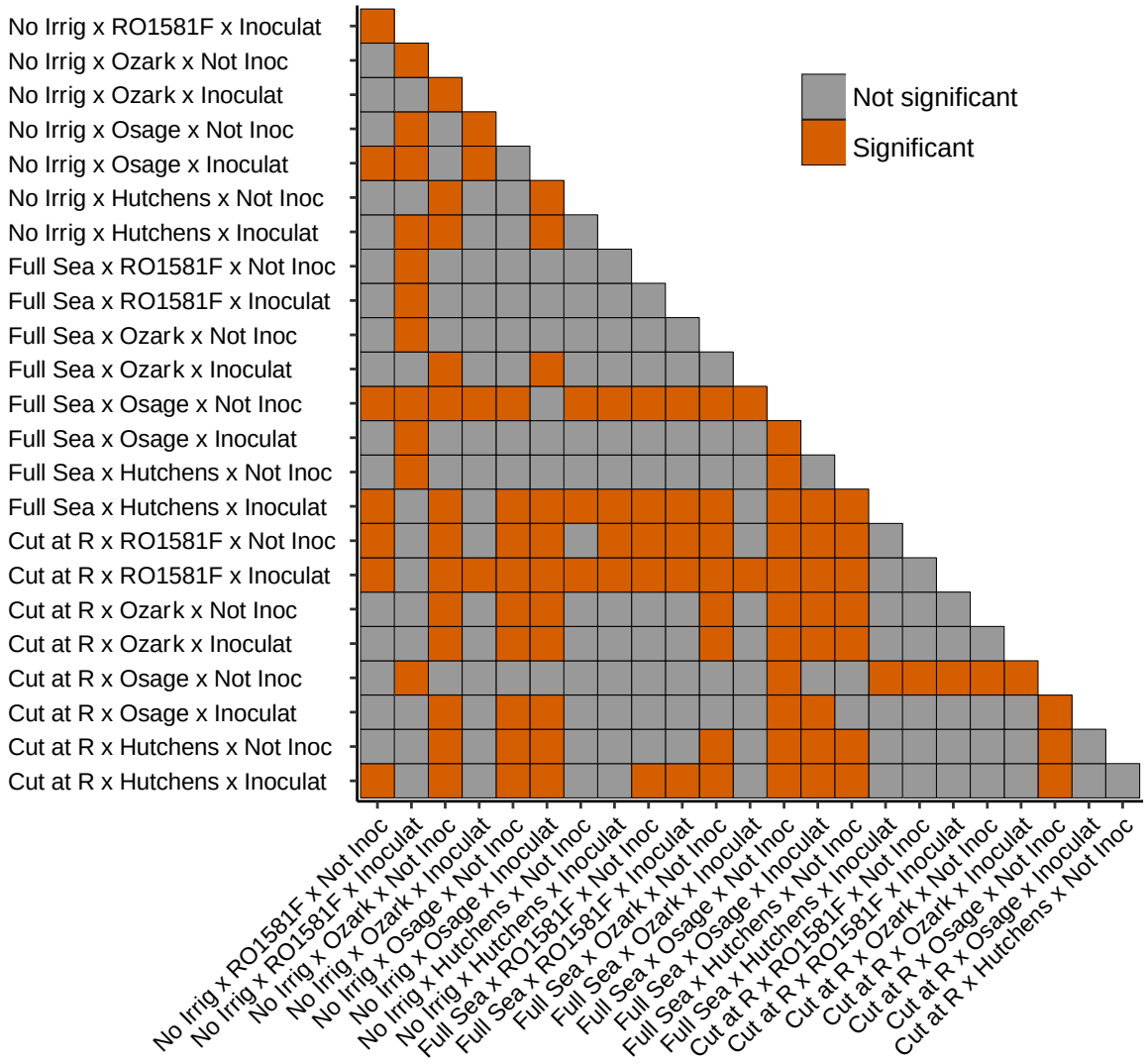

Figure 2. All contrasts from irrigation x cultivar x inoculation 3-way interaction for charcoal rot severity measured with 1-5 disease scale. Contrasts were considered significant when $P<0.05$. Analysis of variance, least squares means, and contrasts were obtained with the GLIMMIX procedure in SAS 9.4. RSS severity scale was treated as ordered categorical with Multinomial distribution.

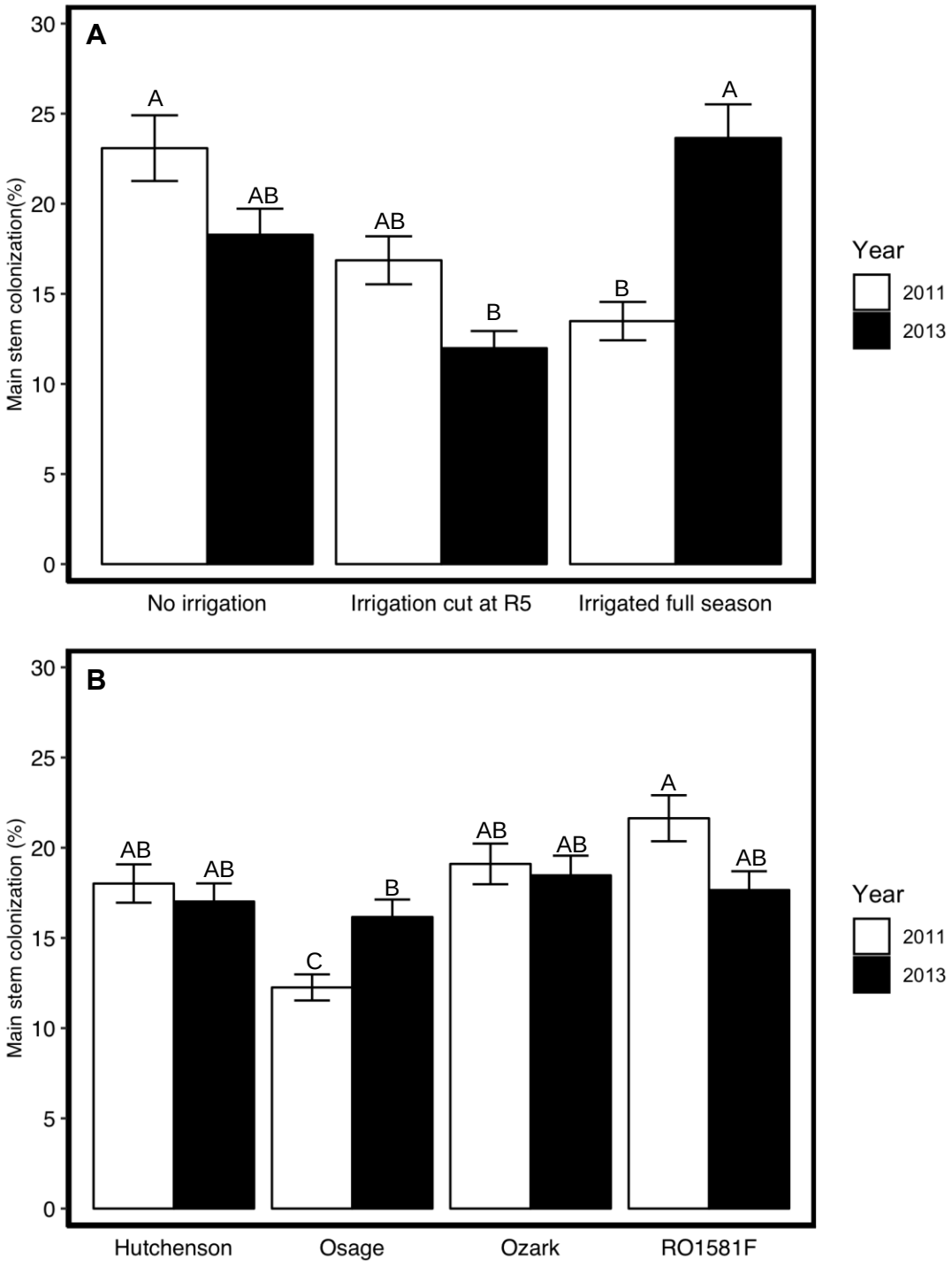

Figure 3. Proportion of main stem colonization. The proportion of main stem length colonized by *M. phaseolina* was affected by the interactions of cultivar by year and irrigation by year. Bars within each panel with different letters are significantly different ($P<0.05$) according to Tukey's range test. Error bars represent the standard error of the mean.

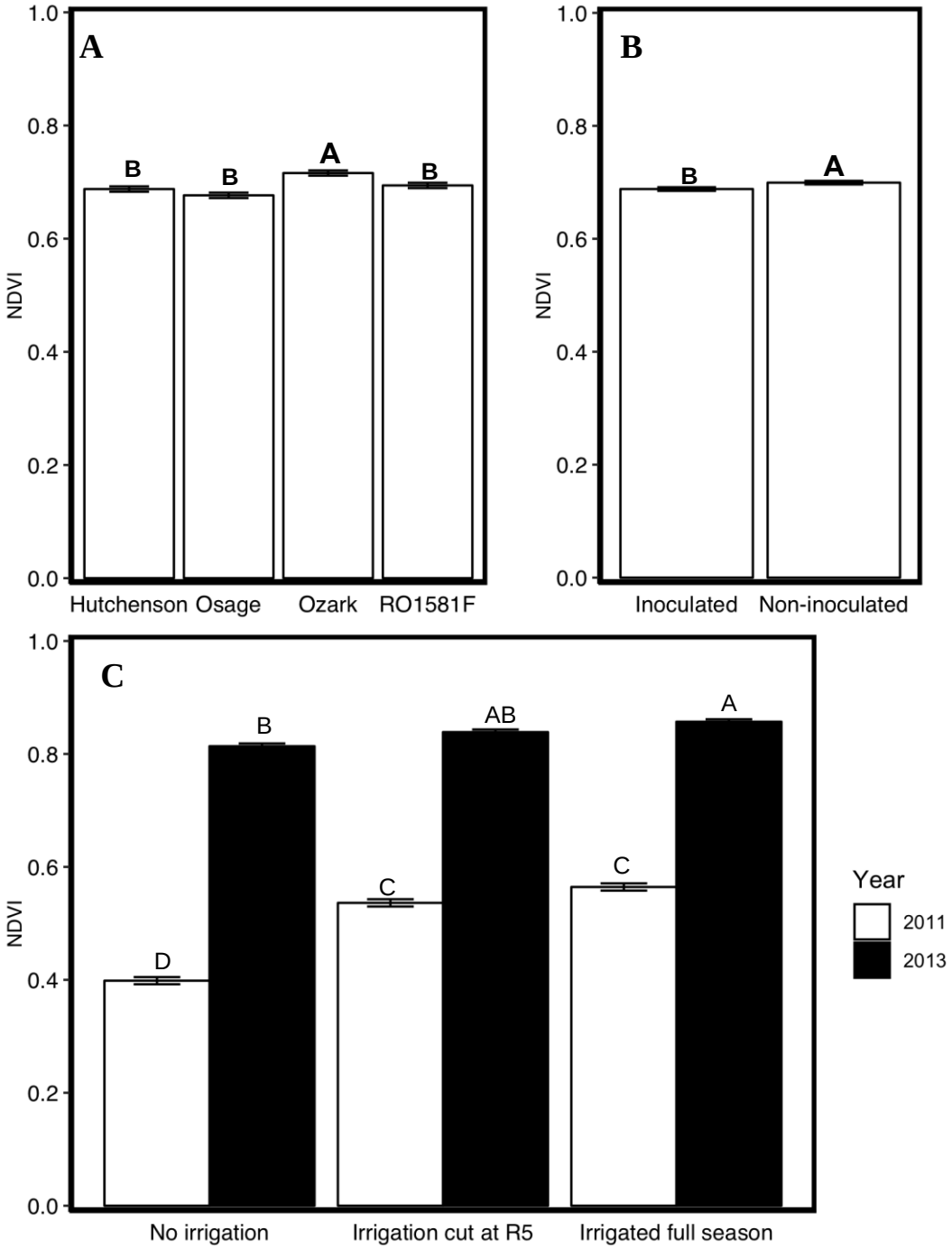

Figure 4. NDVI at R3 developmental stage reviews soybean plants were significantly more stressed in 2011 than in 2013. **(A)** Cultivar had a significant effect on NDVI measure at R3. The cultivar Ozark presented significantly higher NDVI than Hutcheson, Osage, and RO1581F. **(B)** Non-inoculated treatments had significantly higher NDVI measurements than inoculated treatments. **(C)** Plants had significantly lower NDVI in 2011 for all irrigation regimes than in 2013. Bars within each panel with different letters are significantly different (P<0.05) according to Tukey's range test. Error bars represent the standard error of the mean.

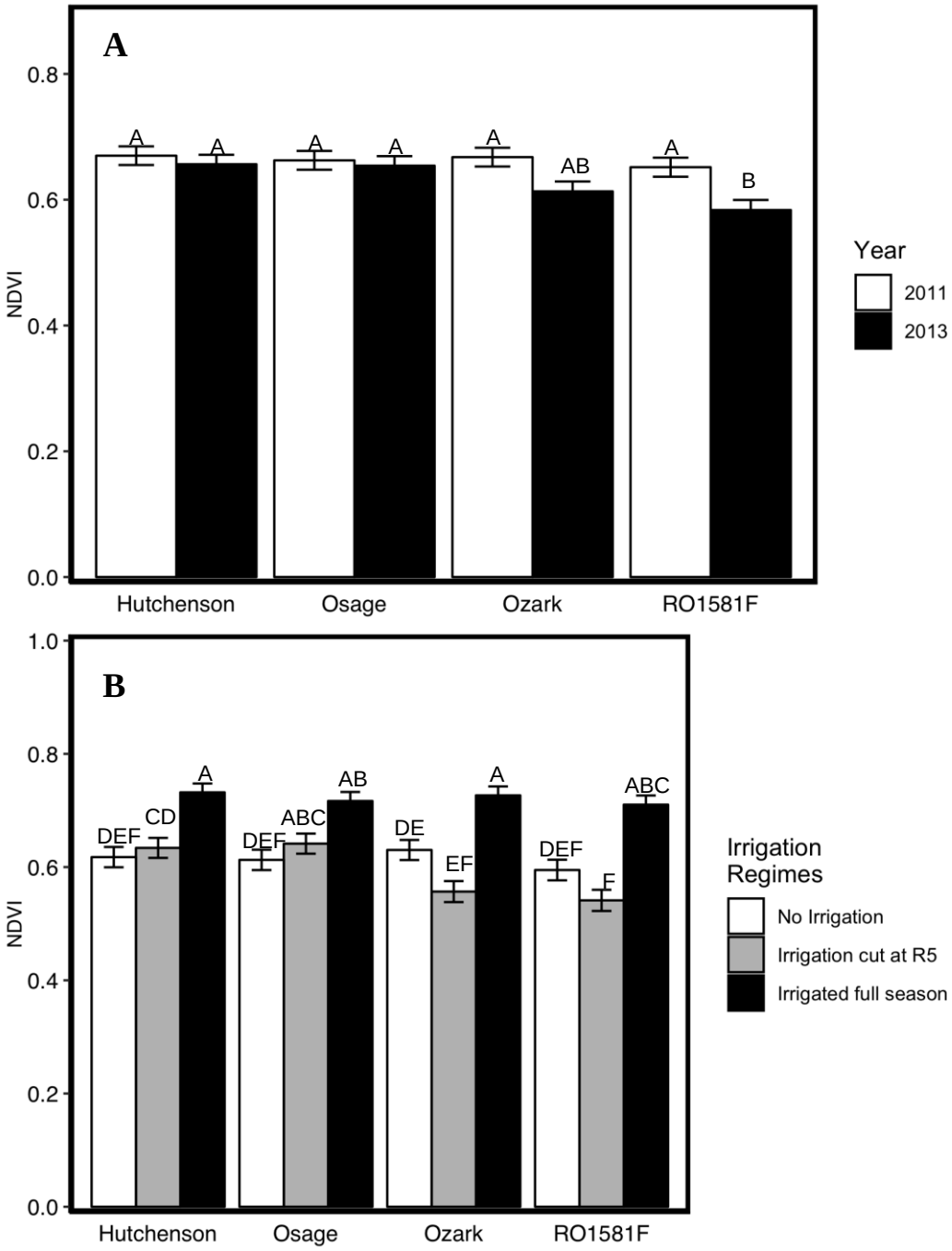

Figure 5. NDVI at R6 developmental stage. At R6, significant interactions of cultivar by year and cultivar by irrigation were observed. **(A)** RO1581F had significantly lower NDVI at 2013, all other cultivars had similar NDVI measurements in both years. **(B)** Full-season irrigation and irrigation cut at R5 presented similar NDVI measurements for the cultivar Osage. Whereas, Hutcheson, Ozark, and RO1581F presented significantly lower NDVI measurements when irrigation was cut at R5 when compared to cull season irrigation. Bars within each panel with different letters are significantly different (P<0.05) according to Tukey's range test. Error bars represent the standard error of the mean.

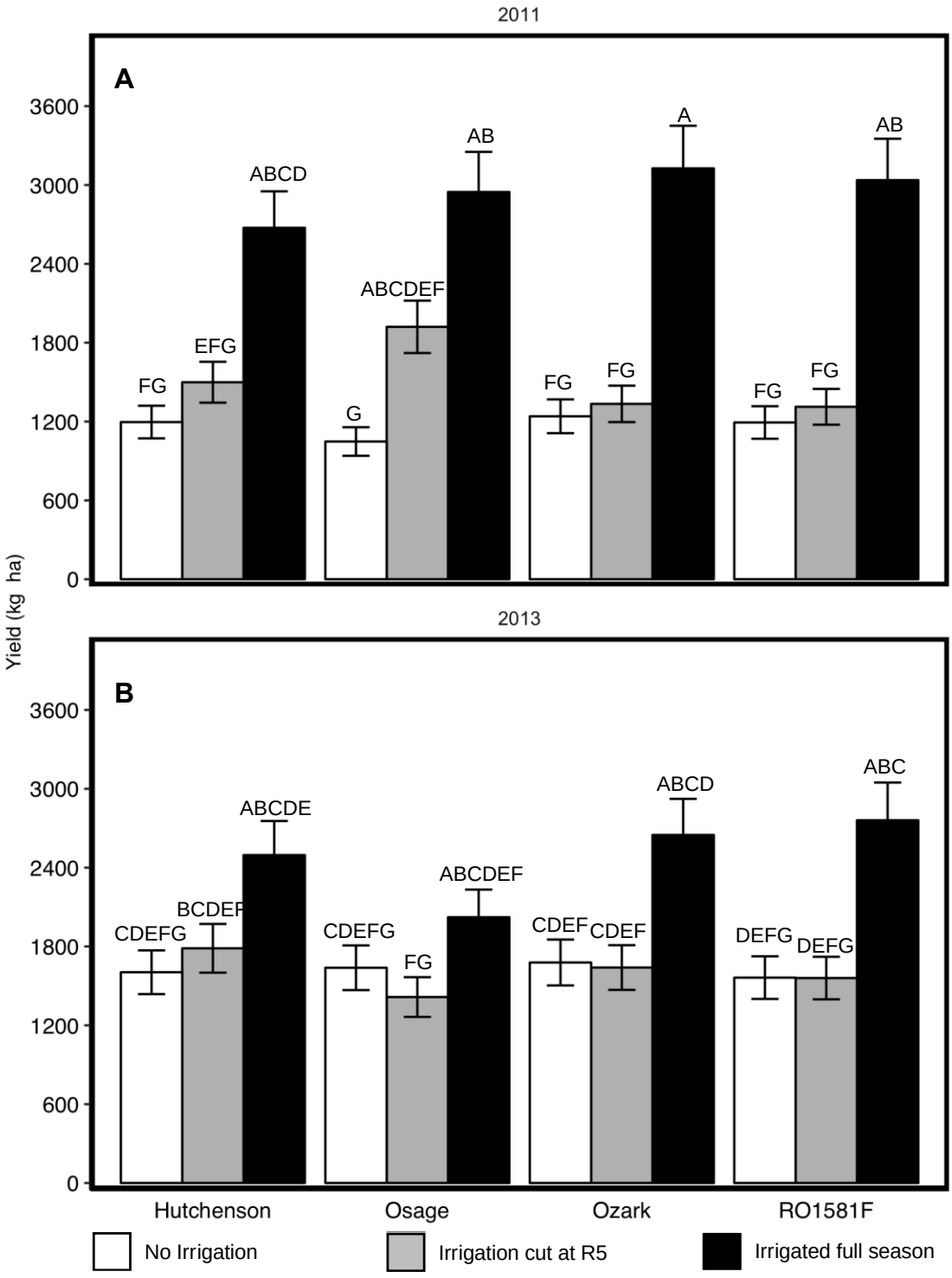

Figure 6. Effect of Irrigation, inoculation and cultivar on soybean yield. Bars within each panel with different letters are significantly different (P<0.05) according to Tukey's range test. Error bars represent the standard error of the mean.

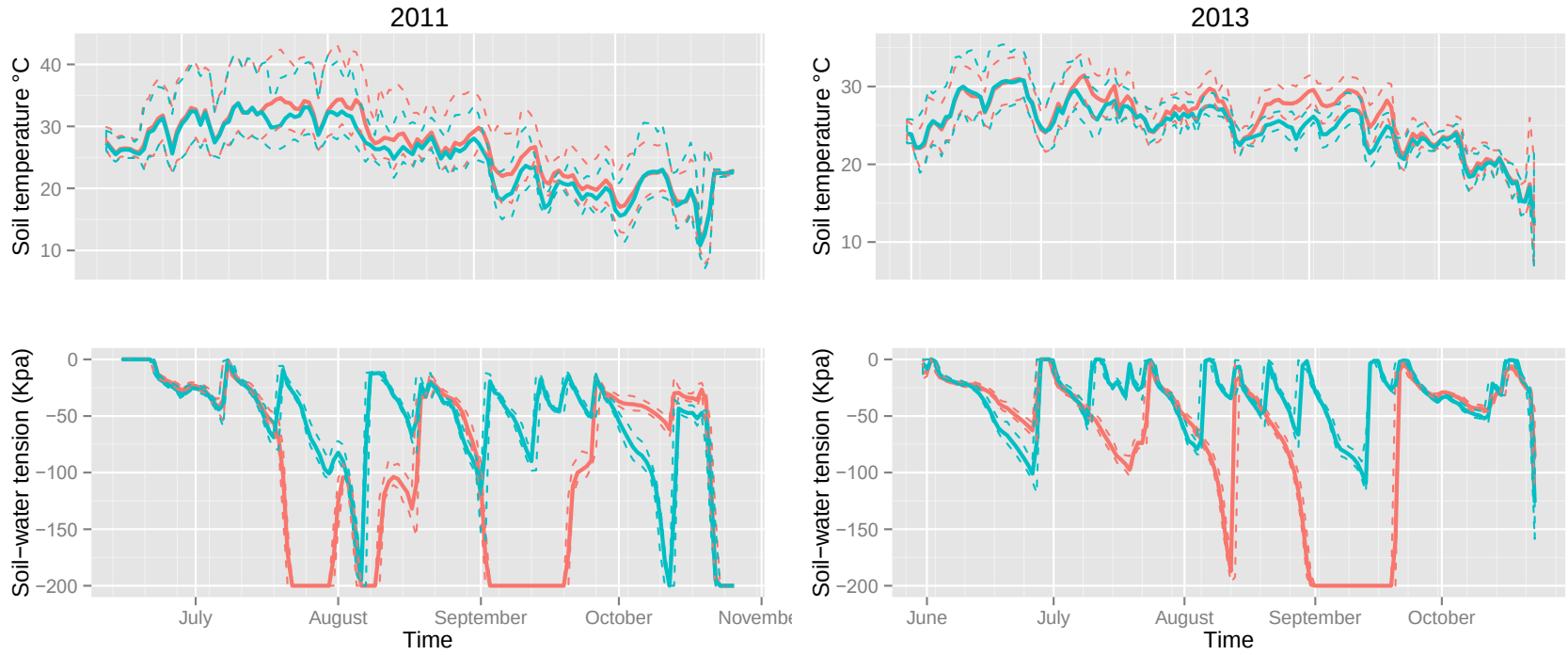

Figure 7. Soil temperature and moisture. Solid lines indicate daily mean values while dashed lines indicate daily maximum and minimum. Measurements were taken at a depth of10 cm. Sensor were 5cm offset from soybean planting row atop of a furrow bed. Blue lines are soil temperature and moisture measured in irrigated plots. Red lines are soil temperature and moisture measured in non-irrigated plots. Dashed lines around solid lines represent the daily maximum and minimum values.

Chapter III: Zone lines associated with P. longicolla alter soybean root colonization by M. phaseolina

Abstract

Charcoal rot is an economically important soybean disease caused by *M. phaseolina*. During plant senescence *M. phaseolina* produces large numbers of melanized microsclerotia in stem and root tissues that serve as primary inoculum for future epidemics. The amount of microsclerotia in soybean tap rots and the extent of stem in which they are produced are used to rate charcoal rot disease severity. Zone lines are often associated with wood decaying fungi that densely colonize a layer of three to five host cells with dark pigmented hyphae. The objectives of this study were: (I) to determine if zone lines incidence is affected by location and soybean cultivar and (II) to investigate the fungi associated with zone lines in soybean tap roots. In the growing season of 2012, a set of 18 cultivars of maturity groups (MG) II to V were grown at two locations, Rohwer and Stuttgart, AR. A second set of cultivars, 14 from MG IV and 12 from MG V, was grown in Marianna, AR. Only cultivars Osage, R01581F, and DK4866 were present at all locations. Cultivar had a significant effect on the presence of zone lines at Stuttgart (P 0.002) and at Rohwer (P<0001), where incidence ranged from 0-49% and 5-72%, respectively, but not at Marianna (P 0.519) where incidence ranged from 38-87%. Incidence was significantly higher at Rohwer than at Stuttgart (P<.0001), but there was a significant interaction between location and cultivar (P<0.001). When isolations were made from tissues enclosed by the zone lines, *P. longicolla* was isolated from 95.4% of roots while *M. phaseolina* was isolated from only 2.5% of roots and other filamentous fungi comprised 1.9% (n=368). DNA sequencing of ITS, EF-1α and β-tubulin confirmed the identity of *P. longicolla* and showed tap root isolates were indistinguishable from previously characterized seed isolates, phylogenetically. Our results

indicate that zone lines in soybean taproots associated with *P. longicolla* seem to restrict colonization of *M. phaseolina*, which could be a confounding variable when screening for charcoal rot resistance, especially since zone lines incidence seems to be affected by cultivar and location.

Introduction

The Ascomycota fungi *Macrophomina phaseolina* and *Phomopsis longicolla* are economically important soybean pathogens worldwide (Bellaloui et al. 2008; Wrather et al. 2010; Zorrilla et al. 1994). *M. phaseolina*, the causal agent of charcoal rot, is a soil born fungus that infects soybean roots early in the season then systemically colonizes the root system and basal stem (Mengistu et al. 2011). In most epidemics, soybean plants remain symptomless and no signs of the pathogen are seen until the beginning of plant senescence (Short et al. 1978; Wyllie and Calvert 1969). However, in some cases charcoal rot is reported to cause wilt and premature plant death, particularly when associated with drought stress (Hartman, et al. 1999; Mengistu et al. 2011; Navi and Yang 2008). Following the premature plant death or late senescence stages, *M. phaseolina* rapidly produces large numbers of microsclerotia in roots and stems of colonized plants (Kendig et al. 2000; Short et al. 1978). As a result, a distinct light silvery-gray to blackish discoloration is observed in dead colonized plants. Besides the characteristic discoloration, zone lines are also often seen in dead colonized tissues and have been considered a sign of charcoal rot (Romero Luna et al. 2017). However, recent studies have shown that black zone lines in stems and roots of dead or senesced soybean plants are caused by *P. longicolla* and not *M. phaseolina* (Ghissi et al. 2014; Olson et al. 2015; Vidić et al. 2013). Zone lines are layers of two to five host cells densely colonized with dark pigmented hyphae;

they are a common sign of fungi associated with wood decay (Campbell 1933; Li 1983; Robinson and Laks 2010).

P. longicolla is a soil and seed born pathogen that causes pod and stem blight and seed decay in soybean (Hobbs et al. 1985; Sinclair 1993). *P. longicolla*, alike *M. phaseolina*, is ubiquitously present in soybean production areas, has prolonged incubation periods, and produce copious amounts of structures, i.e. pycnidia, during plant senescence (Almeida et al. 2008; Short et al. 1978; Sinclair 1993; Wrather et al. 2010). *P. longicolla* can successfully overwinter in production areas in colonized plant debris and is capable of asymptomatically infecting soybean plants during vegetative and reproductive developmental stages (Roy and Abney 1988; Rupe 1990; Rupe and Ferriss 1987). Following infection, *P. longicolla* maintains an endophytic-like lifestyle for most of crop development causing no apparent symptoms nor exhibiting any signs of colonization (Rupe and Ferriss 1987). At senescence, *P. longicolla* infects seeds and under conducive environmental condition can cause severe seed decay (Baker et al. 1987). Additionally, once plants mature, *P. longicolla* produces large numbers of pycnidia on the surfaces of aerial plant parts. In particular, characteristic vertical-row alignment pattern of pycnidia are distinctively observed on soybean plants main stem (Baker et al. 1987; Hartman et al. 1999; Roy and Abney 1988).

Zone lines are macroscopic black lines seen in decaying woody plant tissues (Campbell 1933). They vary from a few millimeters to a several centimeters, straight or tortuous. In some cases, they can be observed as stand-alone lines, but more often form an enclosed shape, e.g. an ellipsoid (Li 1983; Olson et al. 2015). Zone lines are formed by intense colonization of plant material by pigmented fungal tissue and are often observed during wood decay (Lopez-Real 1975). Several species of filamentous fungi have cause zone lines including *Xylaria polymorpha*

(Robinson and Laks 2010), *Polyporus squamosus* (Campbell and Munson 1936), *Armillaria melea* (Campbell 1934), and *Phellinus weirri* (Li 1981). However, *P. longicolla* is the first species observed to cause zone lines in soybean (Olson et al. 2015). *Phomopsis spp*. causes zone lines in alfalfa (Nikandrow 1989, 1990) and elm trees (Brayford 1990; Webber 1981; Webber and Gibbs 1984). *Phomopsis spp*. isolated from elm trees produces barrage zones in culture when colony margins of genetic distinct isolates meet or are in proximity to colonies from different fungal species (Webber 1981). Zone lines in plant debris have been considered a possible survival structure and are demonstrably associated with long term viability of *Poria weirii* in soil environment (Nelson 1964).

P. longicolla causes zone lines in soybean (Olson et al. 2015). However, there has not been documentation of how prevalent this phenomenon is in field conditions. Additionally, it remains unknown if cultivar has an effect in the incidence of zone lines in soybean. This study endeavored to understand how commonly zone lines are produced in soybean tap roots and if their incidence is affected by cultivar. Additionally, field observations have suggested that signs of *M. phaseolina* seem to not be produced in taproot tissues covered by zone lines. Thus, in this study it was investigated if *M. phaseolina* colonization is restricted from soybean root tissues where zone lines are present.

Materials and methods

Plant material and *M. phaseolina* infestation. Zone lines incidence was assessed in soybean tap roots of diverse plant materials grown in multiple locations in Arkansas. A total of 41 soybean genotypes, including cultivars and advanced breeding lines, were grown in *M. phaseolina* artificially infested soil in three locations in the state of Arkansas during the growing season of 2012. The primary purpose of these tests was to compare cultivar responses to charcoal

rot. A set of 18 genotypes, of maturity groups II to V, was grown in Stuttgart and Rohwer, AR. A second set of 26 genotypes, of maturity groups IV and V, was grown in Marianna, AR. There were three genotypes present in both sets, 'Osage', 'R01581F', and 'DK4866'. A randomized complete block design was employed in all locations with four replications in the trials at Stuttgart and Rohwer, and five in the trial at Marianna. Experimental units consisted of four-row plots of 6.1 meters in length with 81 cm between rows seeded with 32 seeds m^{-1}. Before planting, soil was tilled and bedded.

All plots were artificially infested with *M. phaseolina*. Initial inoculum was produced by growing *M. phaseolina* on sterile sorghum seeds. The *M. phaseolina* soybean isolate MP-Conway was selected for having high aggressiveness (Twizeyimana et al. 2012). Inoculum was initially grown on potato dextrose agar (PDA; Becton Dickinson and Company, Franklin Lakes, NJ, USA) at room temperature for seven days. Autoclave safe bags containing one liter of dried sorghum seeds and 0.3 liter of distilled water were autoclaved twice and cooled at room temperature for two days. One Petri dish of *M. phaseolina* was sectioned into rectangles of approximate 0.5 cm^2 and added to one bag of sterilized and cooled sorghum seeds. Inoculum was periodically mixed to promote uniform colonization and incubated for 3 weeks under room temperature. After incubation, colonized sorghum seeds were air dried for five days on a wire screen in a fume hood. Once dried, inoculum was stored in paper bags at room temperature until used. The inoculum mixture was planted with the soybean seeds at a rate of 1.6 grams per meter of row.

Sample collection and processing. At the R7 reproductive stage, ten plants per plot were dug from the two outer rows of each plot and washed with running tap water for removal of debris and soil residue. Only plants with yellow or brown stems were collected. Plants were air

dried on a greenhouse bench and stems were separated from roots at the soil line and discarded. Taproots were split in half with sharp trimming shears, and the presence of zone lines was recorded for each individual root by visual examination. A dissecting scope was used to confirm the presence of small zone lines when necessary. Roots were cleaned and disinfested before further processing. The split taproots were washed in running tap water for 5 minutes for removal of remaining soil particles and contaminating debris. Then, clean roots were surface disinfested by submergence in 0.5% sodium hypochlorite for two minutes, blotted dry with sterile paper towels, and air dried at room temperature for 24 hours. Roots were stored in paper bags at room temperature until isolations could be performed.

Isolations were made from roots selected from a single replication for each location. First, a single experimental block from each experiment was randomly chosen. Roots with zone lines large enough to be dissected, at least 5mm in dimensions, were selected to undergo isolation. Isolations were performed on one half of each longitudinally-split tap root, while the other was discarded. A sharp sterile knife was used to remove a thin layer (2 to 3 mm) of tissue from atop the root site to be sampled for isolation. The knife was sterilized with 70% ethanol and flamed between every root. Tissue specimen of approximately 2 to 4 mm^2 were cut and removed from sampled tap root with a sharp scalpel. From every sampled tap root, two specimens were collected from the following sites:1) the center of a zone line, 2) tissue often of light-yellow discoloration enclosed by zone lines, 3) the black lines themselves, and tissue 2 to 4 mm outside the zone lines **(Fig. 1)**. Isolations were carried out under aseptic conditions in a laminar-flow cabinet with the aid of a dissecting scope. Specimens from each root site were plated equidistantly on a Petri dish containing PDA and incubated at room temperature. After ten days, plates were visually assayed for the presence of *M. phaseolina* and *P. longicolla*. Notes on the

presence of *Fusarium spp*. and other unidentified filamentous fungi also were taken. In total, isolations were made from 368 soybean tap roots with zone lines. During isolations, soybean tap roots were classified as having 1) no visible *M. phaseolina* microsclerotia, 2) having microsclerotia further than 0.5 cm from zone lines, or 3) having visible microsclerotia adjacent to the zone line sampled.

Identification of *P. longicolla*. DNA sequencing of house-keeping loci was used to confirm morphological identification of selected *P. longicolla* isolates. Two sets of 14 *P. longicolla* isolates were selected from isolates recovered from either root tissues within the zone lines or from tissues outside the zone lines. Three commonly used barcoding loci for phylogenetic studies in filamentous fungi, including population studies in *Phomopsis*/*Diaporthe* were chosen and amplified on selected isolates. Strains were single spored and grown on potato dextrose broth (PDB; Becton Dickinson and Company, Franklin Lakes, NJ, USA) incubated at room temperature in the dark. After five days, tissue was harvested and DNA extracted via cetyl trimethylammonium bromide (CTAB) method as described (Li et al. 2013). PCR amplification of internal transcribed spacer (ITS), elongation factor 1α, and β-tubulin was done with primers and conditions described in identifying *Phomopsis spp*. (Table 1; Udayanga et al. 2012). Forward and reverse sequencing of amplicons were obtained from Genewiz (South Plainfield, NJ, USA) via Sanger method. Sequences were converted to fastq format with the SeqIO.parse function from Biopython v1.70 (Cock et al. 2009) and trimmed with trimfq from seqtk v1.0-r68 (https://github.com/lh3/seqtk, accessed: March 2019) using error rate threshold of 0.05. Forward and reverse sequences were assembled with CAP3 version 02/10/15 (Huang and Madan 1999). Sequences were aligned with MAFFT v7.407 (Katoh and Standley 2013) with parameters --localpair and --maxiterate 1000. The alignments were visualized and their ends were manually

trimmed with Jalview v2.10.4 (Waterhouse et al. 2009). The alignments were concatenated and a maximum likelihood phylogenetic tree was inferred with RAxML v8.2.11 (Stamatakis 2014) with settings adjusted for 100 rapid bootstrap replicates and GTRGAMMA as the nucleotide substitution model. The tree was visualized and exported with FigTree v1.4.3 (http://tree.bio.ed.ac.uk/software/figtree/, accessed: March 2019). Nucleotide sequences of other *Diaporthe* species were obtained from GenBank using the ncbi-acc-download script (https://github.com/kblin/ncbi-genome-download, accessed: March 2019) based on the accession numbers provided in other studies (Gomes et al. 2013; Udayanga et al. 2012). Nucleotide sequences of *Stenocarpella maydis* A1-1 was obtained by homology searches performed with BLASTn (Altschul et al. 1997) against its genome assembly (GenBak accession GCA_002270565.1; Zaccaron et al. 2017).

Statistical analysis. Incidence of zone lines was statistically analyzed with SAS 9.4. Analysis of variance was performed with the GLIMMIX procedure assuming binomial distribution for the presence of zone lines and a logit link function option. The Stuttgart and Rohwer locations were analyzed together with location as a fixed effect. The dataset generated by isolations of fungi from soybean roots was zero-inflated, precluding parametric statistical analyzes.

Results

Zone line incidence. Zone lines were observed in 48.14 % of the 2740 senesced soybean tap roots examined. For the 18 cultivars grown at Rohwer and Stuttgart, there were significant location and cultivar main effects and a significant location by cultivar interaction (Table 2). The incidence of zone lines was significantly higher ($P<.0001$) at Rohwer (44%) than at Stuttgart (17%). The range in incidences ranged from 5 to 72% and 0 to 49% at Rohwer and Stuttgart, respectively (Table 3). Some cultivars had similar incidences of zone lines between the locations

such as Osage, R01581F, JTN-5208, and Jack. Others like Pharaoh, EXP2XC3810, and Spencer, had significantly higher incidences at Rohwer than at Stuttgart. There was a high incidence of zone lines at Marianna (67.62%) ranging from 38 to 87% (Table 4). There were no significant differences among cultivars. The tests had three cultivars in common: Osage, R01581F, and DK4866. Incidences for Osage were 67,44, and 73%, for R01581F were 49, 49, and 38%, and for DK4866 were 71, 11, and 73% at Rohwer, Stuttgart, and Marianna, respectively (Tables 3 and 4).

Zone line isolations. The predominate fungi isolated in association with the zone lines were *P. lonogicolla* and *M. phaseolina* with recovery rates of 75.2% and 18.4%, respectively. Meanwhile, other filamentous fungi were isolated at a rate of 9.9%, reaching 21% when tissues outside the zone lines were sampled. More than half of roots where other fungi were isolated, it was a *Fusarium* spp. (58%). The isolation of *P. longicolla* was particularly frequent for isolations taken from the line or the tissue enclosed by the line with rates of 91.6 and 95.2%, respectively **(Fig. 2)**. When signs of charcoal rot were seen adjacent to the zone lines, *M. phaseolina* was isolated from tissues enclosed by zone lines at a rate of 3.9%. In the outer tissue (tissue not enclosed by the zone line), *P. longicolla* was still the predominate species isolated when *M. phaseolina* was either present, but not up to the line or not visibly present recovered at a rate of 41.2 and 64.5, respectively. *M. phaseolina* was the predominate fungus (93.8%) isolated from the outer tissue when *M. phaseolina* was visibly present up to the line. Other fungi were a minor component of the isolations, but were most frequent in the outer tissue when *M. phaseolina* was not visibly present (28.7). The incidences of other fungi from the enclosed tissue was very small (1.2%).

Identification of *P. longicolla* associated with zone lines. Isolates of *P. longicolla* were identified based on culture morphology and alpha conidia. Sequencing the ITS and the EF1-α, and β-tubulin genes, 28 randomly selected isolates identified as *P. longicolla*. When these sequences, along with published sequences of other fungi, were used to construct a phylogenetic tree, all of the 28 isolates clustered with the *P. longicolla* type-strains TWH_P74 (Li et al. 2015) and other *P. longicolla* strains isolated from soybean seeds previously described (Gomes et al. 2013; Udayanga et al. 2012). These isolates were distinct from other similar fungi associated with soybean: *Diaporthe phaseolorum, D. sojae*, and *D. aspalathi* **(Fig. 3)**.

Discussion

Zone lines in soybean roots are associated with *P. longicolla*. Our findings strongly support *P. longicolla* as zone lines causal agent in soybean roots, as previously reported (Ghissi et al. 2014; Olson et al. 2015). *P. longicolla* was isolated almost exclusively from soybean taproot tissues enclosed by zone lines from plants of multiple locations and cultivars. *Phomopsis* species have been known to produce zone lines in taxonomically diverse plants, including areca palm (Saccardo, 1913), alfalfa (Nikandrow 1989), and elm trees (Webber and Gibbs 1984). The function of such zone lines and their impact on Phomopsis spp. fitness remains unknown. However, zone lines caused wood decaying fungi have been associated with increased survivability in soil (Nelson 1964).

Cultivar and location had strong effect on the incidence of zone lines. Zone lines were observed in some degree in every one of the 41 soybean genotypes assayed. However, soybean genotype was found to significantly impact incidence of zone lines. These findings suggest the expression of zone lines in soybean may be, at least in part, quantitatively and genetically controlled. *Phomopsis spp.* production of zone lines has been linked to response to the proximity

of a colony of a genetically different filamentous fungus, including members of the same species. Thus, a possible host genetic control of zone lines incidence in soybean may not related exclusively to soybean resistance to root colonization by *P. longicolla*. Thus, zone lines incidence may be affected by soybean susceptibility to infection by other filamentous fungi. Additionally, the location where cultivars were grown significantly change their level of zone lines incidence, indicating environmental conditions, the difference in microbial community, or their interplay may play a role in zone lines development in soybean. It remains unclear if soybean root colonization by *Phomopsis longicolla* and later formation of zone lines have an impact on crop performance. Similarly, zone lines interplay with root-colonizing pathogens and their diseases remain unknown.

Zone lines restricted soybean root colonization by *M. phaseolina*. Virtually no signs of *M. phaseolina* were observed in soybean root tissues enclosed by zone lines. Additionally, *M. phaseolina* was isolated from these tissues in very low levels, even when collected from roots with severe charcoal rot. The mechanism by which employed by *P. longicolla* to suppress *M. phaseolina* root colonization is not known. However, multiple metabolites with antimicrobial properties have been identified in *Phomopsis spp*., including *P. longicolla* (Ahmed et al. 2011; Choi et al. 2013; Corrado and Rodrigues 2004; Horn et al. 1995). The recently published *P. longicolla* draft genome shows it possesses one of the largest set of genes involved in the production of secondary metabolites among sequenced fungi to date. The secretion of antimicrobial metabolites could explain *M. phaseolina* growth restriction observed in soybean taproots, although such interaction has not been observed in growth media. *Phomopsis sp*. zone lines has been show to act as biocontrol to scolytid beetles, vectors of *Ceratocystis ulmi*, causal agent of Dutch elm disease (Webber 1981). When beetles breeding galleries overlapped with

zone lines, it was observed a severe decrease in numbers and fitness of beetle offspring, reducing their vectoring ability. Thus, supporting the presence of a level of biotoxicity present in *Phomopsis spp*. zone lines.

Zone lines and root colonization by *P. longicolla* should be further studied and considered during epidemiological and resistance screening studies. The present work shows *Phomopsis longicolla* zone lines incidence may be genetically controlled by the host and impact root colonization by *M. phaseolina*. It is unclear if the charcoal rot impact on soybean yield is affected by zone lines. However, this work suggests that zone lines could be a confounding factor when assessing charcoal rot severity in soybean by currently used methods. In particular, methods using CFU quantification. It is unclear if zone lines or root colonization by *Phomopsis longicolla* impacts the presence of other filamentous fungi in soybean roots, either pathogens or growth promoting. Together, this work brings to light the importance of considering zone lines caused by *P. longicolla* when assessing for root diseases resistance or evaluating disease management practices.

Literature cited

Ahmed, I., Hussain, H., Schulz, B., Draeger, S., Padula, D., Pescitelli, G., van Ree, T., and Krohn, K. 2011. Three New Antimicrobial Metabolites from the Endophytic Fungus *Phomopsis* sp. Eur. J. Org. Chem. 2011:2867–2873

Almeida, Á. M. R., Sosa-Gomez, D. R., Binneck, E., Marin, S. R. R., Zucchi, M. I., Abdelnoor, R. V., and Souto, E. R. 2008. Effect of crop rotation on specialization and genetic diversity of *Macrophomina phaseolina*. Tropical Plant Pathology. 33:257–264

Altschul, S. F., Madden, T. L., Schäffer, A. A., Zhang, J., Zhang, Z., Miller, W., and Lipman, D. J. 1997. Gapped BLAST and PSI-BLAST: a new generation of protein database search programs. Nucleic Acids Res. 25:3389–3402

Baker, D. M., Minor, H. C., Brown, M. F., and Brown, E. A. 1987. Infection of immature soybean pods and seeds by *Phomopsis longicolla*. Can. J. Microbiol. 33:797–801

Bellaloui, N., Mengistu, A., and Paris, R. L. 2008. Soybean seed composition in cultivars differing in resistance to charcoal rot (*Macrophomina phaseolina*). Journal of Agricultural Science. 146:667–675

Brayford, D. 1990. Vegetative incompatibility in *Phomopsis* from elm. Mycological Research. 94:745–752

Campbell, A. H. 1933. Zone lines in plant tissues I. The black lines formed by *Xylaria polymorpha* (pers.) Grev. Ln hardwoods. Annals of Applied Biology. 20:123–145

Campbell, A. H. 1934. Zone Lines in Plant Tissues: II. The Black Lines Formed by *Armillaria mellea* (Vahl) Quel. Annals of Applied Biology. 21:1–22

Campbell, A. H., and Munson, R. G. 1936. Zone lines in plant tissues. III. The black lines formed by *Polyporus squamosus* (Huds.) Fr. Annals of Applied Biology. 23:453–464

Choi, J. N., Kim, J., Ponnusamy, K., Lim, C., Kim, J. G., Muthaiya, M. J., and Lee, C. H. 2013. Identification of a new phomoxanthone antibiotic from Phomopsis longicolla and its antimicrobial correlation with other metabolites during fermentation. The Journal of Antibiotics. 66:231

Cock, P. J. A., Antao, T., Chang, J. T., Chapman, B. A., Cox, C. J., Dalke, A., Friedberg, I., Hamelryck, T., Kauff, F., Wilczynski, B., and de Hoon, M. J. L. 2009. Biopython: freely available Python tools for computational molecular biology and bioinformatics. Bioinformatics. 25:1422–1423

Corrado, M., and Rodrigues, K. F. 2004. Antimicrobial evaluation of fungal extracts produced by endophytic strains of *Phomopsis* sp. J. Basic Microbiol. 44:157–160

Ghissi, V. C., Reis, E. M., and Deuner, C. C. 2014. Etiology of phomopsis root rot in soybean. Summa Phytopathologica. 40:270–272

Gomes, R. R., Glienke, C., Videira, S. I. R., Lombard, L., Groenewald, J. Z., and Crous, P. W. 2013. *Diaporthe*: a genus of endophytic, saprobic and plant pathogenic fungi. Persoonia. 31:1–41

Hartman, G. L., Sinclair, J. B., and Rupe, J. C., eds. 1999. *Compendium of soybean diseases*. Fourth Edition. American Phytopathological Society (APS Press), St. Paul.

Hobbs, T. W., Schmitthenner, A. F., and Kuter, G. A. 1985. A New *Phomopsis* Species from Soybean. Mycologia. 77:535

Horn, W. S., Simmonds, M. S. J., Schwartz, R. E., and Blaney, W. M. 1995. Phomopsichalasin, a novel antimicrobial agent from an endophytic *Phomopsis* sp. Tetrahedron. 51:3969–3978

Huang, X., and Madan, A. 1999. CAP3: A DNA sequence assembly program. Genome Res. 9:868–877

Katoh, K., and Standley, D. M. 2013. MAFFT multiple sequence alignment software version 7: improvements in performance and usability. Mol. Biol. Evol. 30:772–780

Kendig, S. R., Rupe, J. C., and Scott, H. D. 2000. Effect of Irrigation and Soil Water Stress on Densities of *Macrophomina phaseolina* in Soil and Roots of Two Soybean Cultivars. Plant Disease. 84:895–900

Li, C. Y. 1983. Melanin-like Pigment in Zone Lines of *Phellinus weirii*-Colonized Wood. Mycologia. 75:562

Li, C. Y. 1981. Phenoloxidase and Peroxidase Activities in Zone Lines of *Phellinus weirii*. Mycologia. 73:811

Li, S., Ridenour, J. B., Kim, H., Hirsch, R. L., Rupe, J. C., and Bluhm, B. H. 2013. Agrobacterium tumefaciens-mediated transformation of the soybean pathogen *Phomopsis longicolla*. Journal of Microbiological Methods. 92:244–245

Li, S., Song, Q., Ji, P., and Cregan, P. 2015. Draft Genome Sequence of Phomopsis longicolla Type Strain TWH P74, a Fungus Causing Phomopsis Seed Decay in Soybean. Genome Announc. 3

Lopez-Real, J. M. 1975. Formation of pseudosclerotia (‘zone lines’) in wood decayed by *Armillaria mellea* and *Stereum hirsutum*: I. Morphological aspects. Transactions of the British Mycological Society. 64:465-IN7

Mengistu, A., Smith, J. R., Ray, J. D., and Bellaloui, N. 2011. Seasonal progress of charcoal rot and its impact on soybean productivity. Plant Disease. 95:1159–1166

Navi, S. S., and Yang, X. B. 2008. Foliar symptom expression in association with early infection and xylem colonization by *Fusarium virguliforme* (formerly *F. solani* f. sp. *glycines*), the causal agent of soybean sudden death syndrome. Plant Health Progress. :0222–01

Nelson, E. E. 1964. Some probable relationships of soil fungi and zone lines to survival of *Poria weirii* in buried wood blocks. Phytopathology. 54:120–121

Nikandrow, A. 1990. Acrocalymma medicaginis and *Phomopsis* sp. as Causal Agents of Crown Rot of Lucerne in Australia. Journal of Phytopathology. 130:24–36

Nikandrow, A. 1989. Zone lines diagnostic of *Phomopsis* sp. in lucerne crown rot. Australasian Plant Pathology. 18:86–89

Olson, T. R., Gebreil, A., Micijevic, A., Wise, K. A., Mueller, D. S., Chilvers, M. I., and Mathew, F. M. 2015. Association of *Diaporthe longicolla* with Black Zone Lines on Mature Soybean Plants. Plant Health Progress.

Robinson, S. C., and Laks, P. E. 2010. Wood Species and Culture Age Affect Zone Line Production of *Xylaria polymorpha*. Open Mycology Journal. 4:18–21

Romero Luna, M. P., Mueller, D., Mengistu, A., Singh, A. K., Hartman, G. L., and Wise, K. A. 2017. Advancing Our Understanding of Charcoal Rot in Soybeans. J Integr Pest Manag. 8

Roy, K. W., and Abney, T. S. 1988. Colonization of pods and infection of seeds by *Phomopsis longicolla* in susceptible and resistant soybean lines inoculated in the greenhouse. Canadian Journal of Plant Pathology. 10:317–320

Rupe, J. C. 1990. Effect of temperature on the rate of infection of soybean seedlings by *Phomopsis longicolla*. Canadian Journal of Plant Pathology. 12:43–47

Rupe, J., and Ferriss, R. 1987. A Model for Predicting the Effects of Microclimate on Infection of Soybean by *Phomopsis longicolla*. Phytopathology. 77:1162–1166

Saccardo, P.A. 1913. Notae mycologicae. Series XV. Fungi ex Gallia, Germania, Italia, Melita (Malta), Mexico, India, Japonia. Ann. mycol. 11:14–21

Short, G. E., Wyllie, T. D., and Ammon, V. D. 1978. Quantitative enumeration of *Macrophomina phaseolina* in soybean tissues. Phytopathology. 68:736–741

Sinclair, J. B. 1993. Phomopsis Seed Decay of Soybeans- A Prototype for Studying Seed Disease. Plant Disease. 77:329

Stamatakis, A. 2014. RAxML version 8: a tool for phylogenetic analysis and post-analysis of large phylogenies. Bioinformatics. 30:1312–1313

Twizeyimana, M., Hill, C. B., Pawlowski, M., Paul, C., and Hartman, G. L. 2012. A Cut-Stem Inoculation Technique to Evaluate Soybean for Resistance to *Macrophomina phaseolina*. Plant Disease. 96:1210–1215

Udayanga, D., Liu, X., Crous, P. W., McKenzie, E. H. C., Chukeatirote, E., and Hyde, K. D. 2012. A multi-locus phylogenetic evaluation of *Diaporthe* (*Phomopsis*). Fungal Diversity. 56:157–171

Vidić, M., Petrović, K., Đorđević, V., and Riccioni, L. 2013. Occurrence of *Phomopsis longicolla* β Conidia in Naturally Infected Soybean. J Phytopathol. 161:470–477

Waterhouse, A. M., Procter, J. B., Martin, D. M. A., Clamp, M., and Barton, G. J. 2009. Jalview Version 2--a multiple sequence alignment editor and analysis workbench. Bioinformatics. 25:1189–1191

Webber, J. 1981. A natural biological control of Dutch elm disease. Nature. 292:449–451

Webber, J. F., and Gibbs, J. N. 1984. Colonization of elm bark by *Phomopsis oblonga*. Transactions of the British Mycological Society. 82:348–352

Wrather, A., Shannon, G., Balardin, R., Carregal, L., Escobar, R., Gupta, G. K., Ma, Z., Morel, W., Ploper, D., and Tenuta, A. 2010. Effect of diseases on soybean yield in the top eight producing countries in 2006. Plant Health Progress.

Wyllie, T. D., and Calvert, O. H. 1969. Effect of flower removal and pod set on formation of sclerotia and infection of *Glycine max* by *Macrophomina phaseoli*. Phytopathology. 59:1243–1245

Zaccaron, A. Z., Woloshuk, C. P., and Bluhm, B. H. 2017. Comparative genomics of maize ear rot pathogens reveals expansion of carbohydrate-active enzymes and secondary metabolism backbone genes in *Stenocarpella maydis*. Fungal Biology. 121:966–983

Zorrilla, G., Knapp, A. D., and McGee, D. C. 1994. Severity of Phomopsis Seed Decay, Seed Quality Evaluation, and Field Performance of Soybean. Crop Science. 34:172

Tables

Table 1. Primers used to amplify the loci for phylogenetic analysis (Udayanga et al. 2012).

Locus	Primer	Sequence
ITS	ITS1	CTTGGTCATTTAGAGGAAGTAA
	ITS4	TCCTCCGCTTATTGATATGC
CAL	CAL228F	GAGTTCAAGGAGGCCTTCTCCC
	CAL737R	CATCTTTCTGCCCATCATGG
EF-1α	EF1-728F	CATCGAGAAGTTCGAGAAGG
	EF1-986R	TACTTCAAGGAACCCTTACC
β-tubulin	Bt2a	GGTAACCAAATCGGTGCTGCTTTC
	Bt2b	ACCCTCAGTGTAGTGACCCTTGGC

Table 2. Analysis of variance for incidence of zone lines in soybean roots during the growing season of 2013.

Location	Effect	Num DF	Den DF	F Value	*P*
Rohwer and Stuttgart	Location	1	11.13	51.1	<.0001
	Cultivar	17	69.69	1.46	0.155
	Location*Cultivar	8	75.9	3.73	0.001
Mariana	Cultivar	25	84.86	1.48	0.0976

Table 3. Incidence of zone lines in soybean cultivars grown at Rohwer and Stuttgart, AR during the growing season of 2012. Significant groupings were adjusted by Tukey-Kramer test at significance level of *P*=0.05. Location was treated as a fixed effect, enabling comparisons of cultivars across both locations.

Cultivar	MG	Estimate			
		Rohwer		Stuttgart	
Jack	II	5	C	0	C
K07-1544	III	17	BC	0	C
NKBrandS39-A3	III	13	BC	0	C
Exp2_XC3810	Late III	71	A	2	C
Exp1_Stine39LA02	Late III	14	BC	14	BC
Pharaoh	Early IV	72	A	5	C
Spencer	Early IV	64	AB	8	C
DT97-4290	IV	34	B	2	C
JTN-4307	IV	14	BC	21	BC
DK4866	Late IV	71	A	11	BC
LS980358	Late IV	62	AB	12	BC
CPL-RC5007	V	71	A	28	BC
Osage	V	67	AB	44	AB
R01581F	V	49	AB	49	AB
JTN-5208	V	44	AB	45	AB
JTN-5308	V	42	AB	19	BC
MorsoyRT5388N	V	40	B	34	B
CPL-RC5663	V	36	B	21	BC

Table 4. Incidence of zone lines in soybean cultivars grown at Marianna, AR during the growing season of 2013. Cultivar did not explain significant variations in zone line incidence.

Cultivar	MG	Incidence (%)	Standard error
HBK4924	IV	81	7.07
DG4880	IV	79	7.49
R04_122	IV	79	7.38
DG4925	IV	78	7.72
Progeny4510	IV	76	8.24
DG4765	IV	75	8.41
DK4866	IV	73	8.99
R05_4114	IV	71	9.05
Progeny4710	IV	71	9.05
DG4755	IV	65	9.90
DG4825	IV	64	9.98
P94Y81	IV	61	10.36
P94Y70	IV	61	10.18
DG4670	IV	54	10.73
Ozark	V	87	5.55
R04_572	V	78	7.83
R05_235	V	75	8.29
DG5475	V	74	8.53
Osage	V	73	8.77
Progeny5210	V	72	8.84
DG5565	V	67	9.50
RO1_416F	V	67	9.61
R06_4433	V	59	10.33
DG5175	V	59	10.41
DG5625	V	52	10.79
R01581F	V	38	10.19

Figures

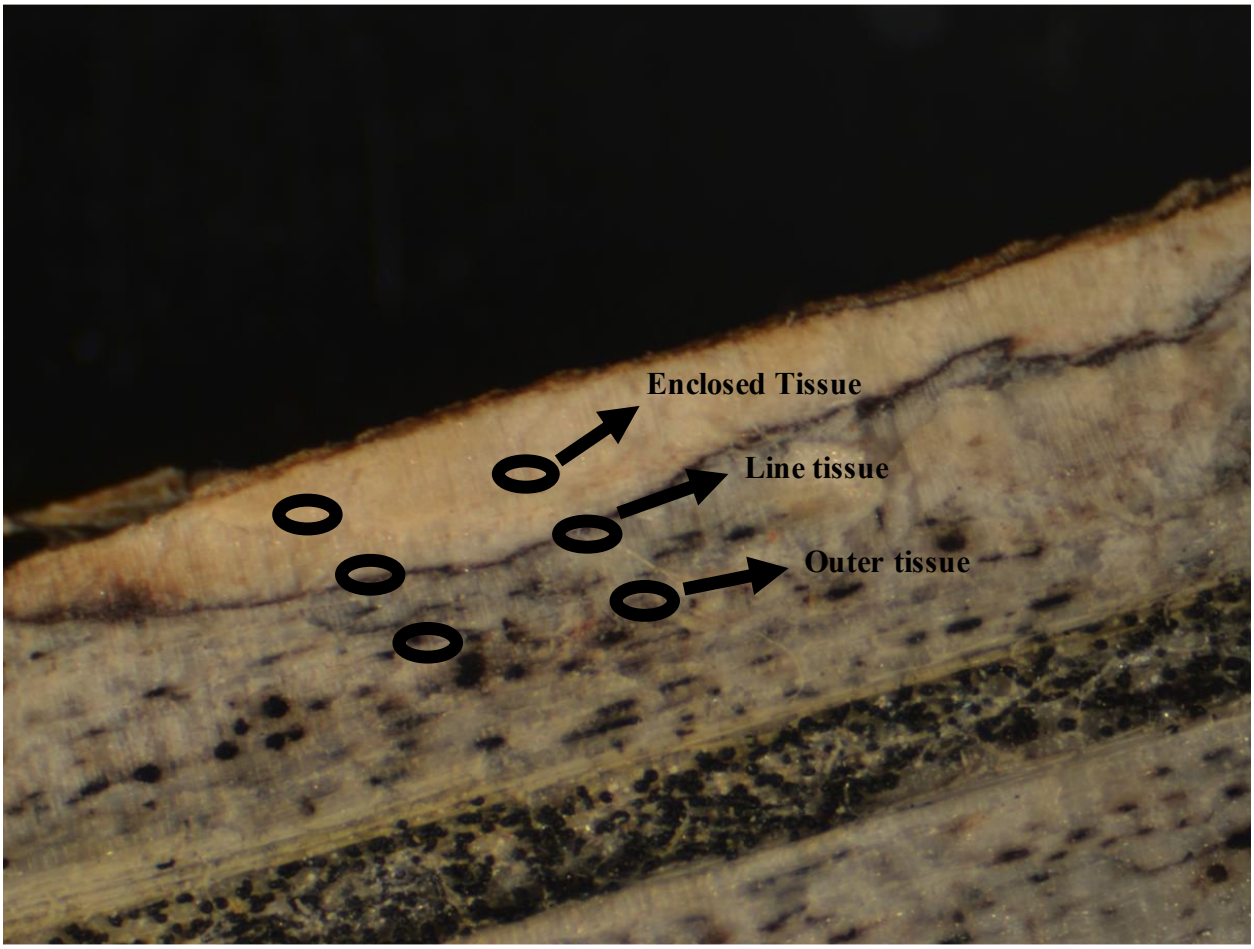

Figure 1. Signs of zone lines in soybean roots in the presence of charcoal rot and isolation location on a root specimen. Zone lines can be seen restricting the presence of microsclerotia, signs of *M. phaseolina* colonization, on a soybean taproot tissues enclosed by zone lines. The ellipses illustrate the three different sampling sites where tissue was taken for isolations.

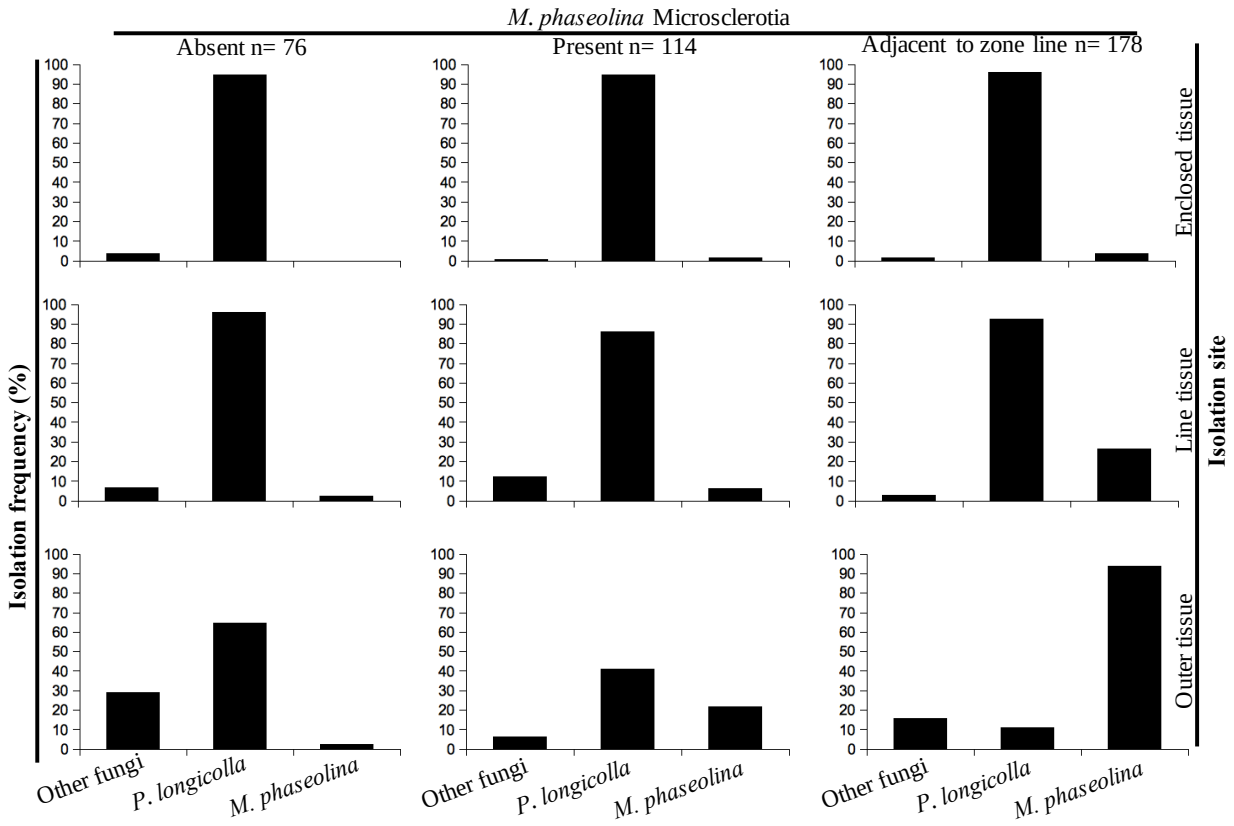

Figure 2. *P. longicolla* was the predominantly fungus isolated from zone lines in soybean tap roots. Isolations were performed on soybean taproots with zone lines. Specimen were collected and plated from tissues within the zone line, the black line itself, and tissues just outside the zone line. *P. longicolla* was recovered from virtually every specimen collected from the center of zone lines. *M. phaseolina* was only predominant on specimen collected outside the zone lines in roots with severe charcoal rot. Rate of isolations represent the proportion of sampled roots where that particular taxa was recovered. Because more than one taxon could at times be recovered, the isolation frequency depicted for each set might not total '100%'.

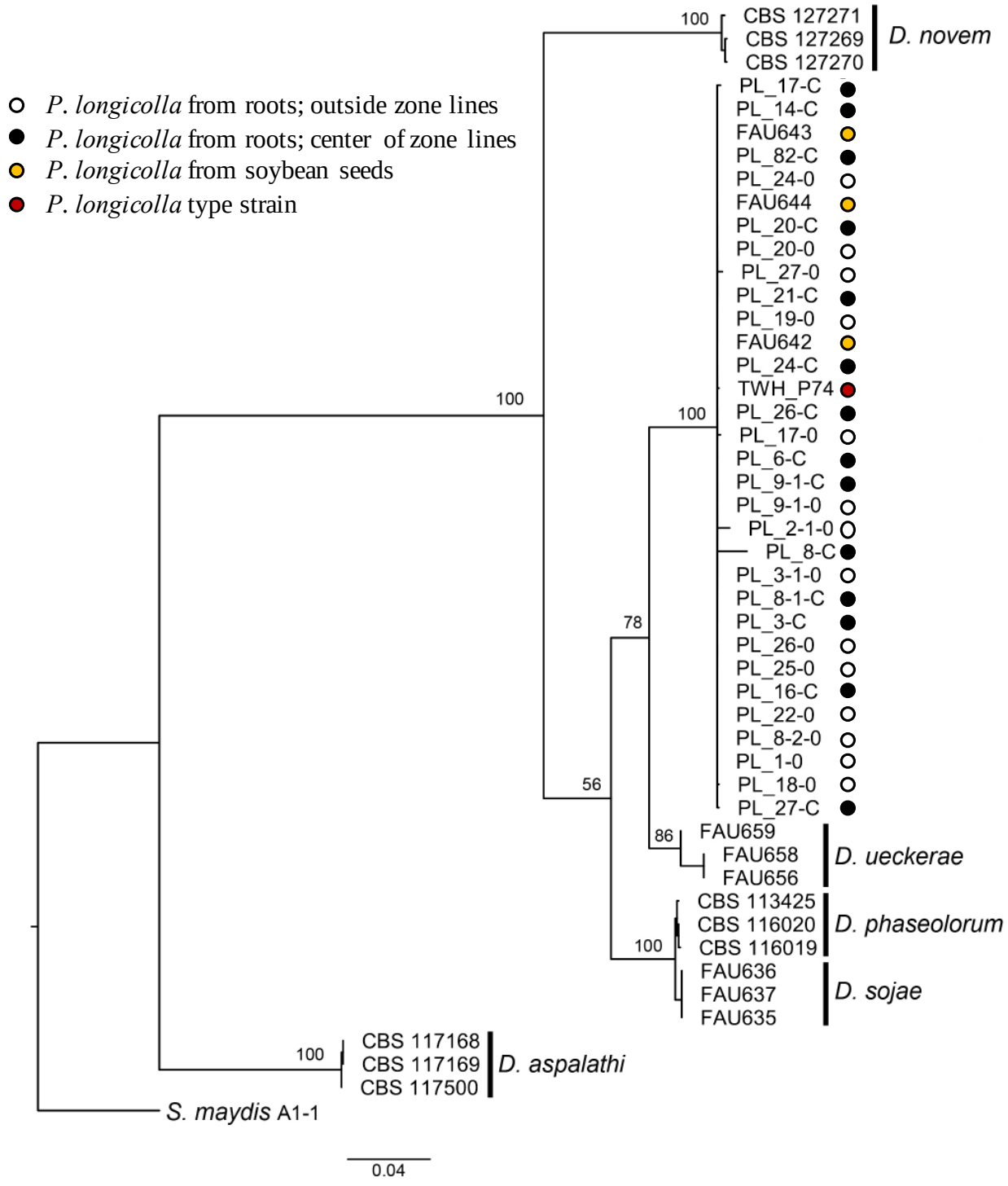
P. longicolla from roots; outside zone lines
P. longicolla from roots; center of zone lines
P. longicolla from soybean seeds
P. longicolla type strain
100
CBS 127271
CBS 127269
CBS 127270
D. novem
PL_17-C
PL_14-C
FAU643
PL_82-C
PL_24-0
FAU644
PL_20-C
PL_20-0
PL_27-0
PL_21-C
PL_19-0
FAU642
PL_24-C
TWH_P74
PL_26-C
PL_17-0
PL_6-C
PL_9-1-C
PL_9-1-0
PL_2-1-0
PL_8-C
PL_3-1-0
PL_8-1-C
PL_3-C
PL_26-0
PL_25-0
PL_16-C
PL_22-0
PL_8-2-0
PL_1-0
PL_18-0
PL_27-C
100
100
78
56
86
FAU659
FAU658
FAU656
D. ueckerae
CBS 113425
CBS 116020
CBS 116019
D. phaseolorum
100
FAU636
FAU637
FAU635
D. sojae
100
CBS 117168
CBS 117169
CBS 117500
D. aspalathi
S. maydis A1-1
0.04

Figure 3. *Phomopsis sp*. strains isolated from soybean taproot zone lines group with *P. longicolla* type strain. 28 *P. longicolla* strains were isolated from soybean tap roots from plant grown at Marianna, AR, Stuttgart, AR, and Rohwer, AR. 14 strains were recovered from within zone lines and 14 strains recovered from outside the zone lines. The ITS, EF-1α, and β-tubulin loci were amplified, sequenced and employed for the construction of the phylogenetic tree. Publicly available sequences of other *Diaporthe spp*. and *Phomopsis spp*. reported to be isolated from soybean plants were also used. Tree was rooted with *Stenocarpella maydis* as the outgroup. All 28 P. longicolla strains isolated from soybean tap roots clustered together with known *P. longicolla,* including the type-strain THW_P74.

Chapter IV: A forward genetic screen in *Phomopsis longicolla* provides unique insights into pathogenesis

Abstract

Phomopsis longicolla (Hobbs) causes Phomopsis seed decay of soybean (*Glycine max*), and lesions on soybean stems, pods, and petioles. *P. longicolla* can exist endophytically within soybean stems, which has given rise to the hypothesis that pathogenesis occurs when the fungus transitions from endophytic or hemibiotrophic growth to necrotrophy. In this study, a forward genetic screen was performed to elucidate genetic mechanisms underlying necrotrophy. Insertional mutants were created via *Agrobacterium*-mediated transformation and evaluated for their ability to induce necrosis in soybean stems using a cut stem assay. A significant reduction in soybean stem necrosis was observed in nine insertional mutants when compared to the wild-type strain. No consistent gain-of-function mutations (increased necrosis) were observed. One mutant, PL343, was found to be impaired in stem lesion formation, seed infection, and colonization despite wild-type growth in defined culture media. The genomic lesion in mutant PL343 was characterized with a modified RADseq approach that enriched T-DNA insertion-junctions. Next-generation DNA sequencing identified a single copy of the disruption cassette in the promoter region of a cellobiose dehydrogenase gene (*CDH*). This study describes new biological resources to dissect the interaction between *P. longicolla* and soybean, and provides new insight into conserved mechanisms underlying stem and seed necrosis caused by *P. longicolla*.

Introduction

Phomopsis longicolla, a ubiquitous and important seed pathogen of soybean (*Glycine max*), is a member of the *Diaporthe-Phomopsis* species complex that includes *D. phaseolorum* f.

sp. *sojae*, *D. phaseolorum* f. sp. *caulivora*, and *D. phaseolorum* f. sp. *meridionalis* (Gomes et al. 2013a; Hobbs and Phillips 1985; Hobbs et al. 1985; Kmetz 1978; Mengistu et al. 2014; Nevena et al. 1997). *P. longicolla* is predominantly associated with Phomopsis seed decay (PSD) in the U.S. (Hobbs et al. 1985), although it has been reported to cause stem lesions in other regions of the world (Cui et al. 2009). Symptoms of PSD include shriveled and elongated seeds with chalky and cracked seed coats. These symptoms are easily discernable from other common soybean seed diseases, such as purple seed stain caused by *Cercospora* spp. (Hartman, et al. 1999). In addition to decreasing the nutritional quality of infected seeds (Hepperly and Sinclair 1978; Mayhew and Caviness 1994), *P. longicolla* can substantially impair seed germination and vigor, which negatively affects seedling emergence in laboratory and field conditions (McGee et al. 1980; Mengistu and Heatherly 2006). Besides colonizing pods and seeds, *P. longicolla* can asymptomatically infect vegetative tissues as early as three weeks after seedling emergence, with symptoms only observed upon senescence (Walcott et al. 1998; Impullitti and Malvick 2013).

PSD is endemic throughout North American soybean production areas, and has been described as one of the most common diseases affecting soybean seeds in the U.S. (Sinclair 1992). In recent years, PSD has increased in incidence and severity in Southeastern states, partly due to the prevalence of the early soybean production system (ESPS) in the region (TeKrony et al. 1996; Logan et al. 1998). The ESPS encourages early planting of soybean with relatively early maturity to avoid late-summer stresses of heat and periodic droughts that occur throughout the region. Due to early planting, the reproductive stages of soybean development may occur during periods of high temperature and humidity, both of which favor PSD development (Shortt 1981). Delayed harvests also favor PSD, as the pathogen has an extended opportunity to colonize seeds before seed moisture can be adequately reduced by controlled drying (Wilcox et

al. 1974). Beyond the Southeastern U.S., PSD occurs periodically in the Midwest when environmental conditions are favorable or harvests are substantially delayed (Kmetz 1978; Shortt 1981). The potential implications of climate change on PSD are difficult to project. However, several long-term forecasting models suggest the increased occurrence of extreme weather events, including heat waves, flooding, and storms (Pachauri et al. 2014), which could conceivably favor increased incidence of PSD across U.S. soybean producing regions.

The relationship between *P. longicolla* and soybean is complex and may involve more than one type of association. In addition to causing PSD, *P. longicolla* is commonly found as an asymptomatic endophyte in soybean vegetative tissues, including stems, leaves, and petioles (Kmetz 1978). Interestingly, *P. longicolla* is reported to endophytically associate with a range of taxonomically diverse plants, including *Euphorbia nutans* (Euphorbiaceae), *Abutilon theophrasti* (Malvaceae), *Ipomoea lacunosa* (Convolvulaceae), *Xanthium strumarium* (Asteraceae), and a tropical red seaweed *Bostrychia radicans* (Rhodomelaceae) (Erbert et al. 2012; Gomes et al. 2013; Udayanga et al. 2011), which suggests it has evolved broadly effective mechanisms of endophytism. *P. longicolla* produces a wide variety of anti-microbial compounds, such as 3-nitropropionic acid (Flores et al. 2013), 18-deoxy-cytochalasin H, mycophenolic acid, and dicerandrol C (Erbert et al. 2012). During colonization of soybean roots and stems, *P. longicolla* has been observed to form zone lines (Olson et al. 2015), structures that are postulated to be analogous to barrage zones on defined media (Brayford 1990). These observations suggest *P. longicolla* could function as a beneficial endophyte in soybean, although the exact nature of the relationship requires further elucidation.

The potential duality underlying the endophytic/pathogenic basis of the *P. longicolla*/soybean relationship has led to fundamental questions about how to dissect

pathogenesis. A cut stem assay is commonly used to assess *P. longicolla* virulence and soybean resistance (Li et al. 2010), in which soybean stems are cut and inoculated with an agar plug colonized by the pathogen. However, *P. longicolla* is reported to produce appressoria during infection of soybean pods (Baker et al. 1987), which suggests a degree of developmental specialization during plant infection. The cut stem assay is predicated on wounding, e.g., cutting the stem, which would presumably bypass specialized infectious development during pathogenesis. Additionally, soybean seeds and pods could express resistance responses not observed in stems, and thus a cut stem assay may not fully capture the range of phenotypes associated with PSD.

Despite its importance as the causal agent of PSD, few studies have explored the molecular basis of pathogenesis in *P. longicolla*. Recently, new molecular resources have become available, including a protocol for genetic transformation (Li et al. 2013) and draft genome sequences for two isolates of *P. longicolla,* including the type isolate (Li et al. 2015). However, functional genomics approaches have not yet been applied to the *P. longicolla*/soybean pathosystem. Forward genetic screens provide a powerful tool for the molecular dissection of pathogenesis in filamentous fungi. Forward genetic screens have been used effectively to discover novel genes and dissect pathogenesis in several filamentous fungi, including *Fusarium graminearum*, *Colletotrichum higginsianum*, *Magnaporthe grisea*, and *Leptosphaeria maculan* (Gupta and Chattoo 2007; Idnurm and Howlett 2002; Korn et al. 2015; Seong et al. 2005).

In this study, a forward genetic screen was developed to dissect the molecular basis of pathogenicity in *P. longicolla*. To this end, a collection of random insertional mutants was created via *Agrobacterium*-mediated transformation and initially screened for virulence using the cut stem assay. From the primary screen, a subset of mutants was analyzed in greater depth,

including the ability to infect and colonize soybean seeds. This study represents the first application of molecular genetics to dissect mechanisms of virulence in the *P. longicolla*/soybean pathosystem.

Materials and methods

Generation of *P. longicolla* mutant collection. Mutagenesis in *P. longicolla* was achieved via *Agrobacterium tumefaciens*-mediated transformation of wild-type strain PL2010AR, as previously described (Li et al. 2013). *A. tumefaciens* strain AGL-1 (Lazo et al. 1991) carrying the pBHt2_sGFP plasmid derived from pBHt2 (Mullins et al. 2001), was used to produce random mutants of *P. longicolla*. Briefly, for each transformation event, PL2010AR mycelia were harvested from one seven-day-old culture growing on 0.2× strength potato dextrose agar medium (PDA; BD Diagnostic Systems, Sparks, MD, USA) and suspended in 1 ml of sterile water. Fungal tissue was fragmented using glass beads in a TissueLyser (Quiagen, Germantown, MD, USA) at a rate of 30 cycles per second for 90 seconds. One ml of fragmented *P. longicolla* hyphae was mixed with 1 ml of an induced *A. tumefaciens* cell culture with OD_{600} of 0.2, and subsequently spread on sterile cellophane disks overlaying induction media agar (Mullins et al. 2001). Following incubation in the dark at room temperature for three days, cellophane discs were inverted and transferred to plates containing 0.2× strength PDA amended with cefotaxime (200 μg ml^{-1}) and hygromycin B (100 μg ml^{-1}) (Research Products International, Mt. Prospect, IL, USA). Cellophane discs were removed and discarded after two days, and *P. longicolla* colonies visually expressing GFP were transferred to 24-well plates containing 0.2× strength PDA amended with hygromycin B (100 μg ml^{-1}) after an additional 2-3 days. Cultures were initially incubated at room temperature and then moved to 4°C for short-term storage. Colonized

cubes of 0.2× strength PDA amended with hygromycin (100 μg ml^{-1}) were suspended in 50% glycerol (*v*:*v*) solution and stored at -80°C for long-term storage of all mutants generated.

Southern blot analysis. Tissue was prepared for each strain by culturing in potato dextrose broth medium (PDB; BD Diagnostic Systems, Sparks, MD, USA) for seven days on an orbital shaker at 80 RPM at room temperature. Fungal genomic DNA was isolated with a modified cetyltrimethylammonium bromide (CTAB) method (Leslie and Summerell 2006). Briefly, DNA was digested with HindIII and probed for the hygromycin phosphotransferase-encoding gene *hph*. A 350-base pair *hph*-specific probe was amplified via PCR with primers HYG-F and HYG-R (Li et al. 2013). The probe was labeled with ^{32}P and purified as described previously (Flaherty et al. 2003). Hybridizations were performed as described by Sambrook and Russell (2001). Following hybridization, blots were washed as described by Flaherty et al. (2003), exposed to a phosphorimaging screen, and visualized with a Typhoon FLA 9500 (GE Healthcare Bio-Sciences, Pittsburgh, PA, USA).

Pathogenicity screen. Wild-type strain PL2010AR and 1114 random mutants were evaluated for pathogenesis on soybean cultivar 'Hutcheson' (Buss et al. 1988) with a slightly modified cut stem assay (Li et al. 2010). Fungal strains were grown on 0.2× strength PDA for 4 days in an incubator in a 12:12 hour light-dark cycle at 25°C. Soybean plants were grown in 48-well insert trays until the first trifoliate leaf was fully expanded (V2 stage; approximately 20 days after planting), at which point the main stem was cleaved with a razor blade 2 cm above the unifoliate leaf node. For inoculations, the base (wide end) of a sterile micropipette tip (200 μl) was used to collect a plug of 0.2× strength PDA medium colonized with fungal mycelia. The base of the micropipette tip containing the inoculum was placed atop the cut stem to create direct contact between the cut stem and the colonized media. After 10 days, the micropipette tip was removed

and the length of necrotic lesion was measured from the edge of the cut stem. Each of the 1114 mutant strains and the wild type were inoculated on 3 and 79 plants, respectively. From the 1114 screened mutants, 44 mutants were selected for phenotypic validation with the same cut stem method. For this secondary round of screening, replicates (three per strain) were comprised of four plants grown side-by-side in a randomized complete block design. From the 44 mutants screened a second time, a final set of 19 mutants was selected, each of which underwent three rounds of hyphal-tip purification before the cut stem assay was performed twice more as described above.

Seed infection assay. Soybean plants were inoculated during pod filling stage (R5) with conidial suspensions. Seed infection rate was assessed by plating mature seeds on PDA. Inoculum was produced by growing strains on oatmeal agar medium (OA; BD Diagnostic Systems, Sparks, MD, USA) at room temperature for seven days in a 12:12 hour light:dark cycle. Conidia were gently dislodged from pycnidia with a cell spreader in 5 ml of sterile deionized water per plate. Conidial suspensions were filtered through two layers of sterile cheesecloth, and adjusted to 10^5 conidia ml^{-1} in 100 µl l^{-1} of Tween-20. Soybean plants (cultivar 'Traff'; PI 490930; maturity group 000) were grown in 4-inch pots on a greenhouse bench in a 14:10 hour light:dark cycle. At pod filling stage (R5; approximately 50 days after planting), conidial suspensions were sprayed on all aboveground plant parts with an air brush until runoff. Twelve plants were inoculated with each strain or mock inoculated with 100 µl l^{-1} Tween-20. Immediately after inoculation, plants were placed in a dew chamber for 48 hours and then returned to the green house where they were kept until harvest maturity. Plants were bottom watered as needed in trays, without wetting aerial tissues. A randomized complete block design was used with each plant considered an independent experimental unit (n=12). Three treatments

were applied, the inoculation of wither the wild-type strain and the mutant PL343, and mock inoculated plants. At harvest, seeds were collected from pods and grouped by plant. For surface sterilization, seeds were dipped in 0.5% sodium hypochlorite for 30 seconds, followed by 30 seconds in 70% ethanol. After rising in sterile deionized water for 30 seconds twice, seeds were plated on full-strength PDA amended with 100 μg ml^{-1} of carbenicillin (Research Products International, Mt Prospect, IL, USA). A maximum of five seeds were plated per 90-mm petri dish, and plates were incubated in the dark at room temperature. The emergence of *P. longicolla* from each seed was visually assessed and recorded five days after plating. The experiment was performed twice.

Seed colonization. Physiologically mature soybean seeds were wounded and inoculated with *P. longicolla* strains and colonization was estimated by quantifying seed ergosterol content. Seeds were produced by growing soybean cultivar Traff as described above. Pods were hand harvested at the onset of yellowing during late reproductive stages (R6-R7; approximately 70 days after planting). Pods, and then seeds, were surface disinfested as described above and allowed to dry on sterile paper towels in a laminar flow hood. Seeds were placed in sterile 24-well plates, one seed per well, and wounded by inserting a sterile 12-gage hypodermic needle to a depth of approximately 4 mm. A 5 mm-diameter plug of colonized 0.2× strength PDA medium or uninoculated medium (mock treatment) was placed atop the wound. Plates were kept in the dark at room temperature. Ten days after inoculation, seeds were flash frozen in liquid nitrogen and ground to a fine powder with a mortar and pestle. Ergosterol extraction was performed by incubating 500 mg of ground tissue (fresh weight) in 2 ml of 2:1 chloroform:methanol (*v*:*v*) at room temperature on an orbital shaker at 50 rpm overnight. The extract was filtered through a nylon syringe filter (0.2 μm; VWR International, Radnor, PA, USA). Ergosterol quantification

was performed as previously described (Smith et al. 2014). Briefly, extracts were separated on a high-performance liquid chromatography (HPLC) system (Shimadzu, Columbia, MD, USA) equipped with an ODS 5u column (250 mm × 4.6 mm; Phenomenex, Torrance, CA, USA), and ergosterol was detected with a UV photo diode array detector (Shimadzu). Peaks were detected at $\lambda = 282$ nm. The concentration of ergosterol was determined by comparing peak area in samples to a standard curve generated by analysis of HPLC-grade ergosterol (Sigma-Aldrich, St. Louis, MO, USA). Experimental units were comprised of four seeds, each treatment had three replicates, and the entire experiment was performed twice in a randomized complete block design.

Characterization of T-DNA insertion. We developed a simple and cost-effective method to pinpoint T-DNA insertion sites by enriching a DNA library with T-DNA insertion break junctions via MoNSTR-seq (Zaccaron et al. 2018). The method development is detailed in chapter V of this document. Briefly, DNA from each strain containing a T-DNA insertion was digested with AseI and BpuEI (New England BioLabs, Ipswich, MA, USA). These sites were known to be present within 100bp of right and left borders in the inserted T-DNA. Sequencing adapters were designed and ligated to the digested DNA sticky-overhangs. Then, DNA was digested with Fragmentase (New England BioLabs, Ipswich, MA, USA). A sequencing adapter was ligated at the blunt end left by Fragmentase as described by Zaccaron et al. (2018). Enrichment of T-DNA insertion sites was achieved by PCR-amplification with primers targeting the ligated adapters, followed by size selection of 480bp. Cleanup steps were performed after digestion and ligation steps with AMPureXP beads (Beckman Coulter Inc., Brea, California, USA). Following amplification, template was prepared on the Ion Torrent One Touch 2 system (Life Technologies, Grand Island, NY, USA) and sequenced with Ion PGM on an Ion 314 V2

chip following the manufacturer's protocols. Reads were first mapped to the T-DNA cassette and then mapped to the *P. longicolla* MSPL 10-6 draft genome (Genbank accession AYRD00000000) with bwa version 0.7.10-r789 (Li and Durbin 2009) and processed with SAMtools version 0.1.18 (Li et al. 2009).

P. longicolla carbohydrate-active enzymes from AA family were identified with dbCAN (Yin et al. 2012). Protein sequences from AA8 enzymes were aligned with MAFFT v7.407 (Katoh et al. 2002) with default settings. The *P. longicolla* protein encoded by gene g16049 (AA3 enzyme) was used as an outgroup. Aligned sites containing more than 50% gaps were removed with trimAl v1.2 (Capella-Gutiérrez et al. 2009). A maximum likelihood tree was constructed with RAxML v8.2.11 (Stamatakis 2014) with settings adjusted to perform 100 rapid bootstrap replicates and to detect the best amino acid substitution model (parameter PROTGAMMAAUTO). The constructed tree was visualized and edited with FigTree v1.4.3 (http://tree.bio.ed.ac.uk/software/figtree/, accessed: October 2018).

Quantitative reverse transcription-PCR (RT-qPCR). Relative expression of g4703 was assessed via RT-qPCR in strains growing on full-strength PDA and on 0.5% carboxymethyl cellulose agar (CMC) (Yeoh et al. 1985). Petri dishes with either PDA or CMC were overlaid with sterile cellophane discs, inoculated in the center of the plate with a 5 mm plug of colonized PDA, and incubated in the dark at room temperature. After six days, colonized cellophane discs were removed, ground to a fine powder under liquid nitrogen, and total RNA was extracted using Ribozol (Amresco, Solon, OH, USA). For each sample, two μg of total RNA was treated with DNase (Promega, Madison, WI, USA) for 30 minutes at 37 °C to remove genomic DNA. Two μg of DNA-free RNA were used to synthesize cDNA with M-MLV reverse transcriptase (Promega, Madison, WI, USA). Primer quest (Integrated DNA Technologies, Coralville, IA,

USA) was used to design primer sets 343RTF1/R1 and PlTubF1/R1 to amplify *CDH1* and *beta tubulin*, respectively **(Table 1)**. Sequences for the genes were obtained from the *Phomopsis longicolla* genome (GenBank accession AYRD00000000). All primers were obtained from Integrated DNA Technologies. Quantitative PCR reactions were performed in the AB StepOnePlus instrument (Applied Biosystems, Foster City, CA, USA) and the data were collected with the StepOnePlus software (version 2.1; Applied Biosystems, Foster City, CA, USA). Reaction mixtures (10 µl) consisted of the following: 5 µl SYBR green PCR master mix (Thermo Fisher Scientific, Waltham, MA), 500 nM each of forward and reverse primers, and 4 µl of cDNA template diluted 1:100 in nuclease free water. PCR conditions consisted of 1 cycle for 10 minutes at 95 °C, 15 seconds at 95 °C, and 1 minute at 58 °C (40 cycles). Relative expression of *CDH1* was quantified with the comparative cycle threshold method with *beta tubulin* as the endogenous control. Each treatment had three replicates, each consisting of three colonized cellophane discs. Quantitative PCR was performed on three technical replicates for each experimental unit, and the entire experiment was performed twice. A complete randomized design was used.

Statistics. Pathogenicity selected mutants acquired via cut stem assay were statistically compared to the wild-type strain via the many-to-one Dunnett's test. First, an analysis of variance was conducted with the 'aov' function in R (R Core Team). After uncovering the significant effect of mutants on pathogenicity, a two-tailed Dunnett's test was computed with the 'multcomp' package (Hothorn and Westfall, 2008) in R with the wild-type strain as the standard. Simple linear regression was computed with the lm function in R. Tukey test applied to radial growth, seed infection rate, and ergosterol concentration was computed with lme4 package (Bates et al. 2015) in R. Incidence rate was treated as a Beta distributed variable, while length of

colonization, ergosterol concentration and radial growth were treated as Gamma distributed variables.

Results

Creation of a panel of *P. longicolla* mutants. Creating *P. longicolla* mutants via Agrobacterium-mediated transformation was highly efficient, and mutants displayed strong, stable expression of GFP. Numerous macromorphological phenotypes were observed when mutants were cultured in defined media, including altered rates of radial growth, irregular colony margins, increased or decreased pigmentation, and decreased rates of pycnidiation and conidiation. In total, 1719 mutants were isolated from three transformation events and placed in 50% glycerol (*v*:*v*) solution at -80°C for long term storage. From the 1719 mutants created, 1114 were screened for pathogenesis with a modified cut stem assay (Li et al. 2010).

Cut stem pathogenicity screen. To identify genes in *P. longicolla* associated with pathogenesis, 1114 insertional mutants were evaluated with a modified cut stem assay (Li et al. 2010). In the preliminary screen, ten days after inoculation, wild-type strain PL2010AR caused necrotic lesions averaging 27.8 mm (n=79) in length, while lesions caused by mutant strains averaged 8.67 to 75 mm (n=3) in length **(Fig. 1)**. Although a wide range of lesion lengths was observed, most mutants caused lesions of similar length as the wild-type strain. Additionally, although the wild type and vast majority of mutants produced pycnidia abundantly on necrotic stem tissue; however, a few mutants showed reduced or no pycnidiation.

To confirm pathogenicity phenotypes observed in the preliminary screen, 44 mutant strains displaying abnormal lesion length or mutants with reduced pycnidiation *in planta* were re-screened with the cut stem assay. In this subsequent screen, the wild-type strain induced lesions that averaged 13.83 mm in length, whereas lesions induced by the 44 mutant strains

ranged from 6.92 to 22.75 mm in length. From the 44 re-screened mutants, 19 were selected for further study. Nine of the mutants induced lesions that were significantly ($P < 0.005$) shorter compared to the wild type **(Fig. 1)** in repeated assessments. Of these nine, three also consistently produced fewer pycnidia than the wild type.

Seed infection and colonization. A central goal of this study was to identify genes in *P. longicolla* associated with pathogenesis, i.e. seed decay. To this end, seed infection and colonization was investigated in mutant strain PL343. During growth on PDA medium, PL343 was indistinguishable from PL2010AR in colony morphology and radial growth **(Fig. 2)**. However, PL343 induced significantly shorter lesions on soybean stems. Additionally, a single T-DNA insertion was detected in this strain, according to Southern blot **(Fig. 3)**.

To assess if PL343 had reduced seed infection capability in addition to deficiency in stem lesion formation, soybean plants were inoculated at pod-fill stage (R5) and *P. longicolla* recovery rate from seeds was determined at harvest maturity by plating. *P. longicolla* was recovered from 32.4% of seeds harvested from plants inoculated with the wild-type strain PL2010AR, while the recovery rate from plants inoculated with the mutant-strain PL343 was significantly lower, 7.2%. *P. longicolla* was not recovered from seeds of plants mock inoculated **(Fig. 4A)**. The experiment was replicated with similar results. Seed colonization capability of PL343 was also examined. Strains were inoculated on soybean seeds *in vitro* and ergosterol was measured to estimate colonization. Seeds inoculated with PL343 presented significantly reduced ergosterol content when compared with seeds inoculated with the wild-type PL2010AR, 139.0 and 355.5 $\mu g\ g^{-1}$ respectively. Ergosterol was not detected in soybean seeds mock inoculated **(Fig. 4B)**. The experiment was repeated with similar results.

Characterization of mutant PL343 via MoNSTR-seq. The site of T-DNA integration in the *P. longicolla* mutant PL343 was identified with MoNSTR-seq. A total of 0.5 million reads were obtained for PL343 sequenced library. T-DNA insertion site was identified by sequentially mapping the reads first to the inserted-cassette sequence and then to *P. longicolla* genome. A single insertion was mapped to a site 511 bp upstream of a predicted cellobiose dehydrogenase gene open reading frame, homologue to *CDH2* in *Neurospora crassa* designated g4703 in the *P. longicolla* draft genome **(Fig. 5)**. A Southern blot confirmed a single T-DNA insertion in the PL343 mutant **(Fig 3)**. The insertion site was validated via PCR.

g4703 expression. Expression of *CDH1* was reduced by a large amount in PL343. When the wild-type strain and PL343 were cultivated on PDA, *CDH1* was transcribed at low levels in both strains. However, when strains were cultivated in 0.5% CMC as carbon source, a 60-fold increase was detected in *CDH1* transcripts in the wild type. Meanwhile, PL343 transcription of CDH1 remain at similarly low levels observed in PDA **(Table 2)**

Discussion

In this study, forward genetics was utilized in the *P. longicolla*-soybean pathosystem to identify genes involved in pathogenesis. *Agrobacterium*-mediated transformation approach was used to create *P. longicolla* random mutant library that was screened for pathogenicity. We identified nine *P. longicolla* mutants with impaired pathogenicity, which correspond to approximate 1% of the screened transformants. From the 18 selected for further study due to Pathogenicity impairment, only five had multiple T-DNA insertions indicating this transformation approach and methodology are suitable for forward genetics in this organism. Due to the absence of known sexual stage in *P. longicolla*, it is not possible to separate multiple T-DNA insertions through meiotic segregations. Thus, single T-DNA insertions are preferred

when putatively linking a mutation to the phenotype of interest. This study implicated the *CDH1* ortholog to *P. longicolla* pathogenesis. A single T-DNA insertion was identified in the promoter region of *CDH1* of PL343 strain. Furthermore, analyze of the P. longicolla draft genome and PCR-evidence indicate *CDH1* is a single-copy gene in *P. longicolla*. However, *CDH1* transcription was not abolished in PL343, but was severely reduced when compared to wild-type strain.

The cellobiose dehydrogenase gene, *CDH1*, in *P. longicolla* appears to be a link between pathogenicity and primary metabolism. Cellobiose dehydrogenases are secreted enzymes that catalyze cellulose oxidation, they are also known to be involved in lignin degradation (Tan et al. 2015). CDH act as electron donors for lytic polysaccharide mono-oxygenases (LPMOs) during redox-mediated oxidative cleavage of cellulose and hemicelluloses, greatly improving their efficiency (Kracher and Ludwig 2016). LPMOs are known to be secreted by fungi to degrade plant polysaccharides (Quinlan et al. 2011; Vaaje-Kolstad et al. 2010). Our results indicate that this mechanism for plant biomass degradation is a key component of *P. longicolla* pathogenesis in addition to be important to cellulose metabolism. The disruption of cellobiose dehydrogenase has been reported to reduce, but not completely eliminate, the wood degradation and cellulose utilization capability of the basidiomycetes *Trametes versicolor* (Dumonceaux et al. 2001; Stapleton and Dobson 2003) and *Podospora anserine* (Tangthirasunun et al. 2017). *CDH1* is the first gene implicated in *P. longicolla* pathogenesis.

CDH1 is up-regulated in the presence of carboxymethyl cellulose (CMC). RT-qPCR reviewed that *CDH1* transcription was significantly increased when the wild-type strain was cultivated in 0.5%CMC when compared to PDA. However, PL343 showed *CDH1* transcription at very low levels in both PDA and CMC, but transcription was not abolished. *CDH1* increased

transcription in CMC when compared to PDA in filamentous fungi (Stapleton and Dobson 2003; Tangthirasunun et al. 2017). All together, these results indicate the *CDH1* transcription regulation in PL343 has been disrupted, particularly in response to cellulose-derived compounds. PL343 significantly reduced growth on CMC agar **(Fig. 6)** could be explained by its inefficient utilization as nutritional source due to severely diminished availability of cellobiose dehydrogenase. Similarly, this could partially explain PL343 impaired ability to cause necrosis in stem and colonize seeds of soybean.

Although the mechanistic basis of infection by *P. longicolla* is poorly understood, the genetic screen performed in this study provides a degree of new insight. Typically, PSD is not associated with pod lesions in field conditions, which suggests a stealthy mechanism of entry. *P. longicolla* is reported to form appressoria during external infection of soybean pods (Baker et al. 1987), which suggests a specialized mode of infection. This is in agreement with the endophytic life style observed during early PSD pathogenesis. One possibility is that *P. longicolla* functions as a hemibiotroph during external pod infections. Alternatively, the fungus may gain access to seeds via endophytic colonization of soybean stems and pods. Mechanistically, the endophytic phase of colonization should require manipulation of host defenses, possibly through effectors. Whichever the mechanism of used by *P. longicolla* to gain access to soybean seeds, the disruption of *CDH1* significantly impaired it. Forward genetics is a very useful approach to identify the molecular machinery necessary for penetration, endophytism, and early pathogenesis; however, the cut stem assay may not be suitable for these objectives.

Formation of pycnidia on dead soybean plant material is an important mechanism of dissemination for *P. longicolla*, yet the process remains poorly understood. In Arkansas and other Midsouthern states, pycnidia are commonly observed on senescent tissues such as soybean

petioles and stems. In no-till cropping systems without rotation, pycnidia-laden tissues would presumably overwinter on the ground and persist into the next season of soybean production contributing with primary inoculum for PSD epidemic. Despite the clear importance of pycnidiation in the *P. longicolla*-soybean pathosystem, little is known about its regulation; however, the genetic resources generated in this study could further our understanding. The mutant PL343, with the disrupted *CDH1* gene, in addition to pathogenicity phenotype also did not produced pycnidia *in planta* while producing pycnidia similarly to the wild-type *in vitro* **(Table 3)**. Thus, there appear to be a regulatory link between pycnidiation and necrotrophy or indirectly with carbon primary metabolism. Two other genetically uncharacterized mutants were observed to have reduced pycnidiation *in planta* when compared to the wild-type in addition to have reduced lesion length on cut stem assay. The apparent link between pycnidiation and necrotrophy is not unexpected since pycnidia is produced by *P longicolla* only on dead plant tissue during PSD disease cycle. The putative regulatory link between pycnidiation and the necrotic-saprophitic phase of *P. longicolla*-soybean pathosystem could be used dissect the regulatory mechanisms underlying the end of endophytism at the onset of plant senescence.

In conclusion, our genetic screen has identified 9 mutants with impaired necrotrophic causing capability and one candidate gene putatively associated with pathogenesis in *P. longicolla* on soybean. We have shown that *P. longicolla* can be easily manipulated in a forward genetic screen by generating and phenotyping 1114 insertional random mutants and consequently identifying a gene, *CDH1* linked to *P. longicolla* ability to cause necrotic lesion on soybean stems, infect and colonize soybean seeds, and efficiently use carboxymethyl cellulose as carbon source. This work is the first forward genetic study with *P. longicolla* and *CDH1* is the first gene in this organism to be associated with any function. Thus, this study represents the

first foothold on mechanistically understanding the complex relationship between *P. longicolla* and soybean. Future work will be directed towards elucidating the mechanistic basis for *Phomopsis* seed decay with focus on the molecular signaling associated with the endophytic to saprophytic switch of *P. longicolla* during plant senescence onset.

Literature cited

Bates, D., Mächler, M., Bolker, B., and Walker, S. 2015. Fitting Linear Mixed-Effects Models Using lme4. Journal of Statistical Software *67:* 1-48

Baker, D. M., Minor, H. C., Brown, M. F., and Brown, E. A. 1987. Infection of immature soybean pods and seeds by *Phomopsis longicolla*. Can. J. Microbiol. 33:797-801

Brayford, D. 1990. Vegetative incompatibility in *Phomopsis* from elm. Mycol. Res. 94:745-752

Buss, G. R., Camper, H. M., and Roane, C. W. 1988. Registration of "Hutcheson" soybean. Crop Sci. 28:1024-1025

Capella-Gutiérrez, S., Silla-Martínez, J. M., and Gabaldón, T. 2009. trimAl: a tool for automated alignment trimming in large-scale phylogenetic analyses. Bioinformatics 25:1972-1973

Cui, Y.-L., Duan, C. X., Wang, X.-M., Li, H. J., and Zhu, Z.-D. 2009. First report of *Phomopsis longicolla* causing soybean stem blight in China. Plant Pathol. 58:799-799

Dumonceaux, T., Bartholomew, K., Valeanu, L., Charles, T., and Archibald, F. 2001. Cellobiose dehydrogenase is essential for wood invasion and nonessential for kraft pulp delignification by *Trametes versicolor*. Enzyme Microb. Technol. 29:478-489

Erbert, C., Lopes, A. A., Yokoya, N. S., Furtado, N. A. J. C., Conti, R., Pupo, M. T., Lopes, J. L. C., and Debonsi, H. M. 2012. Antibacterial compound from the endophytic fungus *Phomopsis longicolla* isolated from the tropical red seaweed *Bostrychia radicans*. Bot. Mar. 55:435-440

Flaherty, J. E., Pirttilä, A. M., Bluhm, B. H., and Woloshuk, C. P. 2003. PAC1, a pH-Regulatory Gene from *Fusarium verticillioides*. Appl. Environ. Microbiol. 69:5222-5227

Flores, A. C., Pamphile, J. A., Sarragiotto, M. H., and Clemente, E. 2013. Production of 3-nitropropionic acid by endophytic fungus *Phomopsis longicolla* isolated from *Trichilia elegans* A. JUSS ssp. elegans and evaluation of biological activity. World J. Microbiol. Biotechnol. 29:923-932

Gomes, R. R., Glienke, C., Videira, S. I. R., Lombard, L., Groenewald, J. Z., and Crous, P. W. 2013. *Diaporthe*: a genus of endophytic, saprobic and plant pathogenic fungi. Persoonia Mol. Phylogeny Evol. Fungi. 31:1-41

Gupta, A., and Chattoo, B. B. 2007. A novel gene MGA1 is required for appressorium formation in *Magnaporthe grisea*. Fungal Genet. Biol. 44:1157-1169

Hartman, G. L., Sinclair, J. B., and Rupe, J. C., eds. 1999. Compendium of soybean diseases. Fourth Edition. American Phytopathological Society (APS Press), St. Paul.

Hepperly, P. R., and Sinclair, J. B. 1978. Quality losses in Phomopsis-infected soybean seeds. Phytopathology 68:1684-1687

Hobbs, T., and Phillips, D. 1985. Identification of *Diaporthe* and *Phomopsis* Isolates from Soybean. Phytopathology 75:500-509

Hobbs, T. W., Schmitthenner, A. F., and Kuter, G. A. 1985. A New *Phomopsis* Species from Soybean. Mycologia 77:535-544

Hothorn, T., Bretz F., and Westfall P. 2008. Simultaneous Inference in General Parametric Models. Biometrical Journal 50:346-363

Idnurm, A., and Howlett, B. J. 2002. Isocitrate Lyase Is Essential for Pathogenicity of the Fungus *Leptosphaeria maculans* to Canola (*Brassica napus*). Eukaryot. Cell 1:719-724

Impullitti, A. e., and Malvick, D. k. 2013. Fungal endophyte diversity in soybean. J. Appl. Microbiol. 114:1500-1506

Katoh, K., Misawa, K., Kuma, K., and Miyata, T. 2002. MAFFT: a novel method for rapid multiple sequence alignment based on fast Fourier transform. Nucleic Acids Res. 30:3059-3066

Kmetz, K. T. 1978. Soybean Seed Decay: Prevalence of Infection and Symptom Expression Caused by *Phomopsis* sp., *Diaporthe phaseolorum* var. sojae, and *D. phaseolorum* var. caulivora. Phytopathology 68:836-840

Korn, M., Schmidpeter, J., Dahl, M., Müller, S., Voll, L. M., and Koch, C. 2015. A Genetic Screen for Pathogenicity Genes in the Hemibiotrophic Fungus *Colletotrichum higginsianum* Identifies the Plasma Membrane Proton Pump Pma2 Required for Host Penetration. PLOS ONE 10:e0125960

Kracher, D., and Ludwig, R. 2016. Cellobiose dehydrogenase: An essential enzyme for lignocellulose degradation in nature - A review. Food Environ. 67:145-163

Lazo, G. R., Stein, P. A., and Ludwig, R. A. 1991. A DNA transformation-competent *Arabidopsis* genomic library in *Agrobacterium*. Biotechnol. Nat. Publ. Co. 9:963-967

Leslie, J. F., and Summerell, B. A. 2006. The Fusarium laboratory manual. John Wiley & Sons

Li, H., and Durbin, R. 2009. Fast and accurate short read alignment with Burrows–Wheeler transform. Bioinformatics 25:1754-1760

Li, H., Handsaker, B., Wysoker, A., Fennell, T., Ruan, J., Homer, N., Marth, G., Abecasis, G., and Durbin, R. 2009. The Sequence Alignment/Map format and SAMtools. Bioinformatics 25:2078-2079

Li, S., Hartman, G. L., and Boykin, D. L. 2010. Aggressiveness of *Phomopsis longicolla* and Other *Phomopsis* spp. on Soybean. Plant Dis. 94:1035-1040

Li, S., Ridenour, J. B., Kim, H., Hirsch, R. L., Rupe, J. C., and Bluhm, B. H. 2013. *Agrobacterium tumefaciens*-mediated transformation of the soybean pathogen *Phomopsis longicolla*. J. Microbiol. Methods 92:244-245

Li, S., Song, Q., Ji, P., and Cregan, P. 2015. Draft genome sequence of *Phomopsis longicolla* type strain TWH P74, a fungus causing *Phomopsis* seed decay in soybean. Genome Announc. 3: e00010-15

Logan, J., Mueller, M. A., and Graves, C. R. 1998. A Comparison of Early and Recommended Soybean Production Systems in Tennessee. J. Prod. Agric. 11:319-325

Mayhew, W. L., and Caviness, C. E. 1994. Seed Quality and Yield of Early-Planted, Short-Season Soybean Genotypes. Agron. J. 86:16-19

McGee, D. C., Brandt, C. L., and Burris, J. S. 1980. Seed mycoflora of soybeans relative to fungal interactions, seedling emergence, and carry over of pathogens to subsequent crops. Phytopathology 70:615-617

Mengistu, A., Castlebury, L. A., Morel, W., Ray, J. D., and Smith, J. R. 2014. Pathogenicity of *Diaporthe* spp. isolates recovered from soybean (*Glycine max*) seeds in Paraguay. Can. J. Plant Pathol. 36:470-474

Mengistu, A., and Heatherly, L. G. 2006. Planting date, irrigation, maturity group, year, and environment effects on *Phomopsis longicolla*, seed germination, and seed health rating of soybean in the early soybean production system of the midsouthern USA. Crop Prot. 25:310-317

Mullins, E. D., Chen, X., Romaine, P., Raina, R., Geiser, D. M., and Kang, S. 2001. *Agrobacterium*-Mediated Transformation of *Fusarium oxysporum*: An Efficient Tool for Insertional Mutagenesis and Gene Transfer. Phytopathology 91:173-180

Nevena, M., Jelena, V., and Franić-Mihajlović, D. 1997. A comparative study of *Diaporthe*/*Phomopsis* fungi on soybean from two different regions of the world. Mycopathologia 139:107-113

Olson, T. R., Gebreil, A., Micijevic, A., Wise, K. A., Mueller, D. S., Chilvers, M. I., and Mathew, F. M. 2015. Association of *Diaporthe longicolla* with Black Zone Lines on Mature Soybean Plants. Plant Health Prog. 16:118-122

Pachauri, R. K., Allen, M. R., Barros, V. R., Broome, J., Cramer, W., Christ, R., Church, J. A., Clarke, L., Dahe, Q., Dasgupta, P., and others. 2014. Climate change 2014: synthesis report. Contribution of Working Groups I, II and III to the fifth assessment report of the Intergovernmental Panel on Climate Change. IPCC.

Quinlan, R. J., Sweeney, M. D., Leggio, L. L., Otten, H., Poulsen, J.-C. N., Johansen, K. S., Krogh, K. B. R. M., Jørgensen, C. I., Tovborg, M., Anthonsen, A., Tryfona, T., Walter, C. P., Dupree, P., Xu, F., Davies, G. J., and Walton, P. H. 2011. Insights into the oxidative degradation of cellulose by a copper metalloenzyme that exploits biomass components. Proc. Natl. Acad. Sci. 108:15079-15084

R Core Team. R: A Language and Environment for Statistical Computing. 2019. Vienna, Austria. URL https://www.R-project.org/

Sambrook, J., and Russell, D. 2001. Molecular cloning: a laboratory manual. Cold Spring harbor laboratory Cold Spring Harbor, NY.

Seong, K., Hou, Z., Tracy, M., Kistler, H. C., and Xu, J.-R. 2005. Random Insertional Mutagenesis Identifies Genes Associated with Virulence in the Wheat Scab Fungus *Fusarium graminearum*. Phytopathology 95:744-750

Shortt, B. J. 1981. Epidemiology of Phomopsis Seed Decay of Soybean in Illinois. Plant Dis. 65:62-64

Sinclair, J. B. 1992. Discoloration of Soybean Seeds- An Indicator of Quality. Plant Dis. 76:1087-1091

Smith, J. E., Mengesha, B., Tang, H., Mengiste, T., and Bluhm, B. H. 2014. Resistance to *Botrytis cinerea* in *Solanum lycopersicoides* involves widespread transcriptional reprogramming. BMC Genomics 15:334

Stamatakis, A. 2014. RAxML version 8: a tool for phylogenetic analysis and post-analysis of large phylogenies. Bioinformatics 30:1312-1313

Stapleton, P. C, and Dobson, A. D. W. 2003. Carbon repression of cellobiose dehydrogenase production in the white rot fungus Trametes versicolor is mediated at the level of gene transcription. FEMS Microbiol. Lett. 221:167-172

Tan, T.-C., Kracher, D., Gandini, R., Sygmund, C., Kittl, R., Haltrich, D., Hällberg, B. M., Ludwig, R., and Divne, C. 2015. Structural basis for cellobiose dehydrogenase action during oxidative cellulose degradation. Nat. Commun. 6:7542

Tangthirasunun, N., Navarro, D., Garajova, S., Chevret, D., Tong, L. C. H., Gautier, V., Hyde, K. D., Silar, P., and Berrin, J.-G. 2017. Inactivation of Cellobiose Dehydrogenases Modifies the Cellulose Degradation Mechanism of *Podospora anserina*. Appl. Environ. Microbiol. 83:e02716-16

TeKrony, D. M., Grabau, L. J., DeLacy, M., and Kane, M. 1996. Early Planting of Early-Maturing Soybean: Effects on Seed Germination and *Phomopsis* Infection. Agron. J. 88:428-433

Udayanga, D., Liu, X., McKenzie, E. H. C., Chukeatirote, E., Bahkali, A. H. A., and Hyde, K. D. 2011. The genus *Phomopsis*: biology, applications, species concepts and names of common phytopathogens. Fungal Divers. 50:189-225

Vaaje-Kolstad, G., Westereng, B., Horn, S. J., Liu, Z., Zhai, H., Sørlie, M., and Eijsink, V. G. H. 2010. An oxidative enzyme boosting the enzymatic conversion of recalcitrant polysaccharides. Science 330:219-222

Walcott, R. R., McGee, D. C., and Misra, M. K. 1998. Detection of Asymptomatic Fungal Infections of Soybean Seeds by Ultrasound Analysis. Plant Dis. 82:584-589

Wilcox, J. R., Laviolette, F. A., Athow, K. L., and others. 1974. Deterioration of soybean seed quality associated with delayed harvest. Plant Dis. Report. 58:130-133

Yeoh, H. H., Khew, E., and Lim, G. 1985. A Simple Method for Screening Cellulolytic Fungi. Mycologia 77:161-162

Yin, Y., Mao, X., Yang, J., Chen, X., Mao, F., and Xu, Y. 2012. dbCAN: a web resource for automated carbohydrate-active enzyme annotation. Nucleic Acids Res. 40:445-451

Zaccaron, M., Sharma, S., and Bluhm, B. H. 2018. MoNSTR-seq, a restriction site-associated DNA sequencing technique to characterize *Agrobacterium*-mediated transfer-DNA insertions in *Phomopsis longicolla*. Lett. Appl. Microbiol. 66:19-24

Tables

Table 1. Primers used in this study.

Primer name	Primer sequence	Comment
343RTF1	5' TATTTGCAATGTGCCTCCACGG 3'	qRT-PCR forward primer for CDH
343RTR1	5' ATCACGTAGCCTGTCGCGTA 3'	qRT-PCR reverse primer for CDH
PlTubF1	5' CGACAGCAATGGCGTTTACAAC 3'	qRT-PCR forward primer for tubulin
PlTubR1	5' ATGGTACCGGGCTCGAGAT 3'	qRT-PCR reverse primer for tubulin
PL343F1	5' GTACGGAGTAGGTGTGTCTTTC 3'	Forward primer to confirm insertion of mutagenesis cassette
PL343R1	5' CGGCATGGCGGTTTAATATG 3'	Reverse primer to confirm insertion of mutagenesis cassette
PL343F2	5' CTGTACAGTACCTGCGTCTAATC 3'	Forward primer to confirm insertion of mutagenesis cassette
PL343R2	5' GCATCTCAATTTGTGCGTGTAA 3'	Reverse primer to confirm insertion of mutagenesis cassette

Table 2. RT-qPCR measuring the expression of CDH1 in PL343 and wild type.

PDA		0.5% CMC	
PL2010AR	PL343	PL2010AR	PL343
1.00 (0.70-1.43)	0.44 (0.25-0.77)	61.84 (42.58-89.81)	2.11 (1.17-3.79)

qRT-PCR was performed with SYBR-green as the fluorescence reporter. The expression of the gene was normalized to beta-Tubulin gene as endogenous control. The values show fold differences in expression of the gene compared to the wild type on PDA. $2^{-\Delta\Delta CT}$ was used to calculate the relative expression of the gene. The values in the parentheses represent the range of expression of the gene.

Tables 3. Pycnidiation of multiple strains of P. longicolla.

Strain	Pycnidiation level[a]		
	Preliminary screen	Secondary screen	Final screen
PL343	-	-	-
PL347	-	-	-
PL912	+	+	+
PL1126	-	-	-
PL1404	+	+	+
PL2010AR	+++	+++	+++

[a] +++ indicates wild-type level of pycnidiation. + indicates a reduction in pycnidiation greater than 50% when compared to the wild-type levels, and - indicates absence of pycnidia.

Figures

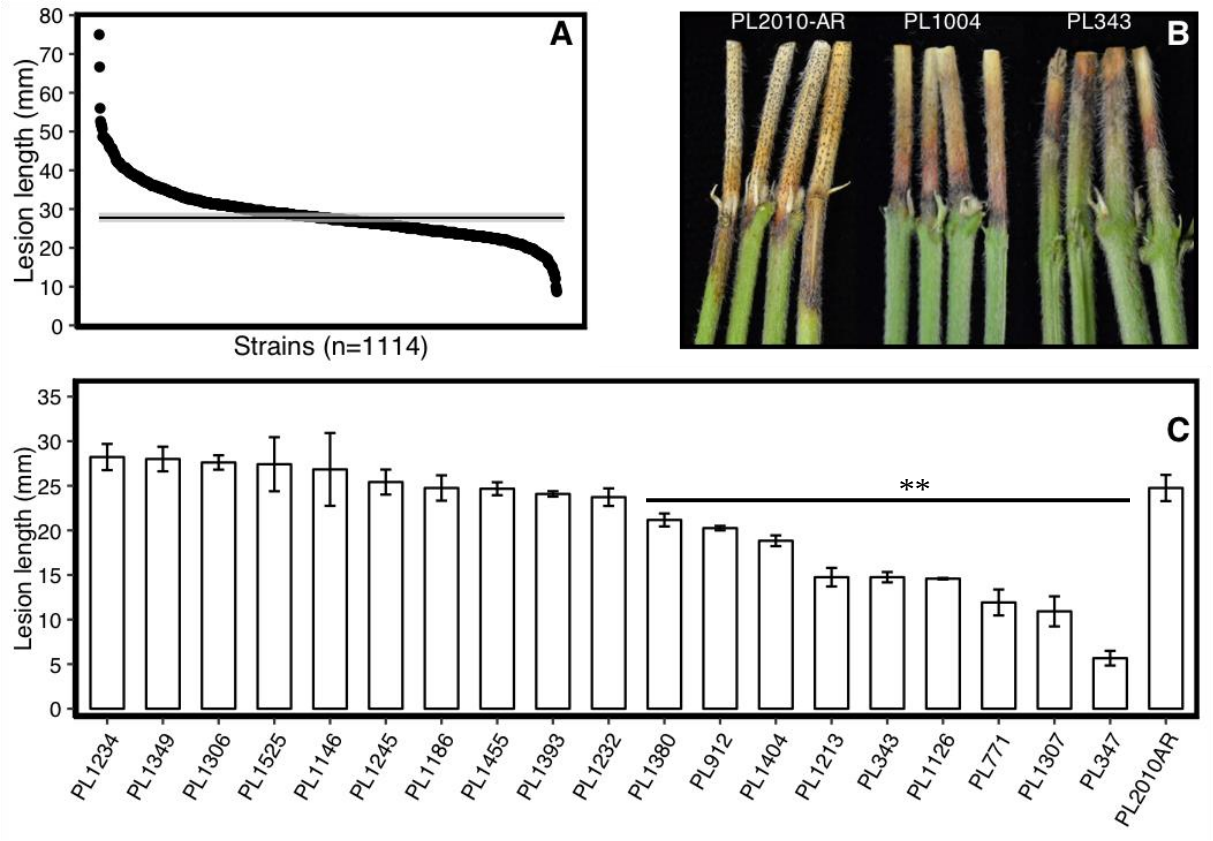

Figure 1. Lesion length on soybean stems inoculated with *P. longicolla*. Strains were inoculated on soybean using the cut stem protocol and lesions were measured ten days thereafter. **(A)** Mean lesion length of 1114 random insertional mutants (n=3), wild type (strain PL2010AR) mean is represented by a black line, respectively (n=79). **(B)** Pycnidiation and lesion on soybean stems inoculated with the wild-type strain PL2010AR, and the insertional mutants PL1004 and PL343. **(C)** Mean lesion length of selected mutants and wild type (n=3), error bars represent the standard error of the mean. *P* values were calculated with Dunnett's many-to-one test with wild type as reference. **Significantly different from wild-type strain ($P<0.01$) according to Dunnett's test.

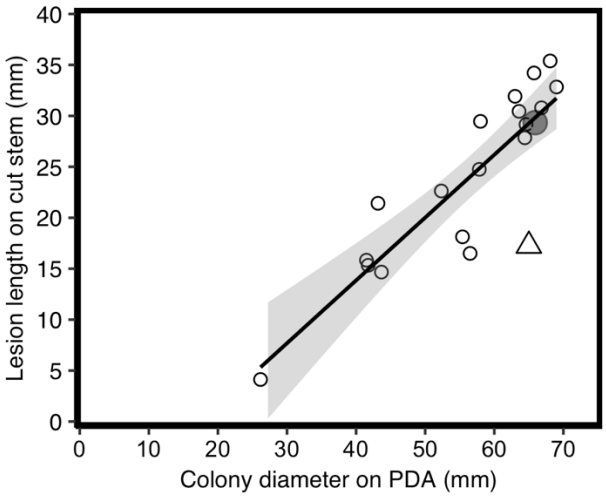

Figure 2. Relationship between colony diameter and lesion length. A significant correlation (R^2= 0.74, P<0.0001) was observed between radial growth and lesion length of 20 strains of *P. longicolla*, including the wild-type strain PL2010-AR **(gray filled circle)**, PL343 **(triangle)**, and other selected mutants **(white filled circle)**. Colony diameter was measured four days after inoculation on full strength PDA plates (n=3) incubated in the dark at room temperature and lesion length was measured ten days after inoculation on soybean cut stems (n=3). Both experiments were repeated once and their average used to compute the linear regression coefficient. Standard error is represented by the gray band around regression line.

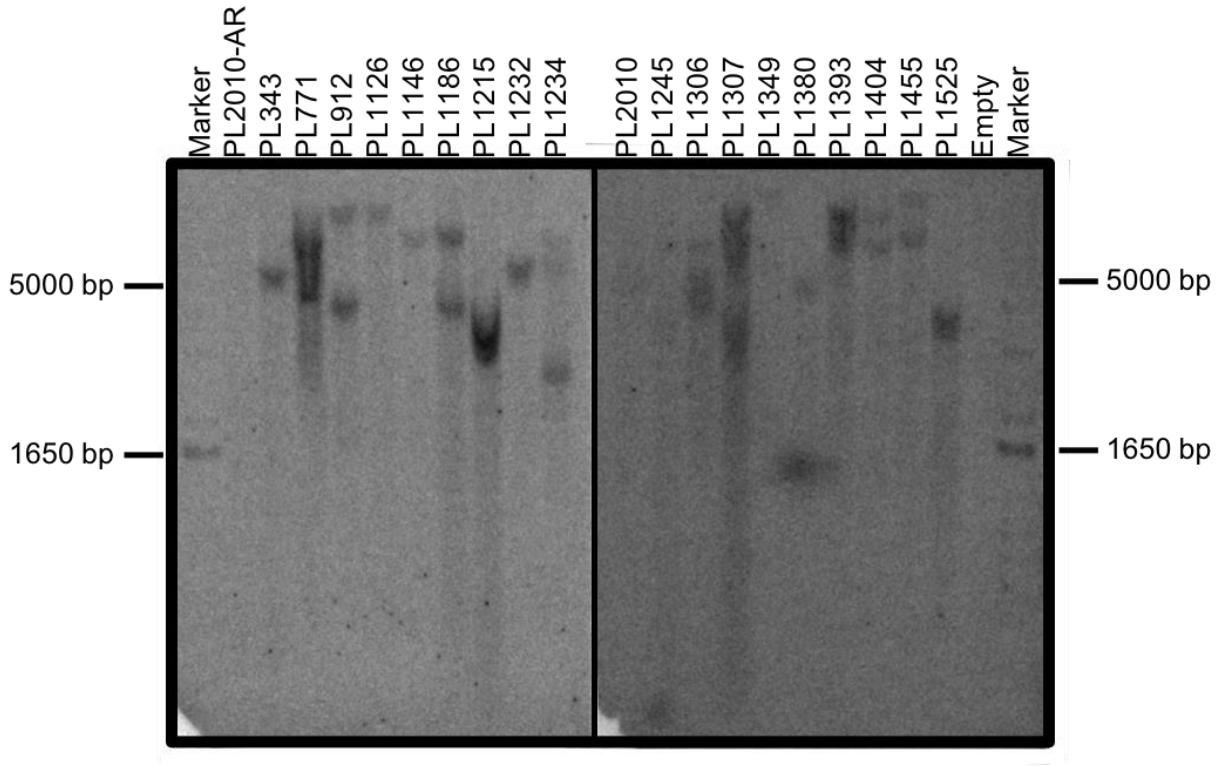

Figure 3. Southern blot of P. longicolla mutant strains.

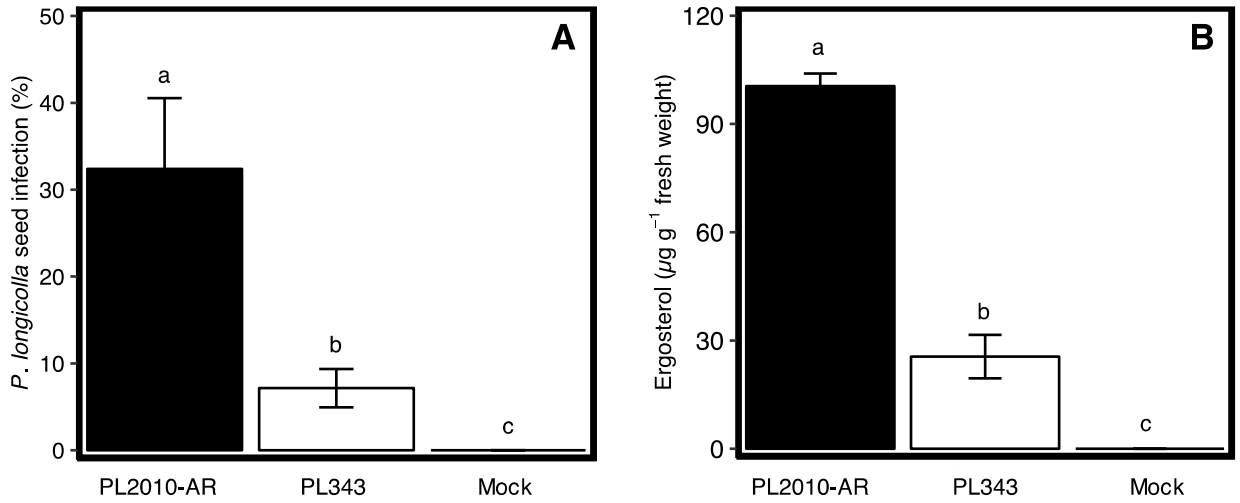

Figure 4. *P. longicolla* mutant PL343 has impaired seed infection and colonization. **(A)** Recovery rate of *P. longicolla* from soybean seeds. Whole plants were inoculated at early pod-filling stage and kept in a mist chamber for 48 hours immediately thereafter and once more at yellow pod stage. At harvest maturity, seeds were hand harvested and plated on full strength PDA after surface disinfestation. *P. longicolla* recovery rate was visually assessed five days thereafter. **(B)** Ergosterol content on soybean seeds inoculated in vitro with *P. longicolla*. All values for Mock were zero in both incidence and ergosterol measurements. Thus, Mock treatment was left out of statistical analyze. Bars with different letters are significantly different ($P<0.01$) according to Tukey's range test.

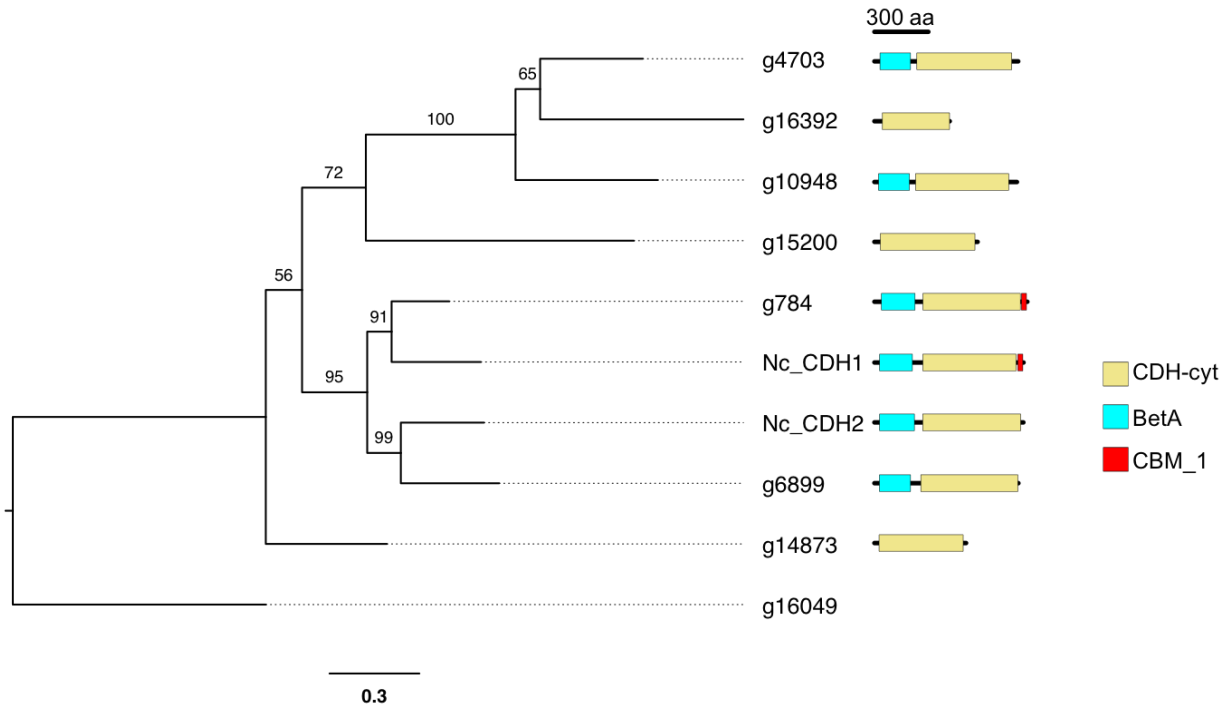

Figure 5. Maximum likelihood phylogenetic tree of *P. longicolla* proteins from the AA8 CAZyme family and *N. crassa CDH1* and *CDH2*. Conserved domain architecture is shown on the right. CDH-cyt: cytochrome domain of cellobiose dehydrogenase; BetA: Choline dehydrogenase; CBM_1: Fungal cellulose binding domain. Bootstrap support (100 replicates) are indicated on the branches. Tree was rooted on a CAZyme AA3 protein from *P. longicolla*.

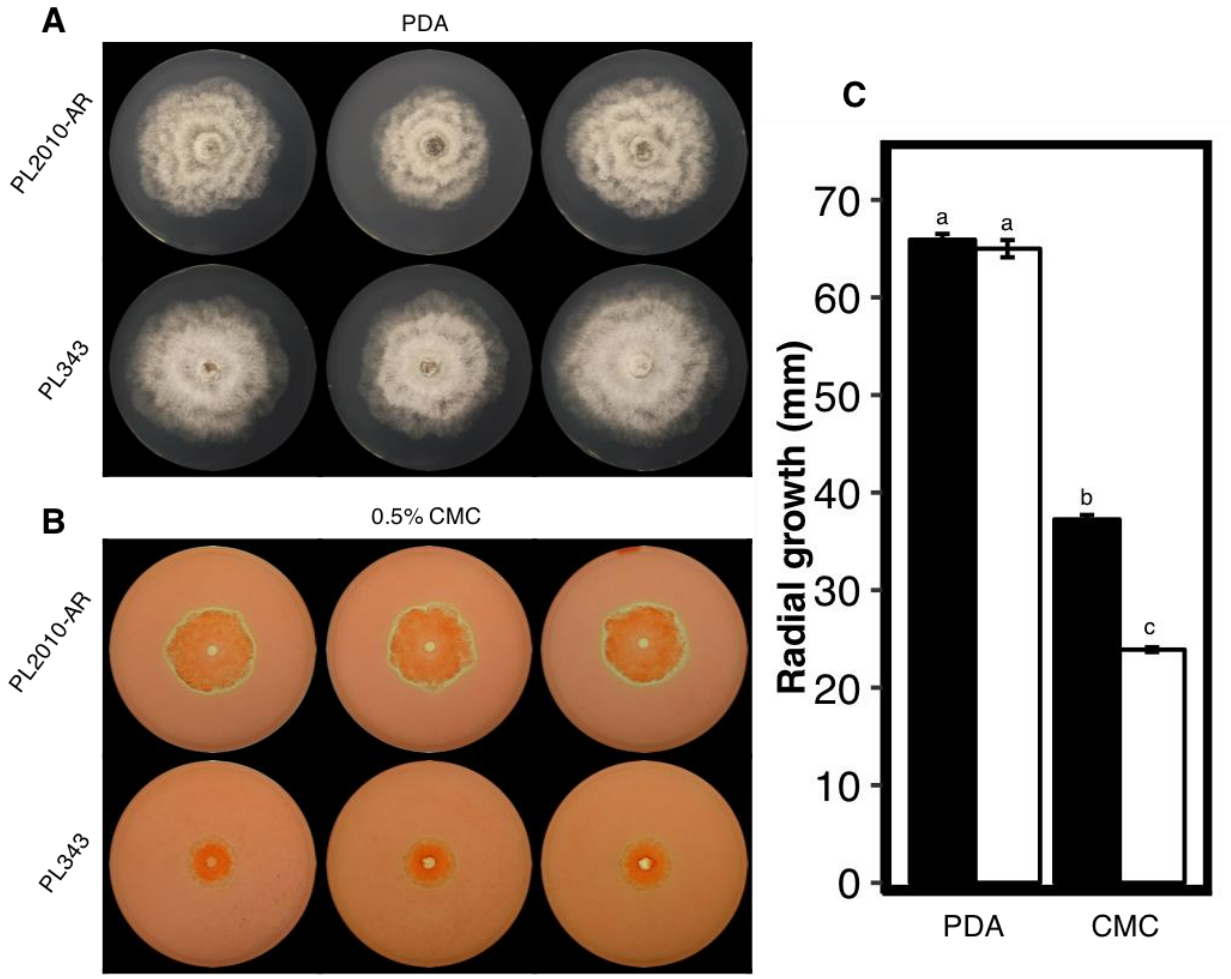

Figure 6. PL343 is hindered in radial growth relative to wild type on CMC (carboxymethyl cellulose) but not PDA (potato dextrose agar). PL2010-AR (wild type) and PL343 were grown on PDA **(A)** and 0.5% CMC **(B)** for 4 days in the dark at room temperature. 0.5% CMC plates were stained with Congo red after incubation. **(C)** Strains were center inoculated with a 5mm plug. Measurements were taken after 4-day incubation in the dark at room temperature. Letters indicate statistically significant differences between strains as determined by Tukey-Kramér test ($P < 0.05$).

Chapter V: MoNSTR-seq, a restriction site-associated DNA sequencing technique to characterize Agrobacterium-mediated transfer-DNA insertions in *Phomopsis longicolla*

Abstract

Phomopsis longicolla (Hobbs) causes Phomopsis seed decay and stem lesions in soybean (*Glycine max*). In this study, a novel, high-throughput adaptation of RAD-seq termed MoNSTR-seq (Mutation analysis via Next-generation DNA Sequencing of T-DNA Regions) was developed to determine the genomic location of T-DNA insertions in *P. longicolla* mutants. Insertional mutants were created via ATMT, and one mutant, strain PL343, was further investigated due to impaired stem lesion formation. MoNSTR-seq, in which DNA libraries are created with two distinct restriction enzymes and customized adapters to simultaneously enrich both T-DNA insertion borders, was developed to characterize the genomic lesion in strain PL343. MoNSTR-seq successfully identified a T-DNA insertion in the predicted promoter region of a gene encoding a cellobiose dehydrogenase (*CDH1*), and the position of the T-DNA insertion in strain PL343 was confirmed by Sanger sequencing. Thus, MoNSTR-seq represents an effective tool for molecular genetics in *P. longicolla,* and is readily adaptable for use in diverse fungal species.

Introduction

Forward genetic screens are a powerful tool for gene discovery and pathway dissection in filamentous fungi. Genetic screens have been used effectively to discover novel genes in plant pathogenic fungi such as *Fusarium graminearum*, *Colletotrichum higginsianum*, *Magnaporthe grisea*, and *Leptosphaeria maculan* (Idnurm and Howlett 2002; Seong et al. 2005; Gupta and Chattoo 2007; Korn et al. 2015). However, a key constraint with forward genetics is the ability to efficiently characterize genomic lesions in mutants. Numerous approaches have been

developed to define insertion sites of mutagenesis cassettes, including plasmid rescue (Tam and Lefebvre 1993), thermal asymmetric interlaced PCR (TAIL PCR; Dent et al. 2005), restriction enzyme site directed amplification PCR (Gonzalez-Ballester et al. 2005), 3'- rapid amplification of cDNA ends (Meslet-Cladiere and Vallon 2012), and site finding PCR (Li et al. 2012). These methods, however, have distinct limitations, particularly regarding throughput. With the advent of next-generation DNA sequencing, whole-genome re-sequencing at varying depths of coverage has been utilized successfully to identify genomic lesions in some species of fungi (Pomraning et al. 2011; Esher et al. 2015). However, costs currently associated with whole-genome resequencing often hinder the application of this approach to large collections of insertional mutants, and may be less effective for non-model organisms due to the limited availability of reference genome sequences.

Restriction Digestion Associated sequencing (RAD-seq) is a reduced representation sequencing strategy in which genomic regions flanking a specific restriction enzyme are selectively enriched for sequencing (Baird et al. 2008). The general workflow consists of digesting genomic DNA with a restriction enzyme, ligating oligonucleotide adapters to the digested DNA, enriching fragments containing the restriction site via PCR amplification, selecting fragments based on size, and sequencing fragments on a next-generation DNA sequencing platform. Distinct advantages of RAD-seq include flexibility regarding the selection of restriction enzymes, no requirement for a reference genome sequence *a priori*, and substantially higher throughput compared to whole-genome re-sequencing. RAD-seq has been widely adopted in taxonomically diverse organisms for population genetics (e.g., Hohenlohe et al. 2010; Cromie et al. 2013; Leboldus et al. 2015), plant breeding (Yang et al. 2011; Pfender et al. 2011), and, more recently, for gene discovery among insertional mutants of green algae

(Zhang et al. 2014). However, RAD-seq has not yet been adapted to characterize random insertional mutations in filamentous fungi.

Phomopsis longicolla is an important pathogen of soybean (Gomes et al. 2013; Mengistu et al. 2014). Although *P. longicolla* is generally associated with Phomopsis seed decay (PSD) in the U.S., it has been reported to cause serious stem canker diseases in other regions of the world (Cui et al. 2009). Despite its importance as a pathogen of soybean, the molecular underpinnings of pathogenesis in *P. longicolla* are unknown. Recently, new molecular resources have become available, including a protocol for genetic transformation (Li et al. 2013) and draft genome sequences for two isolates of *P. longicolla* (Li et al. 2015). However, neither molecular genetics nor functional genomics have been utilized to investigate the *P. longicolla*/soybean pathosystem.

In this study, insertional mutants of *P. longicolla* were created via *Agrobacterium*-mediated transformation, and one mutant was selected for further study based on reduced virulence on soybean stems. Subsequently, a protocol was created utilizing an adaptation of RAD-seq to determine the genomic location of T-DNA insertions in *P. longicolla* mutants. This novel approach, called MoNSTR-seq (Mutation analysis via Next-generation DNA Sequencing of T-DNA Regions), represents a significant advancement for molecular genetics in *P. longicolla* and has broad potential applicability to other fungal systems.

Materials and methods

Generation of *P. longicolla* mutants. Mutants of *P. longicolla*, including strain PL343, were created via *Agrobacterium tumefaciens*-mediated transformation (ATMT) from wild-type strain PL2010AR as previously described (Li et al. 2013). *A. tumefaciens* strain AGL-1 (Lazo et al. 1991) carrying pBHt2_sGFP, derived from pBHt2 (Mullins et al. 2001), was used for mutagenesis.

Southern blot analysis. Fungi were cultured in potato dextrose broth medium (PDB; BD Diagnostic Systems) for seven days at 80 RPM at room temperature. Fungal genomic DNA was isolated from dried tissue as described by Leslie and Summerell (2008). Southern blotting followed the protocol of Sambrook and Russell (2001). DNA was digested and probed as described by Li et al. (2013). The probe was labeled with ^{32}P and purified as described previously (Flaherty et al., 2003). Hybridizations were performed as described by Sambrook and Russell (2001). Following hybridization, blots were washed as described by Flaherty et al. (2003), exposed to a phosphorimaging screen, and visualized with a Typhoon FLA 9500 (GE Healthcare Bio-Sciences, Pittsburgh, PA, USA).

Pathogenicity assay. Fungal strains were evaluated for pathogenesis on soybean cultivar Hutcheson (Buss et al. 1988) with a slightly modified cut stem assay (Li et al. 2010). Fungal strains were grown on 0.2× strength PDA for 4 days in an incubator under 12:12 hours light-dark cycle at 25°C. Soybean plants were grown in 48-cell insert trays until the first trifoliate leaf was fully expanded (V2 stage of growth), at which point the stem was truncated 2 cm above the unifoliate leaf node. For inoculation, the wide end of a sterile micropipette tip (1-200 µl) was used to excise a colonized plug of 0.2× strength PDA medium. The micropipette tip containing the excised plug was placed in full contact with the cut stem (n= 12). After 10 days, the micropipette tip was removed and the length of necrotic lesion was measured starting from the edge of the cut stem.

Characterization of T-DNA insertions via MoNSTR-seq. MoNSTR-seq utilizes relatively rare endonuclease sites (AseI and BpuEI) located 91 and 94 base pairs from T-DNA left and right borders, respectively. RNA-free genomic DNA was extracted from strain PL343 with a CTAB method as described by Li et al. (2013). DNA (1 µg per reaction) was digested with AseI

or BpuEI (New England BioLabs, Ipswich, MA, USA) at 37 °C for 3 hours. Digested DNA was cleaned with a GeneJET gel extraction kit, followed by a DNA clean up microkit (Thermo Fisher Scientific, Waltham, MA, USA). Custom barcoded sequencing adapters were designed containing AseI and BpuEI sticky overhangs by modifying the Ion Torrent sequencing adapter (Integrated DNA Technologies, Coralville, IA, USA; **Table 1**). Two µl of 20 µM solutions of each adapter, 1_ AseI and 2_BpuEI, were ligated with T4 DNA ligase to digested DNA in separate ligation reactions for 10 minutes at room temperature. After the ligation step, another round of clean up was performed as described above to remove unligated adapters. The ligated DNA samples were then combined and fragmented with Fragmentase® followed by end repair as per manufacturer's instructions (New England BioLabs). The Ion Torrent sequencing adapter P1 obtained from Integrated DNA Technologies (Coralville, IA, USA) was ligated to the fragmented DNA with the NEBNext Fast DNA Library Prep Kit (New England BioLabs). The adapter-ligated DNA fragments were size selected for 480-bp fragments with Agilent AMPureXP beads (Beckman Coulter Inc., Brea, California, USA). Finally, the library was amplified with primers complimentary to the P1 adapter and the 1_ AseI or 2_BpuEI adapters with the following parameters: 95 °C for 30s, 14 cycles of 95 °C for 30s, 56 °C for 30s, and 72 °C for 30s, followed by 72 °C for 5 min. Following amplification, the template was sequenced with the Ion PGM platform with an Ion 314 V2 chip following the manufacturer's protocol. Reads were first mapped to the T-DNA cassette and then mapped to the *P. longicolla* MSPL 10-6 draft genome (Genbank accession AYRD00000000) using bwa version 0.7.10-r789 (Li and Durbin 2009) and processed using SAMtools version 0.1.18 (Li et al. 2009).

Results

To identify genes in *P. longicolla* associated with pathogenesis, a collection of ATMT mutants was screened with a cut stem assay (Li et al. 2010). Ten days after inoculation, PL343 caused stem lesions averaging 14.75 mm long, significantly (P<0.001) shorter than lesions caused the wild type-strain, which averaged approximately 24.74 mm **(Fig. 1A).** The growth of strain PL343 was significantly impaired when provided cellulose as a carbon source in a defined culture medium, yet was indistinguishable from the wild type on potato dextrose agar **(Fig. 1B)**.

The MoNSTR-seq protocol was developed to identify the site of T-DNA integration in strain PL343. Unique restriction enzyme sites were identified within 90-95 bp of the left and right borders of the mutagenesis cassette (**Fig. 2**). Genomic DNA from the mutant strain was digested and adapters with corresponding overhangs were ligated before sequencing the fragments **(Fig. 2)**. Thus, the libraries were designed to be enriched for sequences containing the break junction on either side of the mutagenesis cassette. A total of 0.5 million reads were obtained for strain PL343 from one Ion Torrent 314 chip. The T-DNA insertion site was identified by sequentially mapping reads first to the cassette and then to the draft genome of strain MSPL 10-6 (GenBank accession SAMN01162173; Li et al. 2015). A read spanning the right break junction was mapped to the genome. The T-DNA insertion was mapped to a site 511 bp upstream of the putative start codon of a gene predicted to encode a cellobiose dehydrogenase homologous to *CDH1* of *Neurospora crassa* (**Fig. 3A**). Southern blot analysis indicated the presence of a single T-DNA insertion in strain PL343 **(Fig. 3B)**. The T-DNA insertion discovered via MoNSTR-seq was validated by PCR with primers flanking the putative insertion site. The difference in band size between the wild type and PL343 was consistent with the length of the insertion cassette **(Fig. 3C)**. Sanger sequencing of the PCR products confirmed the

position of the T-DNA insertion and revealed a deletion of 87 bp from the left border of the cassette. This deletion likely accounts for the absence of reads mapping to the left border junction in the *P. longicolla* genome.

Discussion

The T-DNA insertion in the putative promoter of *CDH1* in strain PL343 provides a plausible explanation for the mutant's phenotype. The impaired capability of this mutant to induce necrosis on soybean stems, of which the predominant carbohydrate is cellulose, implicates *CDH1* in cellulose catabolism and pathogenesis. Cellobiose dehydrogenase enzymes, such as those encoded by putative orthologs of *CDH1*, have long been associated with cellulose degradation (Ayers et al., 1978). The recent discovery that cellobiose dehydrogenases act in concert with lytic polysaccharide monooxygenases via an oxidative mechanism to depolymerize cellulose (Tan et al., 2015) suggests that this specific mechanism of cellulose catabolism may be paramount for carbohydrate acquisition in *P. longicolla* during pathogenesis. However, a thorough functional characterization of *CDH1* in *P. longicolla* will require additional effort, including targeted gene disruption and complementation assays.

MoNSTR-seq represents a distinct improvement over genome walking (Shyamala and Ames 1989) and plasmid rescue (Tam and Lefebvre 1993), two methods commonly used for insertion site determination in filamentous fungi. MoNSTR-seq is relatively inexpensive and simple to perform, allows high throughput characterization of mutants, and is adaptable to various next-generation DNA sequencing platforms. Additionally, MoNSTR-seq could readily be adapted to detect a wide range of cassette truncation scenarios, a major limitation of current gene discovery methods, including a recent RAD-seq derived technique in *Chlamydomonas* (ChlaMmeseq; Zhang et al, 2014). For example, combining long-read DNA sequencing and a

rare endonuclease site in the T-DNA would enable MoNSTR-seq to overcome large T-DNA truncation events. Alternatively, short-read technologies coupled with multiple endonuclease sites could be used to address the same constraint. Although in this paper a single mutant strain was investigated, MoNSTR-seq can be used in high-throughput genotyping of mutant pools using barcoded adapters. With T-DNA break junction enrichment, MoNSTR-seq circumvents whole genome re-sequencing, which increases throughput, and decreases per-strain sequencing expenses.

Additional advantages of MoNSTR-seq include the ability to obtain a considerable amount of sequence data spanning T-DNA insertion sites, which is particularly useful when T-DNA insertion occurs in a repetitive region. In principle, MoNSTR-seq is not affected by genome complexity or size, and it also dispenses the need of a draft genome. Additionally, the method can be widely adapted to existing fungal mutant collections generated using T-DNA insertion. However, MoNSTR-seq is not likely to identify whole-plasmid insertions due to its dependence upon targeted endonuclease-sites within the T-DNA.

On the whole, MoNSTR-seq makes the characterization of T-DNA break junctions in *P. longicolla* mutants created via ATMT more affordable and technically accessible. This technique facilitates the application of forward genetics as a tool for gene discovery in *P. longicolla*. Relatively minor modifications of MoNSTR-seq should accelerate gene discovery in collections of ATMT-derived mutants in a myriad of organisms.

Literature cited

Ayers, A., Ayers, S. and Eriksson, K.-E.L. 1978. Cellobiose oxidase purification and partial characterization of a hemoprotein from *Sporotrichum pulverulentum*. Eur J Biochem. 90:171-181

Baird, N.A., Etter, P.D., Atwood, T.S., Currey, M.C., Shiver, A.L., Lewis, Z.A., Selker, E.U., Cresko, W.A. and Johnson, E.A. 2008. Rapid SNP discovery and genetic mapping using sequenced RAD markers. PloS One 3:e3376

Bates, D., Mächler, M., Bolker, B., and Walker, S. 2015. Fitting Linear Mixed-Effects Models Using lme4. Journal of Statistical Software 67:1-48

Buss, G. R., Camper, H. M., and Roane, C. W. 1988. Registration of "Hutcheson" soybean. Crop Sci. 28:1024-1025

Cromie, G.A., Hyma, K.E., Ludlow, C.L., Garmendia-Torres, C., Gilbert, T.L., May, P., Huang, A.A., Dudley, A.M. and Fay J.C. 2013. Genomic sequence diversity and population structure of *Saccharomyces cerevisiae* assessed by RAD-seq. Genes Genomes Genetics 3:2063-2172

Cui, Y.-L., Duan, C.-X., Wang, X.-M., Li, H.-J., and Zhu, Z.-D. 2009. First report of *Phomopsis longicolla* causing soybean stem blight in China. Plant Pathol. 58:799-799

Dent, R.M., Haglund, C.M., Chin, B.L., Kobayashi, M.C. and Niyogi, K.K. 2005. Functional genomics of eukaryotic photosynthesis using insertional mutagenesis of *Chlamydomonas reinhardtii*. Plant Physiol. 137:545-556

Esher, S.K., Granek, J.A. and Alspaugh, J.A. 2015. Rapid mapping of insertional mutations to probe cell wall regulation in *Cryptococcus neoformans*. Fungal Genet Biol. 82:9-21

Flaherty, J.E., Pirttila, A.M., Bluhm, B.H. and Woloshuk, C.P. 2003. PAC1, a pH-regulatory gene from *Fusarium verticillioides*. Appl Environ Microbiol. 69:5222-5227

Gomes, R. R., Glienke, C., Videira, S. I. R., Lombard, L., Groenewald, J. Z., and Crous, P. W. 2013. *Diaporthe*: a genus of endophytic, saprobic and plant pathogenic fungi. Persoonia: Mol Phylogeny Evol Fungi 31:1-41

González-Ballester, D., Montaigu, A., Galván, A. and Fernández, E. 2005. Restriction enzyme site-directed amplification PCR: a tool to identify regions flanking a marker DNA. Anal Biochem. 340:330-335

Gupta, A., and Chattoo, B. B. 2007. A novel gene MGA1 is required for appressorium formation in *Magnaporthe grisea*. Fungal Genet Biol. 44:1157-1169

Hohenlohe, P.A., Bassham, S., Etter, P.D., Stiffler, N., Johnson, E.A., and Cresko, W.A. 2010. Population Genomics of Parallel Adaptation in Threespine Stickleback using Sequenced RAD Tags. PloS Gen. 6:e1000862

Idnurm, A., and Howlett, B. J. 2002. Isocitrate lyase is essential for pathogenicity of the fungus *Leptosphaeria maculans* to canola (*Brassica napus*). Eukaryot Cell 1:719-724

Korn, M., Schmidpeter, J., Dahl, M., Müller, S., Voll, L. M., and Koch, C. 2015. A genetic screen for pathogenicity genes in the hemibiotrophic fungus *Colletotrichum higginsianum* identifies the plasma membrane proton pump Pma2 required for host penetration. PLoS One 10:e0125960

Lazo, G. R., Stein, P. A., and Ludwig, R. A. 1991. A DNA transformation-competent *Arabidopsis* genomic library in Agrobacterium. Biotechnol Nat Publ Co. 9:963-967

Leboldus, J.M., Kinzer, K., Richards, J., Ya, Z., Yan, C., Friesen, T.L. and Brueggeman, R. 2015. Genotype-by-sequencing of the plant-pathogenic fungi *Pyrenophora teres* and *Sphaerulina musiva* utilizing Ion Torrent sequence technology. Mol Plant Pathol. 16:623-632

Leslie, J. F., and Summerell, B. A. 2008. The Fusarium laboratory manual. John Wiley & Sons.

Li, H., and Durbin, R. 2009. Fast and accurate short read alignment with Burrows-Wheeler transform. Bioinformatics 25:1754-1760.

Li, H., Handsaker, B., Wysoker, A., Fennell, T., Ruan, J., Homer, N., Marth, G., Abecasis, G., Durbin, R., and 1000 Genome Project Data Processing Subgroup. 2009. The sequence alignment/map format and SAMtools. Bioinformatics 25:2078-2079

Li, S., Hartman, G. L., and Boykin, D. L. 2010. Aggressiveness of *Phomopsis longicolla* and Other *Phomopsis spp*. on Soybean. Plant Dis. 94:1035-1040

Li, X., Moelleringa, E.R., Liu, B., Johnny, C., Fedewac, M., Sears, B.B., Kuoc, M.H. and Benning, C. 2012. A galactoglycerolipid lipase is required for triacylglycerol accumulation and survival following nitrogen deprivation in *Chlamydomonas reinhardtii*. Plant Cell 24:4670-4686

Li, S., Ridenour, J. B., Kim, H., Hirsch, R. L., Rupe, J. C., and Bluhm, B. H. 2013. *Agrobacterium tumefaciens*-mediated transformation of the soybean pathogen *Phomopsis longicolla*. J. Microbiol. Methods. 92:244-245

Li, S., Song, Q., Ji, P., and Cregan, P. 2015. Draft genome sequence of *Phomopsis longicolla* type strain TWH P74, a fungus causing phomopsis seed decay in soybean. Genome Announc. 3:e00010-15

Mengistu, A., Castlebury, L. A., Morel, W., Ray, J. D., and Smith, J. R. 2014. Pathogenicity of *Diaporthe spp*. isolates recovered from soybean (*Glycine max*) seeds in Paraguay. Can. J. Plant Pathol. 36:470-474

Meslet-Cladière, L. and Vallon, O. 2012. A new method to identify flanking sequence tags in *Chlamydomonas* using 3′-RACE. Plant Methods 8:21

Mullins, E. D., Chen, X., Romaine, P., Raina, R., Geiser, D. M., and Kang, S. 2001. *Agrobacterium*-Mediated Transformation of *Fusarium oxysporum*: An Efficient Tool for Insertional Mutagenesis and Gene Transfer. Phytopathology 91:173-180

Pfender, W.F., Saha, M.C., Johnson, E.A. and Slabaugh, M.B. 2011. Mapping with RAD (restriction-site associated DNA) markers to rapidly identify QTL for stem rust resistance in *Lolium perenne*. Theor and Appl Genet. 122:1467-1480

Pomraning, K.R., Smith, K.M. and Freitag, M. 2011. Bulk Segregant Analysis Followed by High-Throughput Sequencing Reveals the *Neurospora* Cell Cycle Gene, ndc-1, To Be Allelic with the Gene for Ornithine Decarboxylase, spe-1. Eukaryotic Cell 10:724-733

R Core Team. R: A Language and Environment for Statistical Computing. 2019. Vienna, Austria. URL https://www.R-project.org/

Sambrook, J., and Russell, R.W. 2001. *Molecular cloning: A laboratory manual*, 3rd ed. Cold spring harbor laboratory press, Cold Spring Harbor, N.Y.

Seong, K., Hou, Z., Tracy, M., Kistler, H. C., and Xu, J.-R. 2005. Random insertional mutagenesis identifies genes associated with virulence in the wheat scab fungus *Fusarium graminearum*. Phytopathology 95:744-750

Shyamala V. and Ames, G.F. 1989. Genome walking by single-specific-primer polymerase chain reaction: SSP-PCR. Gene 84**:**1-8

Tam, L.W. and Lefebvre, P.A. 1993. Cloning of flagellar genes in *Chlamydomonas reinhardtii* by DNA insertional mutagenesis. Genetics 135:375-384

Tan, T.C., Kracher, D., Gandini, R., Sygmund, C., Kittl, R., Haltrich, D., Hällberg, B.M., Ludwig, R., and Divne, C. 2015. Structural basis for cellobiose dehydrogenase action during oxidative cellulose degradation. Nat Comm. 6:7542

Yang, H., Tao, Y., Zheng, Z., Li, C., Sweetingham M.W. and Howieson, J.G. 2011. Application of next-generation sequencing for rapid marker development in molecular plant breeding: a case study on anthracnose disease resistance in *Lupinus angustifolius* L. BMC Genomics 13:318

Zhang, R., Patena, W., Armbruster, U., Gang, S.S., Blum, S.R. and Jonikas, M.C. 2014. High-Throughput Genotyping of Green Algal Mutants Reveals Random Distribution of

Mutagenic Insertion Sites and Endonucleolytic Cleavage of Transforming DNA. The Plant Cell 26, 1398-1409

Tables

Table 1. Sequences of the modified duplex A-adapters (1_AseI and 2_BpuEI) containing the restriction enzyme overhang, and the adapter P1 used for library preparation in MoNSTR-seq. The letters in bold represent barcodes to distinguish the enzyme sites. *represents Phosphorothioate bonds that prevent action of exo- and endonucleases.

Adapter name	Sequence
A-Adapter	5’ TAATCGTT**ACCTTAGC**TGAGTCGGAGACACGCAGGGATGAGATGG*T*T 3’
1_ASEI	5’ CCATCTCATCCCTGCGTGTCTCCGACTCA**GCTAAGGT**AACGAT 3’
A-Adapter	5’ ATCGTT**CTCCTTAC**TGAGTCGGAGACACGCAGGGATGAGATGG*T*T 3’
2_BpuEI	5’ CCATCTCATCCCTGCGTGTCTCCGACTCA**GTAAGGAG**AACGATTC 3’
Adapter P	5' CCACTACGCCTCCGCTTTCCTCTCTATGGGCAGTCGGTGAT 3’ 5' ATCACCGACTGCCCATAGAGAGGAAAGCGGAGGCGTAGTGGT*T* 3’

Figures

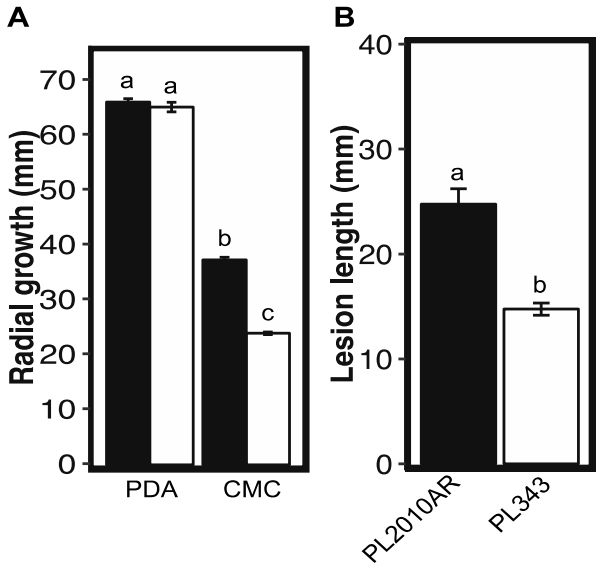

Figure 1. Phenotypic characterization of *P. longicolla* mutant strain PL343. **(A)** Radial growth of strain PL2010AR (wild type; black bars) and mutant strain PL343 (white bars) on potato dextrose agar and carboxymethyl cellulose agar (n= 6). **(B)** Length of necrotic lesions measured 10 days after inoculation on cut soybean stems (n= 12). Letters above bars, in the same plot, indicate significant difference (P<0.001) according to Tukey-Kramer mean test. Error bars represent the standard error of the mean. Statistical test was performed with lme4 (Bates et al. 2015) package in R (R Core Team, 2019) with radial growth and lesion length treated as Gamma distributed variables.

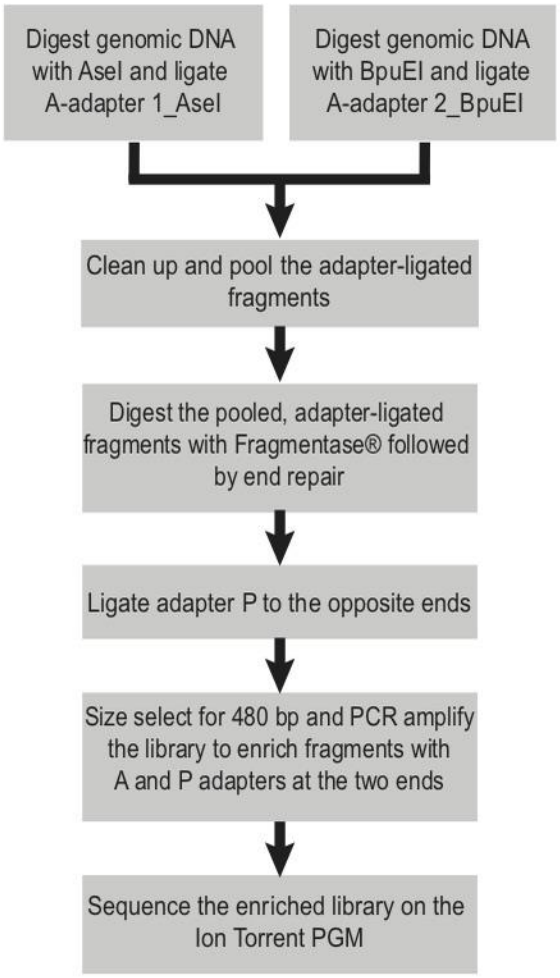

Figure 2: Step-by-step illustration of MoNSTR-seq used to identify a T-DNA break junction in the *P. longicolla* strain PL343.

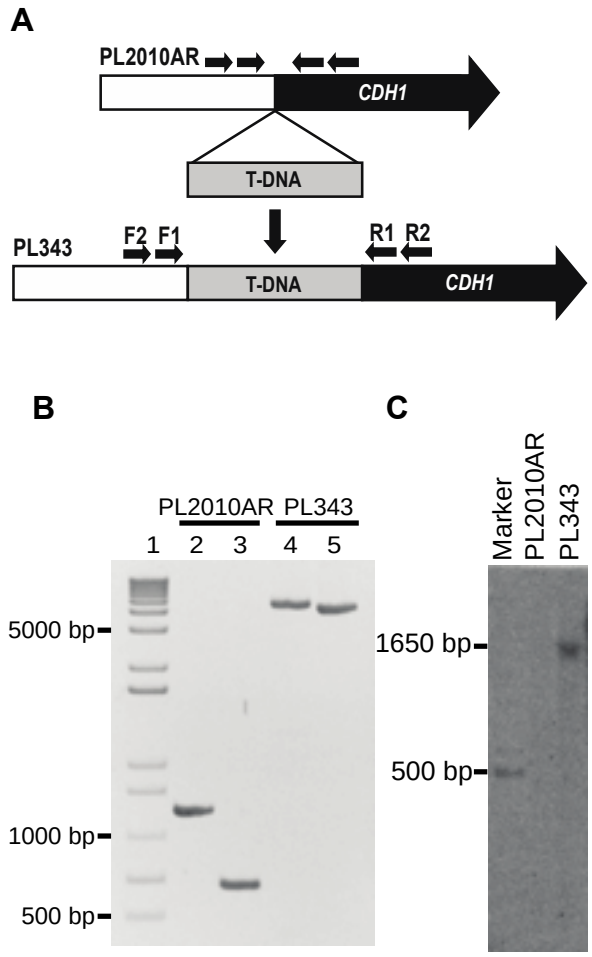

Figure 3: Confirmation of the T-DNA insertion site identified via MoNSTR-seq in the genome of strain PL343. **(A)** Cartoon depicting the T-DNA insertion in strain PL343, including PCR primers designed to flank the predicted insertion site. **(B)** PCR amplification with PCR primers flanking the T-DNA insertion in strain PL343. **(C)** Southern blot indicating the presence of a single T-DNA insertion in strain PL343. Strain PL2010AR was the wild type used in this study.

Chapter VI: *HAP3*, a component of the CCAAT-binding complex of *Phomopsis longicolla*, regulates pathogenesis during infection of soybean

Abstract

Phomopsis longicolla (Hobbs) causes Phomopsis seed decay, one of the most prevalent and potentially damaging diseases of soybean seed. Currently, little is known about the molecular basis of pathogenesis in *P. longicolla*, in part because crucial tools for molecular genetics, such as targeted gene deletion, have not been demonstrated in this organism. In other filamentous fungi, the heterotrimeric CCAAT-binding complex is involved in diverse aspects of growth and development, including secondary metabolism, morphogenesis, and pathogenesis. In this study, a putative component of the CCAAT-binding complex (*HAP3*) was identified and characterized in *P. longicolla*. The *HAP3* gene was successfully deleted via homologous recombination, and the mutant was genetically complemented via reintroduction of the wild-type gene. *HAP3* deletion strains did not produce pycnidia or conidia and were substantially impaired in radial growth. In addition, deletion of *HAP3* significantly reduced *P. longicolla* pathogenicity on soybean seeds and stems. Expression profiling during colonization of soybean seeds identified 2353 genes differentially regulated following deletion of *HAP3*, including genes predicted to encode plant biomass degrading enzymes, effector proteins, and structural and enzymatic components of secondary metabolism. This study established the involvement of the CCAAT-binding complex in *P. longicolla* pathogenesis and demonstrated the feasibility of targeted gene deletion in this organism. Phenotypic similarities between *HAP3* deletion mutants of *P. longicolla* and other filamentous fungi suggest a broad involvement of the CCAAT-binding complex in fungal growth, development, and pathogenesis.

Introduction

Phomopsis longicolla Hobbs (synonym = *Diaporthe longicolla*) is the primary causal agent of Phomopsis seed decay (PSD) of soybean (Hobbs et al. 1985). Soybean seeds affected by PSD are typically shriveled, cracked, chalky, and/or discolored, although symptomless infection can occur when environmental conditions are not conducive for symptom development (Sinclair 1993; Hepperly 1978; Sinclair 1992). PSD reduces seed quality by decreasing seed germination and vigor (Zorrilla et al. 1994). Infected seeds are unable to germinate or germinate poorly, potentially giving rise to infected seedlings with significantly increased rates of pre- and post-emergence damping-off under disease-conducive conditions (Nicholson 1972). PSD affects soybean seed quality in most soybean-growing regions of the world. In the U.S., PSD is particularly problematic in the Mid-South where hot and humid conditions during seed maturation can favor disease development (Kmetz et al. 1979; Rupe 1990). PSD has caused significant economic losses over the past few decades throughout U.S. soybean production regions and has received widespread attention in the Mid-South due to increased usage of early soybean production system (ESPSs) (Wrather et al. 2003, 2004; Mengistu and Heatherly 2006). ESPSs focus on planting early-maturing cultivars early in the spring to avoid late-season droughts that periodically impact the Mid-South; however, soybean seed maturation in ESPSs typically occurs in August, when heat and humidity are ideal for PSD (Egli et al. 2005; TeKrony et al. 1983).

To date, the molecular basis of pathogenesis underlying PSD is poorly understood, in large part due to the unavailability of crucial genetic and genomic resources for *P. longicolla* or related species within the genus. In recent years, significant advancements have been made in support of molecular genetics and functional genomics approaches in *P. longicolla*, including

protocols for genetic transformation (Li et al. 2013) and characterization of T-DNA insertions (Zaccaron et al. 2018), draft genome sequences for two isolates of the pathogen, including the type strain (Li et al. 2014, 2015), and a predicted interactome of protein models (Li et al. 2018). In addition, draft genome sequences are available for *D. helianthi* (Baroncelli et al. 2016), two isolates of *D. ampelina* (Savitha et al. 2016), an unidentified *Diaporthe sp*. (de Sena Filho et al. 2016), and the causal agent of southern stem canker of soybean, *D. aspalathi* (synonym = *Diaporthe phaseolorum var. meridionalis*; Li et al. 2016). Recently, a targeted gene deletion approach utilizing *Agrobacterium tumefaciens* was successfully employed to functionally characterize *DhPKS1* in *D. helianthi* (Ruocco et al. 2018). However, the ability to perform functional genomics in *P. longicolla*, particularly reverse genetics via targeted gene deletion, has not been reported thus far.

The heterotrimeric CCAAT-binding complex (CBC) of eukaryotes is broadly conserved in animals, plants, and fungi (McNabb and Pinto 2005; Edwards et al. 1998; Becker et al. 1991). The fungal CBC was originally described in *Saccharomyces cerevisiae* as the Hap regulatory complex and found to consist of three core subunits: Hap2, Hap3, and Hap5 (Olesen et al. 1987; McNabb et al. 1995). More recently, a fourth subunit of the CBC exclusive to fungi, HapX, has been identified and characterized in filamentous Ascomycetes (Tanaka et al. 2002; Jung et al. 2010). In fungi, all three core components must be present for the functionality of the complex (Ridenour and Bluhm 2014; McNabb et al. 1995). The CBC is a key regulator of iron acquisition and homeostasis (Chakravarti et al. 2017) and the shift from fermentation to aerobic respiration in yeast (McNabb and Pinto 2005). In filamentous fungi, the CBC has been implicated as a regulator of responses to oxidative stress, secondary metabolism, and plant

pathogenesis (Ridenour and Bluhm 2014; Hong et al. 2013; Yin and Keller 2011; Thön et al. 2010).

The objective of this study was to identify potential mechanisms underlying pathogenesis in *P. longicolla*. To this end, *HAP3*, which encodes the ortholog the CBC subunit Hap3, was identified in *P. longicolla* and targeted for deletion using a reverse genetics approach. Subsequently, *HAP3* deletion mutants were evaluated for defects in growth, development, and pathogenicity. Additionally, gene expression profiling was performed to determine how deletion of *HAP3* impacts transcriptional reprogramming during colonization of soybean seeds.

Materials and Methods

***P. longicolla* strains, soybean plants, and growing conditions**. The wild-type strain PL2010AR, described previously (Li et al. 2013), was utilized due to pronounced virulence and amenability to genetic transformation. The *HAP3* ortholog was identified as described below and deleted in strain PL2010AR to create strains PLH100 and PLH101. The wild-type copy of the *HAP3* locus was reintroduced into strain PLH101 to create the genetically complemented strain PLH101C. Each strain was single-spore purified on its respective selective medium and routinely sub-cultured every 10-14 days on V8 agar with antibiotics to maintain selection of deletion or complementation strains. Radial growth rates were assessed by center-inoculating 6-mm colonized-PDA plugs on three Petri dishes containing potato dextrose agar (PDA), V8, or complete medium (Correll 1987; Leslie and Summerell 2006). Cultures were incubated in 12:12 h light-dark cycles at 25°C. The diameter of each colony was measured four days after inoculation. To assess pycnidiation and conidiation, each strain was cultured on three oatmeal agar plates (OMA; Becton Dickinson and Company, Franklin Lakes, NJ, USA) for 14 days at

25°C in a 12:12 h light-dark cycle. All strains were stored as blocks of colonized PDA suspended in 30% glycerol (*v*:*v*) at -80°C.

The fast-maturing soybean cultivar 'Traff' (PI 470930; maturity group 000) was used to assess pathogenicity of *P. longicolla* strains and the differential gene expression experiment. Seeds were surface disinfested for 30 seconds in 70% ethanol followed by 30 seconds in 0.5% sodium hypochlorite and thoroughly rinsed in sterile deionized water before they were sown into flats containing pasteurized potting mixture (Metro-Mix 900; Sun Gro Horticulture, Agawam, MA, USA) in greenhouses at the University of Arkansas - Fayetteville. Healthy and vigorous seedlings were individually transplanted to four-inch pots four days after emergence. The greenhouse temperature was maintained at 20-26°C, with a 14:10 h light-dark cycle. To maximize conditions for production of healthy seeds, plants were watered as needed by flooding the trays containing the pots to avoiding wetting plant canopies.

Identification of *HAP3* in *P. longicolla*. The draft assembly and predicted gene models of *P. longicolla* strain MSPL10-6 (Li et al. 2014) were obtained at http://bioinformatics.towson.edu/Phomopsis_longicolla/Download.aspx, accessed: April 2018. The amino acid sequence of *HAP3* from *Fusarium verticillioides* (Ridenour and Bluhm 2014) was used as the query in homology searches with BLASTp (Altschul et al. 1997) to identify the corresponding homologs in *P. longicolla* and other species. The *P. longicolla HAP3* homolog was manually curated by mapping the amino acid sequence of *F. verticillioides HAP3* to the *P. longicolla* genome with Exonerate v2.2 (Slater and Birney 2005). Introns within *HAP3* of *P. longicolla* were predicted by analyzing the splicing patterns of RNA-seq reads mapped to the *P. longicolla* genome. The species phylogenetic tree was constructed based on 20 universal single-copy orthologs (USCOs) conserved among the analyzed taxa identified with BUSCO v2 (Simão

et al. 2015). Protein sequences of USCOs were individually aligned with ClustalOmega v1.2.3 (Sievers et al. 2011) and gaps were removed with trimAl v1.2 (Capella-Gutiérrez et al. 2009). Alignments were concatenated and a tree was inferred with RAxML v8.2.11 (Stamatakis 2014) with settings adjusted to perform 100 rapid bootstrap replicates and to automatically select the protein substitution model. Amino acid conservation among *HAP3* orthologs was evaluated with local and global alignments constructed with the Smith-Waterman (Smith and Waterman 1981) and Needleman-Wunsch (Needleman and Wunsch 1970) algorithms, respectively, implemented within the EMBOSS suite v6.6.0 (Rice et al. 2000). Protein sequences of *HAP3* orthologs were queried against the NCBI conserved domains database (CDD) v3.16 (Marchler-Bauer et al. 2017) for the identification of the histone-like conserved domain.

Creation of plasmids for targeted deletion and genetic complementation of *HAP3*. Binary vector pCambia2301(CAMBIA Institute; http://www.cambia.org/, accessed: January 2017) was modified by replacing elements between the left and right borders at XhoI and BstEII restriction sites with *hpt* and s*GFP* cassettes flanked by multiple cloning sites (MCS). The resulting plasmid was designated pBYR14. Subsequently, regions upstream (5' flank; 756 bp) and downstream (3' flank; 760 bp) of the predicted *P. longicolla HAP3* open reading frame were inserted into the two MCS regions of pBYR14 to create the gene replacement construct. The 5' flank was amplified from genomic DNA of wild-type *P. longicolla* strain PL2010AR with primers PlHAP3-KpnI-F1/ PlHAP3-ApaI-F2, which introduced KpnI and ApaI restriction sites for directional cloning into the first MCS of pBYR14. Similarly, the 3' flank was amplified by PlHAP3-PacI-F3/ PlHAP3-HindIII-F4 which introduced PacI and HindIII restriction sites for directional cloning into the second MCS of pBYR14. The plasmid carrying the *P. longicolla HAP3* replacement construct was designated pBYR61. To create the *HAP3* complementation

construct, plasmid pCambia2301 was modified to convey geneticin resistance, thus resulting in pBYR48. The *HAP3* gene, including 1000 bp upstream of the predicted start codon and 776 bp downstream from the predicted stop codon, was amplified with primers PacI-PlHAP3-5'F/ PlHAP3-HindIII-F4, which incorporated PacI and HindIII sites into the ends of the amplicon. The resulting product was cloned into the PacI and HindIII sites of pBYR48 to create plasmid pBYR62. The sequences of all primers used in this study are presented in **Table 1**.

Targeted deletion of *HAP3* in *P. longicolla*. To delete *HAP3*, hyphal fragments of *P. longicolla* strain PL2010AR were transformed with pBYR61 via *Agrobacterium*-mediated transformation with strain AGL1 (Lazo et al. 1991), following a previously described protocol (Li et al. 2013). Putative transformants were grown on selective medium containing 75 µg/ml of hygromycin B and screened by PCR to confirm targeted deletion of the *HAP3* gene. Primers PLHAP3_PF/PLHAP3_PR were used to screen for the presence of *HAP3*, and PacI_PLHAP3_5'F/HYGSCRN-A and GFPF/PLHAP3_A2 were used to assess the targeted integration of the knock-out cassette. The potential presence of additional, ectopic insertions was assessed by Southern blot analysis, as described below.

Southern blotting. Tissue was obtained from cultures grown in yeast extract peptone dextrose (YEPD; Murthy et al. 1975) for 5 days on an orbital shaker at 80 RPM at room temperature. Fungal genomic DNA was isolated with a modified cetyltrimethylammonium bromide method (Leslie and Summerell 2006). Southern blots were prepared essentially as described by Sambrook and Russell (2001). Briefly, genomic DNA was digested with KpnI and XcmI (New England Biolabs, Ipswich, MA, USA) and probed for the hygromycin B resistance gene *hph*. The probe consisted of 350 bp from the open reading frame of *hph*. The probe was obtained by PCR amplification with primers HYGF/HYGR followed by purification with GeneJet Gel

Extraction Kit (Thermo Fisher Scientific, Waltham, MA, USA). The probe was then labeled with ^{32}P and hybridization was performed as described by Sambrook and Russell (2001). After probing, blots were washed as described by Flaherty et al. (2003) and visualized with a Typhoon FLA 9500 (GE Healthcare Bio-Sciences, Pittsburgh, PA, USA).

Pathogenicity assays. The ability of strains to cause necrotic lesions on soybean stems and to colonize soybean seeds was estimated with a cut stem assay as described by Li et al. (2010). Briefly, stems of soybean plants (cultivar Traff) were clipped two cm above the first node at the V2 developmental stage and inoculated with a colonized PDA plug held in place by a 1-200µl disposable pipette tip. For negative controls, uninoculated PDA plugs were used. Eight plants were inoculated with each strain or uninoculated medium and placed on a greenhouse bench in a randomized complete block design. Ten days after inoculation, the length of necrotic lesion developed from the inoculation point downward was measured.

The ability of strains to colonize soybean seeds was evaluated by wound-inoculations followed by ergosterol measurements to quantify fungal biomass. Seeds of soybean cultivar Traff were collected at R7 (yellow-senescing stage) from plants cultivated in greenhouse conditions. Seeds were surface disinfested for 30 seconds in 70% ethanol, followed by 30 seconds in 0.5% sodium hypochlorite, two 30-second rinses in sterile deionized water, and dried in a laminar flow hood. Seeds were placed in sterile 24-well culture plates and wounded with a sterile 12-gauge needle. For each strain, three replications of four seeds each were inoculated with 5-mm colonized PDA plugs from six-day-old cultures. For negative controls, non-colonized PDA plugs were used. Inoculated seeds were incubated in the dark at room temperature. Seven days after inoculation, seeds were flash frozen with liquid nitrogen and manually ground into a fine powder with a mortar and pestle. Ergosterol was extracted by

incubating 500 mg of ground seeds with 2 ml of chloroform:methanol (2:1, *v:v*) overnight. Ergosterol was analyzed in an HPLC system with UV detection with peak detection at $\lambda = 282$ nm as previously described (Cooley et al. 2005). Ergosterol was quantified by measuring peak area in samples and comparing it to peak areas of standards (1, 10, 100, and 500 ppm).

Gene expression analysis. The wild-type strain PL2010AR and *HAP3* deletion strain PLH101 were inoculated on seeds of soybean cultivar Traff as described above. Three replications, each containing 24 seeds, were inoculated with either PL2010AR or PLH101. To enrich *P. longicolla* tissue, seed coats were carefully removed from colonized seeds six days after inoculation, and the 24 seed coats in each sample were pooled, flash frozen, and ground in liquid nitrogen with a mortar and pestle. Total RNA was extracted with Ribozol (Amresco, Solon, Ohio, USA). For each sample, 2 μg total RNA was treated with DNase (Promega, Madison, WI, USA) for 30 minutes at 37°C to remove genomic DNA and then used as template to synthesize cDNA with M-MLV reverse transcriptase (Promega, Madison, WI, USA). RNA-seq was performed on three pooled, infected seed coat samples of PL2010AR and PLH101 (as described above) with the Ion Torrent PGM at the University of Arkansas. Sequenced reads were mapped to the soybean (version Gmax_189; Schmutz et al. 2010) and *P. longicolla* MSPL10-6 genomes with GSNAP (Wu et al. 2016) version 2014-10-09. Only reads that exclusively mapped to the *P. longicolla* genome were used in the differential expression analysis.

***P. longicolla* gene annotation**. *P. longicolla* gene models were functionally annotated by querying their protein sequences in a BLASTP search (BLAST v2.2.29) against the NCBI nr database with an E-value cutoff of 1e-5. GO terms and functional descriptions were attributed with Blast2GO v3.0 (Conesa et al. 2005). Genes encoding secreted proteins, candidate effectors, secondary metabolite backbones, carbohydrate-active enzymes (CAZymes), proteases,

peroxidases, and lipases were identified as previously reported by Zaccaron et al. (2017). Genes encoding cytochrome P450 enzymes were identified by the presence of an IPR001128 domain from InterPro, and gene orthologs associated with pathogenesis were identified with a BLASTP search against the PHI database 4.5 (Pathogen-Host Interaction; http://www.phi-base.org, accessed: November 2018) with an E-value cutoff of 1e-5. Cluster of Orthologous Groups (COGs) classification (Tatusov et al. 1997) was performed with the EggNOG-mapper webserver (Huerta-Cepas et al. 2017), with parameters set to use the DIAMOND mapping mode, automatically adjusted taxonomic scope, orthologs that prioritize coverage, and gene ontologies that prioritize quality.

Statistical analyses. Experiments utilized randomized complete block designs and data were analyzed in R version 3.2.4 (R Core Team, 2019). Package lme4 (Bates et al. 2015) was used to perform analysis of variance considering block as a random effect. Multiple comparisons were performed with Tukey-Kramer tests. Radial growth, conidiation, length of necrosis, concentration of ergosterol were treated as Gamma distributed variables. Differential expression analysis of RNA-seq data was performed with the software package DESeq2 (Love et al. 2014).

Results

Identification and targeted deletion of *HAP3* in *P. longicolla.* Homology searches performed with BLASTp revealed a single candidate Hap3 ortholog in *P. longicolla*, encoded by gene g5542. Based on a local alignment, the protein encoded by *P. longicolla* gene g5542 shared 37.2% identity and 49.2% similarity with *S. cerevisiae* Hap3 (GenBank accession CAA52633.1). However, further observations indicated that gene g5542 was not predicted correctly. The protein encoded by gene g5542 contained 839 amino acids, approximately 600 more than previously described fungal Hap3 orthologs (Ridenour and Bluhm 2014). For this reason, *P.*

longicolla gene g5542 was manually curated based on *HAP3* of *F. verticillioides* (Ridenour and Bluhm 2014) and RNA-seq data generated in this study. The curated *P. longicolla HAP3* had a predicted ORF of 1039 bp (**Fig. 1A**), and encoded a 202 amino-acid protein, which contained a histone-fold motif near the N-terminus (**Fig. 1B**). Additionally, the Hap3 protein of *P. longicolla* shared significant homology with *HAP3* orthologs from *S. cerevisiae* (59.7% identity) and *F. verticillioides*, (66.5% identity), based on local amino acid sequence alignments (**Fig. 1B).**

To functionally characterize the role of *HAP3* in *P. longicolla*, the *HAP3* locus was deleted via homologous recombination in the wild-type strain PL2010AR via *Agrobacterium tumefaciens*-mediated transformation (Li et al. 2013). Each transformation event yielded an average of 120 transformants, approximately 60% of which contained homologous recombination of the deletion cassette at the *HAP3* locus based on preliminary PCR analysis. Deletion strains PLH100 and PLH101 were selected for further analysis. The targeted integration of the deletion cassette at the *HAP3* locus was confirmed by PCR via amplification with A1/has and GFPF/A2, while pF/pR was amplified to test for the presence of the wild-type *HAP3*. Furthermore, Southern blots showed a single integration of the deletion cassette in PLH100 and PLH101 **(Figure 2)**. For genetic complementation, the wild-type *HAP3* gene, including the putative promoter region, open reading frame, and putative terminator region, was reintroduced into the *HAP3* deletion strain PLH101, thereby creating the genetically complemented strain PLH101C.

Deletion of *HAP3* impaired growth and asexual reproduction in *P. longicolla*. Compared to the wild-type strain, the *HAP3* deletion strains PLH100 and PLH101, grew significantly less on defined growth media (**Figure 3A and B**). No pycnidia or conidia were observed in the *HAP3* deletion strains after 15 days of growth on oatmeal agar. However, prolific production of both

pycnidia and conidia were observed in the wild type and genetic complement after 10 days **(Fig. 4)**.

HAP3* is important for pathogenesis in *P. longicolla. To investigate the role of *HAP3* in pathogenesis, soybean stems and seeds were inoculated with the wild type, *HAP3* deletion strains, or the genetic complement strain. The wild type and genetic complement caused severe necrosis and prolific production of pycnidia on soybean stems, while the *HAP3* deletion strains caused minimal necrosis and failed to produce pycnidia **(Fig 5A, and B)**. When inoculated on seeds, the wild type and genetic complement produced abundant aerial hyphae over the entire seed coat. In contrast, seeds inoculated with the *HAP3* deletion strains exhibited dark discoloration of the seed coat but no apparent aerial fungal growth was observed **(Fig. 5C)**. In addition, ergosterol measurements indicated that soybean seeds inoculated with the *HAP3* deletion strains had significantly less colonization than seeds inoculated with the wild type or the complementation strain **(Fig. 5D)**. Over all, deletion strains colonized soybean stems and seeds approximately 5-fold less than the wild type as measured by lesion length and ergosterol quantification, respectively. (**Fig. 5B and D**).

Deletion of *HAP3* altered the expression profile of *P. longicolla* during colonization of soybean seeds. To identify genes putatively regulated by *HAP3* during pathogenesis, physiologically mature soybean seeds were inoculated with the *HAP3* deletion strain PLH101 or wild-type strain PL2010AR. RNA was extracted from colonized seed coats and sequenced. Each RNA-seq library produced 630,780 to 1,298,400 reads with an average length of 242 bp. Read mapping indicated that 70-90% of the reads from each library mapped to the *P. longicolla* genome (strain MSPL 10-6), while only 0.2-18% of the reads mapped to the soybean genome, and 9-14% of all reads were unmapped or mapped ambiguously.

A total of 2,353 genes were differentially expressed in the *HAP3* deletion strain. Compared to the wild type during seed colonization, 1.455 genes were upregulated and 898 were downregulated in strain PLH101 **(Fig. 6A)**. Based on COG classifications, the expression of genes with diverse functions were altered upon deletion of *HAP3* **(Fig 6B)**. Genes associated with information storage and processing (e.g., RNA processing and modification, transcription, and replication, recombination and repair) were predominately downregulated in the *HAP3* deletion strain. However, genes functionally related to metabolism (e.g., amino acid transport and metabolism, lipid transport and metabolism, and secondary metabolism biosynthesis, transport and catabolism) were predominately upregulated. Furthermore, GO enrichment analyses indicated significant (FDR < 0.05) over-representation of genes involved in oxidoreductase activities and detoxification among the upregulated genes in *P. longicolla* strain PLH101 during soybean seed colonization **(Table 2)**. Notably, the most upregulated gene was g10996 ($log_2FC = 10.2$; **Fig 6A**), which encoded a putative secreted multicopper oxidase homologous (66% identity) to a bilirubin oxidase (3ABG_A) from the fungus *Albifimbria verrucaria* (Mizutani et al. 2010). On the other hand, genes predicted to encode transmembrane transporters were enriched among the downregulated genes in *P. longicolla* strain PLH101 **(Table 3).**

Deletion of *HAP3* affected the expression of genes involved in plant biomass degradation. To identify differentially expressed genes encoding putative plant cell wall degrading enzymes (PCWDEs), carbohydrate-active enzymes (CAZymes) were evaluated in *P. longicolla*. Among the 1,127 predicted CAZymes, 260 were differentially expressed in strain PLH101, which included genes from all six major classes of CAZymes **(Table 4).** Genes encoding PCWDE usually belong to CAZyme families from the glycoside hydrolases class, such as GH3, GH5 and

GH6 (Juge 2006; Kubicek et al. 2014; Vries and Visser 2001). In *P. longicolla*, 186 genes were predicted to encode PCWDEs, of which 19 were up-regulated and 31 were downregulated in strain PLH101. Specifically, of the 144 genes predicted to be involved in hemicellulose degradation, 10 were overexpressed and 31 were under expressed. On the other hand, of the 42 genes predicted to be involved in pectin degradation, 9 were upregulated and none was downregulated.

Other genes associated with plant biomass degradation were differentially expressed in strain PLH101, including copper-dependent lytic polysaccharide monooxygenases (LPMOs). Out of the 46 putative LPMOs in *P. longicolla*, 15 were downregulated and one was upregulated in strain PLH101 during seed colonization. Additionally, of the five putative cellobiose dehydrogenases in *P. longicolla*, two were downregulated, including gene g784, which is a homolog (63% identity) of *Neurospora crassa* cellobiose dehydrogenase *CDH1*. Cellobiose dehydrogenases act in concert with LPMOs to enhance enzymatic activity towards cellulose, hemicellulose, and starch (Tan et al. 2015). The widespread downregulation of genes coding PCWDEs and LPMOs may partially explain the reduced colonization of soybean seeds and stems caused by deletion of *HAP3*.

Deletion of *HAP3* affected the expression of candidate effector genes in *P. longicolla*.

Deletion of *HAP3* increased the expression of numerous candidate effector genes while downregulating the expression of others **(Fig. 7)**. Specifically, among the 397 genes predicted to encode small secreted proteins (SSPs), 68 (17%) were upregulated and 17 (4%) were downregulated in the PLH101 strain. Some of the differentially expressed SSP genes in *P. longicolla* shared homology with known plant avirulence determinants **(Table 5)**. Notably, the up-regulated candidate effector genes g9614, g1873, and g7272 shared substantial homology

with the necrosis-inducing Phytophthora-associated protein 1 **(NPP1; Figure 8),** which has been shown to trigger plant defense and necrosis (Qutob et al. 2002; Fellbrich et al. 2002). Thirteen *P. longicolla* SSP genes homologous to *Magnaporthe oryzae* cell-death inducing protein 1 and 4 (*MoCDIP1* and *4*; Chen et al. 2013) were also differentially regulated in the *HAP3* deletion strain during seed colonization. Specifically, two *MoCDIP1* homologs were identified, with one up- and one downregulated; 11 *MoCDIP4* homologs were identified, with one up- and 10-downregulated **(Table 4)**. Six other upregulated candidate effectors (genes g9817, g7665, g12120, g15154, g11872, and g7191) encoded proteins containing lysin motif (LysM) domains. LysM proteins bind to chitin and have been reported in other plant pathogenic fungi as effectors that suppress plant chitin-triggered immune responses and protect fungal cell walls against plant chitinases (Akcapinar et al. 2015; Marshall et al. 2011). Interestingly, the most up-regulated candidate effector (gene g6307; log2FC = 8.2) encoded a putative cerato-platanin protein (CPP). Homology searches indicated that *P. longicolla* gene g6307 is taxonomically restricted, with homologs found only in *Diaporthe helianthin* and *D. ampelina*, and the Basidiomycetes *Moniliophthora roreri*, *M. perniciosa* and *Pleurotus ostreatus*.

Genes involved in secondary metabolism were mis-regulated in *P. longicolla* strain PLH101. A total of 111 secondary metabolite backbone genes were identified in *P. longicolla*, including 54 polyketide synthases (PKSs), 34 nonribosomal peptide synthetases (NRPSs), 7 PKS-NRPS hybrids, 7 dimethylallyl tryptophan synthases (DMATs), and 9 terpene synthases (TSs). From these 111 backbone genes, 23 were differentially expressed in *P. longicolla* strain PLH101 **(Fig. 9A)**. Among these were 11 highly-reducing PKSs (10 upregulated and 1 downregulated), one non-reducing PKS (upregulated), and 5 partially-reducing PKSs (3 upregulated and 2 downregulated). Additionally, 73 secondary metabolite gene clusters were identified, which, along with the

predicted backbone genes, accounted for a total of 786 genes associated with secondary metabolism in *P. longicolla*. Of these 786 genes, 129 were up-regulated and 32 were down-regulated in *P. longicolla* strain PLH101 during soybean seed colonization.

Interestingly, deletion of *HAP3* induced the expression of several genes within predicted secondary metabolite gene clusters. Notably cluster8, cluster9, and cluster11, had 15, 10, and 11 genes upregulated, respectively **(Fig. 9B and C)**. Predicted cluster11 shared homology with the azaphilone cluster from *Aspergillus niger* (Zabala et al. 2012). The azaphilone cluster in *Aspergillus niger* has two PKS backbones (*azaA* and *azaB*), which were homologous to g1581 (48% identity) and g1582 (51% identity), respectively. Other genes from the azaphilone cluster with homologs in *P. longicolla* included the O-acetyltransferase *azaD* (g1587; 35% identity), the FAD-linked oxidoreductase *azaG* (g1584; 42% identity), the FAD-dependent monooxygenase *azaH* (g1588; 40% identity), and the dehydrogenase *azaJ* (g1589; 48% identity).

Discussion

HAP3 of *P. longicolla* is predicted to encode a subunit of the CCAAT-Binding Complex (CBC), a global transcriptional regulator that is broadly conserved among taxonomically diverse eukaryotes (Thön et al. 2010). In fungi, the CBC has been described as a transcriptional activator or repressor of genes involved in diverse processes, including primary and secondary metabolism, iron homeostasis, response to environmental stress, and pathogenesis (Hortschansky et al. 2017). However, direct relationships between the CBC and plant pathogenesis have only recently been established among filamentous fungi. In *Fusarium verticillioides*, disruption of the CBC via deletion of *HAP3* impaired fumonisin biosynthesis, kernel colonization, and stalk rot during interactions with maize (Ridenour and Bluhm 2014; Ridenour et al. 2016). Disruption of the CBC also impaired pathogenesis in *F. oxysporum* and *U. maydis* on tomato and maize,

respectively (López-Berges et al. 2012; Mendoza-Mendoza et al. 2009). In this study, disrupting the *HAP3* subunit in *P. longicolla* significantly reduced pathogenesis on soybean seeds and stems. This finding may point to a broader role for the CBC in plant pathogenesis specifically, and plant-fungal interactions in general.

Disruption of the CBC extensively influenced growth and development in *P. longicolla*. The pronounced misregulation of radial growth, asexual reproduction, and secondary metabolism in *HAP3* deletion strains of *P. longicolla* was consistent with *HAP3* deletion strains in other filamentous fungi. For example, deletion of *HAP3* in *F. verticillioides* caused pronounced reductions in radial growth, conidiation, and fumonisin biosynthesis, while simultaneously inducing a derepression of pigmentation (Ridenour and Bluhm 2014; Ridneour et al. 2016). Similarly, disruption of the CBC caused defects in growth, development, and sexual reproduction in *Neurospora crassa* (Chen et al. 1998). Disrupting the CBC also caused similar defects in growth and conidiation in *F. oxysporum* and *U. maydis* (López-Berges et al. 2012; Mendoza-Mendoza et al. 2009). The consistency of these phenotypes across taxonomically diverse species of filamentous fungi suggests at least partially conserved roles for the CBC in fungal growth and development.

The exact mechanism through which the CBC regulates plant pathogenesis in *P. longicolla* is not known. Among human pathogenic fungi such as *A. fumigatus*, the CBC is postulated to maintain iron homeostasis and/or amelioriate the effects of iron starvation during host colonization (Haas 2012). In this study, significant differences in the expression of genes involved in iron scavenging and transport were observed, with the majority of these genes expressed at lower levels in the *HAP3* deletion strain. The role of iron in plant pathogenesis is complex: it is a coveted micronutrient, yet can also be utilized by plants to form reactive oxygen

species and subsequently induce oxidative stress (Aznar et al. 2015). In *P. longicolla*, both iron acquisition and tolerance of oxidative stress could potentially be components of pathogenesis that are impaired upon disruption of the CBC. Additionally, differential gene expression data from the wild type vs. *HAP3* deletion strain suggested additional regulatory functions of the CBC during pathogenesis. For example, disruption of the CBC in *P. longicolla* down regulated numerous genes involved in the catabolism of complex plant-produced carbohydrates, which possibly links the CBC with primary metabolism during pathogenesis. Intriguingly, a subset of genes up-regulated in the *P. longicolla HAP3* deletion strain could potentially trigger host defenses due to aberrant expression. For example, effectors are used by diverse fungal pathogens to manipulate host responses during specific stages of the infection process (Bhattacharjee et al. 2011; Fudal et al. 2018; Mentlak et al. 2012), and the mis-regulation of effector gene expression during pathogenesis could have the unintended consequence of triggering detection by the host (Lo Presti et al. 2015; Stotz et al. 2014). Additionally, one gene encoding a putative cerato-platanin protein was up-regulated during pathogenesis in the *P. longicolla HAP3* deletion strain. Cerato-platanin proteins are a broadly conserved family of fungal genes of somewhat uncertain function, although some are known elicitors of plant defense responses (Gaderer et al. 2014). Further dissection of regulatory pathways underlying pathogenesis in *P. longicolla* will be required to fully understand the role of the CBC in the initiation and progression of plant infection.

In conclusion, this study demonstrated that *HAP3* of *P. longicolla* plays an important role in growth, development, and pathogenesis on soybean. This study also presents the first report of successful targeted gene deletion in *P. longicolla*, which will open new avenues of study in this pathosystem and help to guide the development of molecular genetics techniques in related

Phomopsis species. Additionally, the expression profiling data in this study represents the first such insight into how the CBC reprograms fungal gene expression during plant pathogenesis. These RNA-seq data is publicly available will help in design further experiments to better understand *P. longicolla* association with soybean plants.

Literature cited

Akcapinar, G. B., Kappel, L., Sezerman, O. U., and Seidl-Seiboth, V. 2015. Molecular diversity of LysM carbohydrate-binding motifs in fungi. Curr. Genet. 61:103-113

Altschul, S. F., Madden, T. L., Schäffer, A. A., Zhang, J., Zhang, Z., Miller, W., and Lipman, D. J. 1997. Gapped BLAST and PSI-BLAST: a new generation of protein database search programs. Nucleic Acids Res. 25:3389-3402

Aznar, A., Chen, N. W. G., Thomine, S., and Dellagi, A. 2015. Immunity to plant pathogens and iron homeostasis. Plant Sci. 240:90-97

Baroncelli, R., Scala, F., Vergara, M., Thon, M. R., and Ruocco, M. 2016. Draft whole-genome sequence of the *Diaporthe helianthi* 7/96 strain, causal agent of sunflower stem canker. Genomics Data 10:151-152

Bates, D., Mächler, M., Bolker, B., and Walker, S. 2015. Fitting Linear Mixed-Effects Models Using lme4. J. Stat. Softw. 67:1-48

Becker, D. M., Fikes, J. D., and Guarente, L. 1991. A cDNA encoding a human CCAAT-binding protein cloned by functional complementation in yeast. Proc. Natl. Acad. Sci. 88:1968-1972

Bhattacharjee, S., Halane, M. K., Kim, S. H., and Gassmann, W. 2011. Pathogen Effectors Target *Arabidopsis* EDS1 and Alter Its Interactions with Immune Regulators. Science 334:1405-1408

Capella-Gutiérrez, S., Silla-Martínez, J. M., and Gabaldón, T. 2009. trimAl: a tool for automated alignment trimming in large-scale phylogenetic analyses. Bioinformatics 25:1972-1973

Chakravarti, A., Camp, K., McNabb, D. S., and Pinto, I. 2017. The Iron-Dependent Regulation of the *Candida albicans* Oxidative Stress Response by the CCAAT-Binding Factor. PLOS ONE 12:e0170649

Chen, H., Crabb, J. W., and Kinsey, J. A. 1998. The *Neurospora* aab-1 gene encodes a CCAAT binding protein homologous to yeast HAP5. Genetics 148:123-130

Chen, S., Songkumarn, P., Venu, R. C., Gowda, M., Bellizzi, M., Hu, J., Liu, W., Ebbole, D., Meyers, B., and Mitchell, T. 2013. Identification and characterization of in planta–expressed secreted effector proteins from *Magnaporthe oryzae* that induce cell death in Rice. Mol. Plant. Microbe Interact. 26:191-202

Conesa, A., Götz, S., García-Gómez, J. M., Terol, J., Talón, M., and Robles, M. 2005. Blast2GO: a universal tool for annotation, visualization and analysis in functional genomics research. Bioinforma. Oxf. Engl. 21:3674-3676

Cooley, C., H. Bluhm, B., L. Reuhs, B., and P. Woloshuk, C. 2005. Glass-fiber disks provide suitable medium to study polyol production and gene expression in *Eurotium rubrum*. Mycologia 97:743-750

Correll, J. C. 1987. Nitrate Nonutilizing Mutants of *Fusarium oxysporum* and Their Use in Vegetative Compatibility Tests. Phytopathology 77:1640-1646

Edwards, D., Murray, J. A. H., and Smith, A. G. 1998. Multiple Genes Encoding the Conserved CCAAT-Box Transcription Factor Complex Are Expressed in *Arabidopsis*. Plant Physiol. 117:1015-1022

Egli, D. B., TeKrony, D. M., Heitholt, J. J., and Rupe, J. 2005. Air temperature during seed filling and soybean seed germination and vigor. Crop Sci. 45:1329-1335

Fellbrich, G., Romanski, A., Varet, A., Blume, B., Brunner, F., Engelhardt, S., Felix, G., Kemmerling, B., Krzymowska, M., and Nürnberger, T. 2002. NPP1, a *Phytophthora*-associated trigger of plant defense in parsley and *Arabidopsis*. Plant J. 32:375-390

Flaherty, J. E., Pirttilä, A. M., Bluhm, B. H., and Woloshuk, C. P. 2003. PAC1, a pH-Regulatory Gene from *Fusarium verticillioides*. Appl. Environ. Microbiol. 69:5222-5227

Fudal, I., Balesdent, M.-H., and Rouxel, T. 2018. Effector Biology in Fungal Pathogens of Nonmodel Crop Plants. Trends Plant Sci. 23:753-755

Gaderer, R., Bonazza, K., and Seidl-Seiboth, V. 2014. Cerato-platanins: a fungal protein family with intriguing properties and application potential. Appl. Microbiol. Biotechnol. 98:4795-4803

Haas, H. 2012. Iron - A Key Nexus in the Virulence of *Aspergillus fumigatus*. Front. Microbiol. 3:28

Hepperly, P. R. 1978. Quality Losses in *Phomopsis*-Infected Soybean Seeds. Phytopathology 68:1684-1687

Hobbs, T. W., Schmitthenner, A. F., and Kuter, G. A. 1985. A New *Phomopsis* Species from Soybean. Mycologia 77:535-544

Hong, S.-Y., Roze, L. V., and Linz, J. E. 2013. Oxidative Stress-Related Transcription Factors in the Regulation of Secondary Metabolism. Toxins 5:683-702

Hortschansky, P., Haas, H., Huber, E. M., Groll, M., and Brakhage, A. A. 2017. The CCAAT-binding complex (CBC) in *Aspergillus* species. Biochim. Biophys. Acta BBA - Gene Regul. Mech. 1860:560-570

Huerta-Cepas, J., Forslund, K., Coelho, L. P., Szklarczyk, D., Jensen, L. J., von Mering, C., and Bork, P. 2017. Fast Genome-Wide Functional Annotation through Orthology Assignment by eggNOG-Mapper. Mol. Biol. Evol. 34:2115-2122

Juge, N. 2006. Plant protein inhibitors of cell wall degrading enzymes. Trends Plant Sci. 11:359-367

Jung, W. H., Saikia, S., Hu, G., Wang, J., Fung, C. K.-Y., D'Souza, C., White, R., and Kronstad, J. W. 2010. HapX Positively and Negatively Regulates the Transcriptional Response to Iron Deprivation in *Cryptococcus neoformans*. PLOS Pathog. 6:e1001209

Kmetz, K. T., Ellett, C. W., and Schmitthenner, A. F. 1979. Soybean seed decay: Sources of inoculum and nature of infection. Phytopathology 69:798-801

Kubicek, C. P., Starr, T. L., and Glass, N. L. 2014. Plant cell wall-degrading enzymes and their secretion in plant-pathogenic fungi. Annu. Rev. Phytopathol. 52:427-451

Lazo, G. R., Stein, P. A., and Ludwig, R. A. 1991. A DNA transformation-competent *Arabidopsis* genomic library in Agrobacterium. Biotechnol. Nat. Publ. Co. 9:963-967

Leslie, J. F., and Summerell, B. A. 2006. *The Fusarium laboratory manual*. John Wiley & Sons.

Li, S., Darwish, O., Alkharouf, N., Matthews, B., Ji, P., Domier, L. L., Zhang, N., and Bluhm, B. H. 2014. Draft genome sequence of *Phomopsis longicolla* isolate MSPL 10-6. Genomics Data 3:55-56

Li, S., Hartman, G. L., and Boykin, D. L. 2010. Aggressiveness of *Phomopsis longicolla* and Other *Phomopsis spp*. on Soybean. Plant Dis. 94:1035-1040

Li, S., Musungu, B., Lightfoot, D., and Ji, P. 2018. The Interactomic Analysis Reveals Pathogenic Protein Networks in *Phomopsis longicolla* Underlying Seed Decay of Soybean. Front. Genet. 9:104

Li, S., Ridenour, J. B., Kim, H., Hirsch, R. L., Rupe, J. C., and Bluhm, B. H. 2013. *Agrobacterium tumefaciens*-mediated transformation of the soybean pathogen *Phomopsis longicolla*. J. Microbiol. Methods. 92:244-245

Li, S., Song, Q., Ji, P., and Cregan, P. 2015. Draft Genome Sequence of *Phomopsis longicolla* Type Strain TWH P74, a Fungus Causing *Phomopsis* Seed Decay in Soybean. Genome Announc. 3: e00010-15

Li, S., Song, Q., Martins, A. M., and Cregan, P. 2016. Draft genome sequence of *Diaporthe aspalathi* isolate MS-SSC91, a fungus causing stem canker in soybean. Genomics Data 7:262-263

Lo Presti, L., Lanver, D., Schweizer, G., Tanaka, S., Liang, L., Tollot, M., Zuccaro, A., Reissmann, S., and Kahmann, R. 2015. Fungal Effectors and Plant Susceptibility. Annu. Rev. Plant Biol. 66:513-545

López-Berges, M. S., Capilla, J., Turrà, D., Schafferer, L., Matthijs, S., Jöchl, C., Cornelis, P., Guarro, J., Haas, H., and Pietro, A. D. 2012. HapX-Mediated Iron Homeostasis Is Essential for Rhizosphere Competence and Virulence of the Soilborne Pathogen *Fusarium oxysporum*. Plant Cell 24:3805-3822

Love, M. I., Huber, W., and Anders, S. 2014. Moderated estimation of fold change and dispersion for RNA-seq data with DESeq2. Genome Biol. 15:550

Marchler-Bauer, A., Bo, Y., Han, L., He, J., Lanczycki, C. J., Lu, S., Chitsaz, F., Derbyshire, M. K., Geer, R. C., Gonzales, N. R., Gwadz, M., Hurwitz, D. I., Lu, F., Marchler, G. H., Song, J. S., Thanki, N., Wang, Z., Yamashita, R. A., Zhang, D., Zheng, C., Geer, L. Y., and Bryant, S. H. 2017. CDD/SPARCLE: functional classification of proteins via subfamily domain architectures. Nucleic Acids Res. 45:D200-D203

Marshall, R., Kombrink, A., Motteram, J., Loza-Reyes, E., Lucas, J., Hammond-Kosack, K. E., Thomma, B. P. H. J., and Rudd, J. J. 2011. Analysis of two in planta expressed LysM effector homologs from the fungus *Mycosphaerella graminicola* reveals novel functional properties and varying contributions to virulence on wheat. Plant Physiol. 156:756-769

McNabb, D. S., and Pinto, I. 2005. Assembly of the Hap2p/Hap3p/Hap4p/Hap5p-DNA Complex in *Saccharomyces cerevisiae*. Eukaryot. Cell 4:1829-1839

McNabb, D. S., Xing, Y., and Guarente, L. 1995. Cloning of yeast HAP5: a novel subunit of a heterotrimeric complex required for CCAAT binding. Genes Dev. 9:47-58

Mendoza-Mendoza, A., Eskova, A., Weise, C., Czajkowski, R., and Kahmann, R. 2009. Hap2 regulates the pheromone response transcription factor prf1 in *Ustilago maydis*. Mol. Microbiol. 72:683-698

Mengistu, A., and Heatherly, L. G. 2006. Planting date, irrigation, maturity group, year, and environment effects on *Phomopsis longicolla*, seed germination, and seed health rating of soybean in the early soybean production system of the midsouthern USA. Crop Prot. 25:310-317

Mentlak, T. A., Kombrink, A., Shinya, T., Ryder, L. S., Otomo, I., Saitoh, H., Terauchi, R., Nishizawa, Y., Shibuya, N., Thomma, B. P. H. J., and Talbot, N. J. 2012. Effector-Mediated Suppression of Chitin-Triggered Immunity by *Magnaporthe oryzae* Is Necessary for Rice Blast Disease. Plant Cell 24:322-335

Mizutani, K., Toyoda, M., Sagara, K., Takahashi, N., Sato, A., Kamitaka, Y., Tsujimura, S., Nakanishi, Y., Sugiura, T., Yamaguchi, S., Kano, K., and Mikami, B. 2010. X-ray

analysis of bilirubin oxidase from Myrothecium verrucaria at 2.3 A resolution using a twinned crystal. Acta Crystallograph. Sect. F Struct. Biol. Cryst. Commun. 66:765-770

Murthy, M. S., Rao, B. S., Reddy, N. M., Subrahmanyam, P., and Madhvanath, U. 1975. Non-equivalence of YEPD and synthetic complete media in yeast reversion studies. Mutat. Res. 27:219-223

Needleman, S. B., and Wunsch, C. D. 1970. A general method applicable to the search for similarities in the amino acid sequence of two proteins. J. Mol. Biol. 48:443-453

Nicholson, J. F. 1972. Internal Seed-Borne Nature of *Sclerotinia sclerotiorum* and *Phomopsis sp.* and Their Effects on Soybean Seed Quality. Phytopathology 62:1261-1263

Olesen, J., Hahn, S., and Guarente, L. 1987. Yeast HAP2 and HAP3 activators both bind to the CYC1 upstream activation site, UAS2, in an interdependent manner. Cell 51:953-961

Qutob, D., Kamoun, S., and Gijzen, M. 2002. Expression of a *Phytophthora sojae* necrosis-inducing protein occurs during transition from biotrophy to necrotrophy. Plant J. 32:361-373

R Core Team. R: A Language and Environment for Statistical Computing. 2019. Vienna, Austria. URL https://www.R-project.org/

Rice, P., Longden, I., and Bleasby, A. 2000. EMBOSS: The European Molecular Biology Open Software Suite. Trends Genet. 16:276-277

Ridenour, J. B., and Bluhm, B. H. 2014. The HAP complex in *Fusarium verticillioides* is a key regulator of growth, morphogenesis, secondary metabolism, and pathogenesis. Fungal Genet. Biol. 69:52-64

Ridenour, J. B., Smith, J. E., and Bluhm, B. H. 2016. The HAP Complex Governs Fumonisin Biosynthesis and Maize Kernel Pathogenesis in *Fusarium verticillioides*. J. Food Prot. 79:1498-1507

Ruocco, M., Baroncelli, R., Cacciola, S. O., Pane, C., Monti, M. M., Firrao, G., Vergara, M., Magnano di San Lio, G., Vannacci, G., and Scala, F. 2018. Polyketide synthases of *Diaporthe helianthi* and involvement of DhPKS1 in virulence on sunflower. BMC Genomics 19:27

Rupe, J. 1990. Effect of Temperature on the Rate of Infection of Soybean Seedlings by *Phomopsis longicolla*. Can. J. Plant Pathol. 12:43-47

Sambrook, J., and Russell, D. 2001. *Molecular cloning: a laboratory manual*. Cold Spring harbor laboratory Cold Spring Harbor, NY.

Savitha, J., Bhargavi, S. D., and Praveen, V. K. 2016. Complete Genome Sequence of the Endophytic Fungus *Diaporthe* (*Phomopsis*) *ampelina*. Genome Announc. 4:e00477-16.

Schmutz, J., Cannon, S. B., Schlueter, J., Ma, J., Mitros, T., Nelson, W., Hyten, D. L., Song, Q., Thelen, J. J., Cheng, J., Xu, D., Hellsten, U., May, G. D., Yu, Y., Sakurai, T., Umezawa, T., Bhattacharyya, M. K., Sandhu, D., Valliyodan, B., Lindquist, E., Peto, M., Grant, D., Shu, S., Goodstein, D., Barry, K., Futrell-Griggs, M., Abernathy, B., Du, J., Tian, Z., Zhu, L., Gill, N., Joshi, T., Libault, M., Sethuraman, A., Zhang, X.-C., Shinozaki, K., Nguyen, H. T., Wing, R. A., Cregan, P., Specht, J., Grimwood, J., Rokhsar, D., Stacey, G., Shoemaker, R. C., and Jackson, S. A. 2010. Genome sequence of the palaeopolyploid soybean. Nature 463:178-183

de Sena Filho, J. G., Quin, M. B., Spakowicz, D. J., Shaw, J. J., Kucera, K., Dunican, B., Strobel, S. A., and Schmidt-Dannert, C. 2016. Genome of *Diaporthe sp*. provides insights into the potential inter-phylum transfer of a fungal sesquiterpenoid biosynthetic pathway. Fungal Biol. 120:1050-1063

Sievers, F., Wilm, A., Dineen, D., Gibson, T. J., Karplus, K., Li, W., Lopez, R., McWilliam, H., Remmert, M., Söding, J., Thompson, J. D., and Higgins, D. G. 2011. Fast, scalable generation of high-quality protein multiple sequence alignments using Clustal Omega. Mol. Syst. Biol. 7:539

Simão, F. A., Waterhouse, R. M., Ioannidis, P., Kriventseva, E. V., and Zdobnov, E. M. 2015. BUSCO: assessing genome assembly and annotation completeness with single-copy orthologs. Bioinformatics 31:3210-3212

Sinclair, J. B. 1992. Discoloration of Soybean Seeds- An Indicator of Quality. Plant Dis. 76:1087-1091

Sinclair, J. B. 1993. *Phomopsis* Seed Decay of Soybeans- A Prototype for Studying Seed Disease. Plant Dis. 77:329-334

Slater, G. S. C., and Birney, E. 2005. Automated generation of heuristics for biological sequence comparison. BMC Bioinformatics 6:31

Smith, T. F., and Waterman, M. S. 1981. Identification of common molecular subsequences. J. Mol. Biol. 147:195-197

Stamatakis, A. 2014. RAxML version 8: a tool for phylogenetic analysis and post-analysis of large phylogenies. Bioinformatics 30:1312-1313

Stotz, H. U., Mitrousia, G. K., de Wit, P. J. G. M., and Fitt, B. D. L. 2014. Effector-triggered defence against apoplastic fungal pathogens. Trends Plant Sci. 19:491-500

Tan, T.-C., Kracher, D., Gandini, R., Sygmund, C., Kittl, R., Haltrich, D., Hällberg, B. M., Ludwig, R., and Divne, C. 2015. Structural basis for cellobiose dehydrogenase action during oxidative cellulose degradation. Nat. Commun. 6:7542

Tanaka, A., Kato, M., Nagase, T., Kobayashi, T., and Tsukagoshi, N. 2002. Isolation of genes encoding novel transcription factors which interact with the Hap complex from Aspergillus species. Biochim. Biophys. Acta BBA - Gene Struct. Expr. 1576:176-182

Tatusov, R. L., Koonin, E. V., and Lipman, D. J. 1997. A genomic perspective on protein families. Science 278:631-637

TeKrony, D. M., Egli, D. B., Stuckey, R. E., and Balles, J. 1983. Relationship between weather and soybean seed infection by *Phomopsis sp*. Phytopathology 73:914-918

Thön, M., Al Abdallah, Q., Hortschansky, P., Scharf, D. H., Eisendle, M., Haas, H., and Brakhage, A. A. 2010. The CCAAT-binding complex coordinates the oxidative stress response in eukaryotes. Nucleic Acids Res. 38:1098-1113

Vries, R. P. de, and Visser, J. 2001. Aspergillus Enzymes Involved in Degradation of Plant Cell Wall Polysaccharides. Microbiol Mol Biol Rev. 65:497-522

Wrather, J. A., Shannon, J. G., Stevens, W. E., Sleper, D. A., and Arelli, A. P. 2004. Soybean cultivar and foliar fungicide effects on *Phomopsis sp*. seed infection. Plant Dis. 88:721-723

Wrather, J. A., Sleper, D. A., Stevens, W. E., Shannon, J. G., and Wilson, R. F. 2003. Planting date and cultivar effects on soybean yield, seed quality, and *Phomopsis sp*. seed infection. Plant Dis. 87:529-532

Wu, T. D., Reeder, J., Lawrence, M., Becker, G., and Brauer, M. J. 2016. GMAP and GSNAP for genomic sequence alignment: enhancements to speed, accuracy, and functionality. Stat. Genomics Methods Protoc. 1418:283-334

Yin, W., and Keller, N. P. 2011. Transcriptional regulatory elements in fungal secondary metabolism. J. Microbiol. 49:329-339

Zabala, A. O., Xu, W., Chooi, Y.-H., and Tang, Y. 2012. Characterization of a silent azaphilone gene cluster from *Aspergillus niger* ATCC 1015 reveals a hydroxylation-mediated pyran-ring formation. Chem. Biol. 19:1049-1059

Zaccaron, A. Z., Woloshuk, C. P., and Bluhm, B. H. 2017. Comparative genomics of maize ear rot pathogens reveals expansion of carbohydrate-active enzymes and secondary metabolism backbone genes in *Stenocarpella maydis*. Fungal Biol. 121:966-983

Zaccaron, M., Sharma, S., and Bluhm, B. H. 2018. MoNSTR-seq, a restriction site-associated DNA sequencing technique to characterize *Agrobacterium*-mediated transfer-DNA insertions in *Phomopsis longicolla*. Lett. Appl. Microbiol. 66:19-24

Zorrilla, G., Knapp, A. D., and McGee, D. C. 1994. Severity of *Phomopsis* Seed Decay, Seed Quality Evaluation, and Field Performance of Soybean. Crop Sci. 34:172-177

Tables

Table 1. Names and sequence of primers used in this study

Primer name	Primer sequence
PlHAP3. KpnI_F1	GGCGGTACCATTGTGTCTGCGTCCCAGCCC
PlHAP3. ApaI_F2	GCGGCTGGGCCCATTTGGCTACCTGCAGCGGGTG
PlHAP3. PacI_F3	GCGGCGTTAATTAAAACCCGTGCAGGCAGGCTA
PlHAP3. HindIII_F4	GGGAAGCTTGCGGCGAGGTAGACGATGGTG
PacI_PlHAP3_5'F	GCGGCGTTAATTAAGTCGTTGCGCGCGACTTGA
PLHAP3_A2	CGGTTGCTACAGTCGGATG
PLHAP3_PF	GACGAGGAAGCACAAATGAATG
PLHAP3_PR	CGTGGGACATGGACGAATAG
HYGSCRN-A	CTACTGCTACAAGTGGGGCTGA
GFPF	ATCCTGGGGCACAAGCTG
HYGF	CCAGTGATACACATGGGGATCAGC
HYGR	GGATATGTCCTGCGGGTAAATAGCTG

Table 2. Gene onthology terms enriched among the over-expressed genes in *Phomopsis longicolla* PLH101

GO Name	FDR[1]	*P* value
oxidation-reduction process	3.50E-16	1.39E-19
exopeptidase activity	2.73E-03	2.18E-06
coenzyme binding	1.01E-02	1.08E-05
oxidoreductase activity, acting on CH-OH group of donors	1.34E-02	1.79E-05
oxidoreductase activity, acting on peroxide as acceptor	1.76E-02	2.58E-05
carbohydrate derivative catabolic process	2.11E-02	3.36E-05
cellular oxidant detoxification	3.64E-02	6.30E-05

[1]False discovery rate. *P* values and FDR for enrichment GO groups were obtained from Blast2go.

Table 3. Gene onthology terms enriched among the under-expressed genes in *Phomopsis longicolla* PLH101.

GO Name	FDR	*P* Value
cellulose catabolic process	5.32E-04	4.95E-07
xylan catabolic process	1.67E-02	3.77E-05
galactosidase activity	1.67E-02	3.77E-05
transmembrane transporter activity	4.13E-02	1.15E-04

Table 4. Number of up- and downregulated CAZyme genes in the *P. longicolla* strain PLH101 during soybean seed colonization.

CAZyme class	Total genes	Upregulated	%	Downregulated	%
AA	265	44	16.6	26	9.8
GH	463	55	11.9	59	12.7
GT	127	12	9.4	8	6.3
PL	45	9	20.0	0	0.0
CE	197	31	15.7	9	4.6
CBM	83	15	18.1	9	10.8
Total	1127	157	13.9	103	9.1

Table 5. Genes differentially expressed in PLH101, during soybean seed colonization, with characterized effector-protein homolog.

Gene ID[1]	Log_2(FC)[2]	*P*-value[3]	Homolog effector[4]	Species[5]	Identity (%)[6]	E-value[7]
g9614	8.0	2.49E-13	NPP1	*Phytophthora parasitica*	46.5	2.61E-68
g9817	6.4	8.33E-52	SLP_1	*Magnaporthe oryzae*	60.2	1.31E-62
g1873	5.2	9.42E-25	NPP1	*Phytophthora parasitica*	30.9	1.06E-12
g7665	5.2	2.09E-08	Vd5LysM	*Verticillium dahliae*	34.4	3.49E-62
g6578	5.0	6.94E-08	AVR-Pita1JB	*Magnaporthe oryzae*	26.0	1.28E-11
g12120	4.5	0.00236	Vd4LysM	*Verticillium dahliae*	26.6	1.53E-32
g15154	4.1	0.00088	Vd4LysM	*Verticillium dahliae*	45.0	1.00E-10
g4025	4.0	4.82E-06	MoCDIP1	*Magnaporthe oryzae*	79.7	0
g7272	4.0	0.01148	NPP1	*Phytophthora parasitica*	33.1	2.92E-27
g7830	3.7	2.35E-24	PopW_RSc2775	*Ralstonia solanacearum*	31.5	1.57E-07
g4073	3.3	0.01860	PGIP2	*Botrytis cinerea*	28.5	8.21E-15
g11872	3.0	0.01997	Vd4LysM	*Verticillium dahliae*	39.5	1.85E-51
g7191	2.9	7.79E-05	SLP_1	*Magnaporthe oryzae*	47.8	3.96E-34
g13248	2.8	0.01449	MoCDIP4	*Magnaporthe oryzae*	32.6	1.17E-10
g9318	1.7	1.46E-05	PopW_RSc2775	*Ralstonia solanacearum*	33.5	1.23E-14
g5797	-2.8	4.00E-26	MoCDIP4	*Magnaporthe oryzae*	29.4	2.21E-18
g10901	-3.3	5.93E-08	MoCDIP4	*Magnaporthe oryzae*	29.4	1.63E-13
g10295	-3.4	0.00032	MoCDIP4	*Magnaporthe oryzae*	36.1	4.07E-31
g14659	-3.6	2.74E-12	MoCDIP4	*Magnaporthe oryzae*	67.6	9.16E-10
g1705	-3.8	0.00019	MoCDIP1	*Magnaporthe oryzae*	62.6	1.1E-148
g4533	-3.9	1.11E-06	AVR-Pita1	*Magnaporthe oryzae*	25.5	2.52E-08
g8080	-3.9	3.54E-42	MoCDIP4	*Magnaporthe oryzae*	67.6	3.67E-10
g15887	-4.6	1.38E-14	MoCDIP4	*Magnaporthe oryzae*	34.5	8.32E-12
g6073	-5.2	7.52E-09	MoCDIP4	*Magnaporthe oryzae*	35.4	1.26E-25
g10767	-5.4	6.96E-46	MoCDIP4	*Magnaporthe oryzae*	43.9	1.28E-38
g7593	-5.6	2.64E-08	MoCDIP4	*Magnaporthe oryzae*	31.5	1.25E-15

[1]*Phomopsis longicolla* identification number. [2]Log_2 of fold change in gene expression in the PLH101 HAP3 knock out strain compared to the wild type measured by RNA-seq experiment with three biological replicates. [3]P value for the contrast of wild type and mutant PLH101 expression level for that particular gene. [4]Characterized effector gene in different organism homolog to the respective *P. longicolla* gene. [5]Species of filamentous fungi where the effector gene homolog was characterized. [6]Amino acid level identity between the *P. longicolla* gene and its respective homolog. [7]Number of expected homolog genes by chance, given the size of database queried and the size of quarry. E-score was obtained by the BLAST algorithm.

Figures

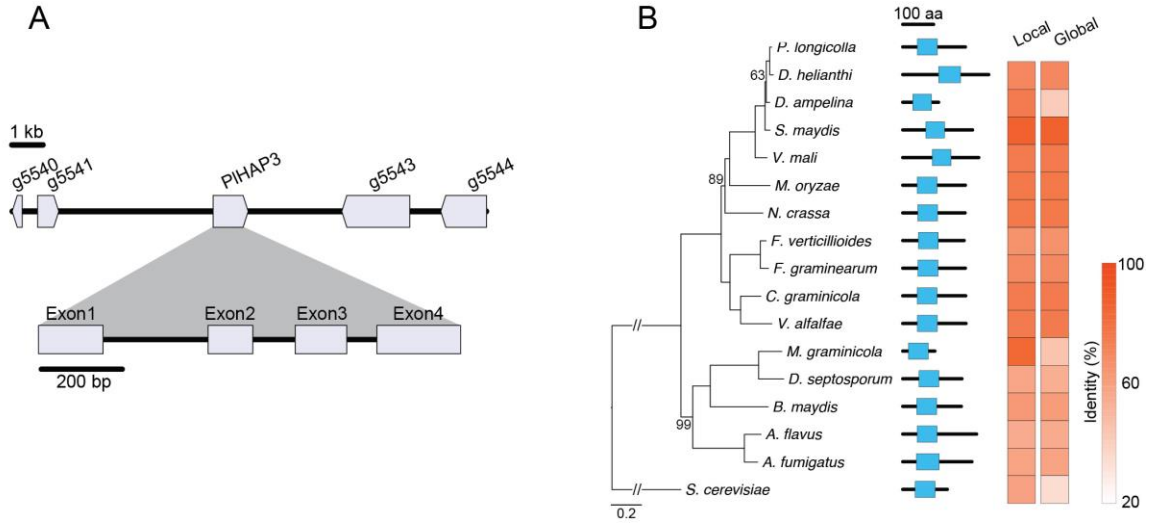

Figure 1. The predicted *HAP3* ortholog in *P. longicolla*. **(A)** Genomic region of *P. longicolla* MSPL 10-6 genome where *HAP3* was located, and the predicted gene structure of *HAP3*. **(B)** Similarity of *HAP3* with its homologs in selected taxa. Protein lengths are shown in scale with the histone-fold motif indicated as rectangles. The heat map shows the identity values (%) of *HAP3* with the corresponding homologs in other species based on local and global amino acid sequence alignments. The species were organized based on their phylogeny, represented by the maximum likelihood phylogenetic tree. Branches with bootstrap support of 100 had their label omitted.

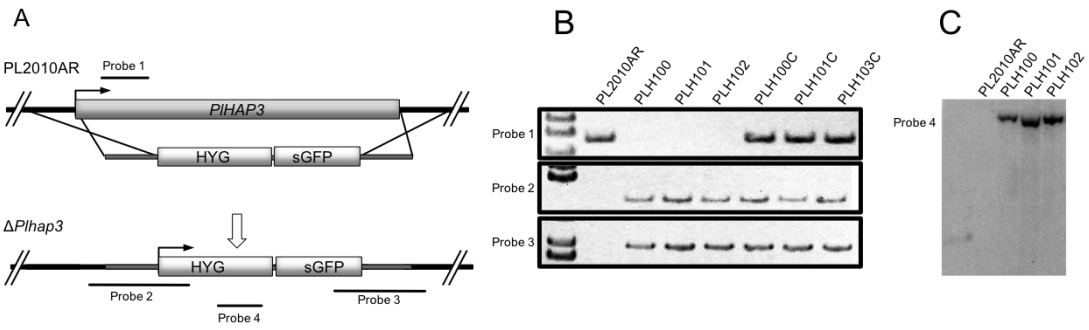

Figure 2. Targeted deletion of *HAP3* in *P. longicolla*. **(A)** Schematic representation of the *HAP3* locus in *P. Longicolla* and the homologous recombination strategy for its targeted deletion. **(B)** *P. longicolla* strains PL2010AR (wild type), PLH100, PLH101, and PLH102 (*HAP3* deletion strains; *Δhap3*), and PLH100C, PLH101C, and PLH102C (*HAP3* complementation strain) were validated by PCR with the following primer pairs: PLHAP3_PF/PLHAP3_PR (Probe 1); PacI_PLHAP3_5'F/HYGSCRN-A (Probe 2); and GFPF/PLHAP3_A2 (Probe 3). **(C)** Genomic DNA was digestion with KpnI and XcmI and probed with the hygromycin phosphotransferase-encoding gene, *hph*, specific probe (Probe 4). The presence of a single band indicates integration of a single copy of the deletion construct into the genome of strains PLH100, PLH101, and PLH102. Arrows indicate gene directionality, and black bars represent the locations of probes relative to genomic loci.

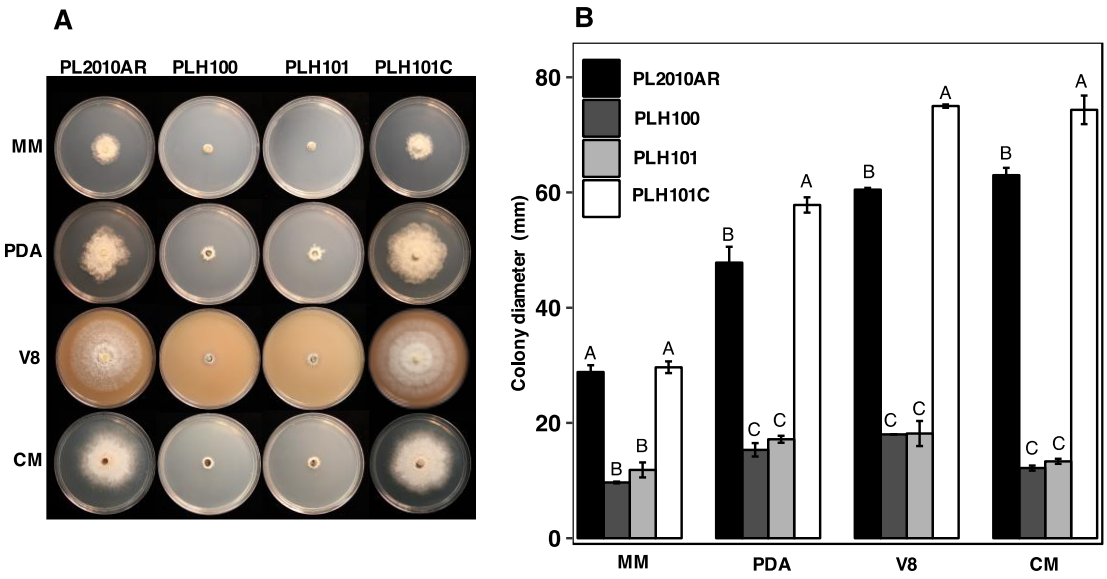

Figure 3. Deletion of *HAP3* impaired *P. longicolla* growth. **(A)** *HAP3* deletion strains presented visually indistinguishable growth phenotype on different growth media. *P. longicolla* strains PL2010AR (wild type), PLH100 and PLH101 (*HAP3* deletion strains), and PLH101C (*HAP3* complementation strain) were grown on MM (minimum medium), PDA (potato dextrose agar), V8 (V8 juice agar), and CM (complete medium) for four days under 12:12 hours light:dark cycle at 25C. **(B)** Statistical comparisons of strains radial growth within the different tested media (n = 3). Error bars represent the estimated standard error for the mean of each combination of strain and medium. Letters indicate statistically significant differences between strains within each medium as determined by Tukey-Kramer HSD at *P*-value <0.05. Statistical comparisons were performed with lme4 package in R treating diameter (mm) as a Gamma distributed variable.

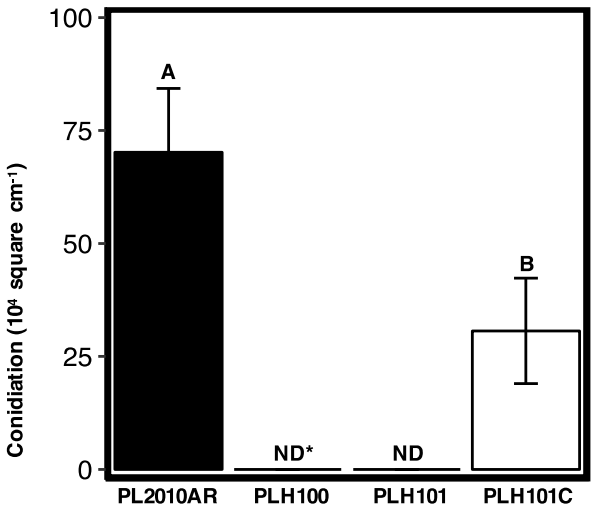

Figure 4. *HAP3* is critical for asexual reproduction of *Phomopsis longicolla*. The wild-type strain PL2010AR, the *HAP3* deletion strains PLH100 and PLH101, and the complementation strain PLH101C were grown on oatmeal agar. Plates were incubated at 25°C under 12:12 h light:dark cycle and conidia were harvested 14 days after inoculation (n=3). Error bars represent the estimated standard error of the mean. Letters indicate statistically significant differences between strains according to Tukey-Kramer HSD at *P* value <0.05. Statistical comparisons were performed with lme4 package in R conidiation as a Gamma distributed variable. *Not detected.

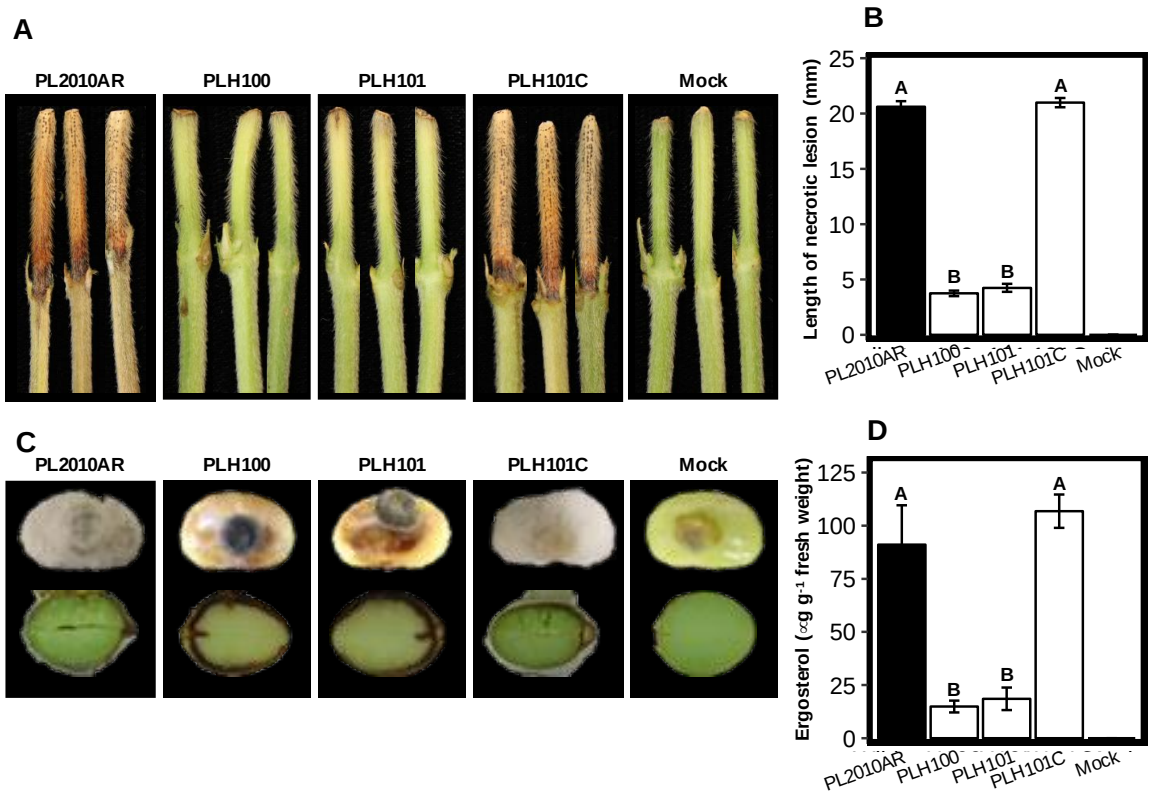

Figure 5. Deletion of *HAP3* impairs *P. longicolla* pathogenicity. **(A)** Necrotic lesions and pycnidiation on stems of soybean cultivar Traff (PI 470930) inoculated with the wild-type strain PL2010AR, *HAP3* deletion strains PLH100 and PLH101, and complementation strain PLH101C. For the negative control, stems were inoculated with sterile 0.2x PDA plugs. **(B)** Ten days after inoculation with the cut-stem method, the length of necrotic lesion was measured. The cut-stem inoculation method was used (n=8). **(C)** *P. longicolla* strains were also inoculated on surface disinfested physiologically-mature soybean seeds of cultivar Traff. Bottom pictures are the cross section of inoculated soybean seeds. **(D)** Ergosterol was extracted from seeds and quantified ten days after inoculation (n=4). Error bars represent the estimated standard error of the mean. Letters indicate statistically significant differences between strains within each media as determined by Tukey-Kramer HSD at *P* value <0.05. Statistical comparisons were performed with lme4 package in R treating lesion length and ergosterol concentration as Gamma distributed variables.

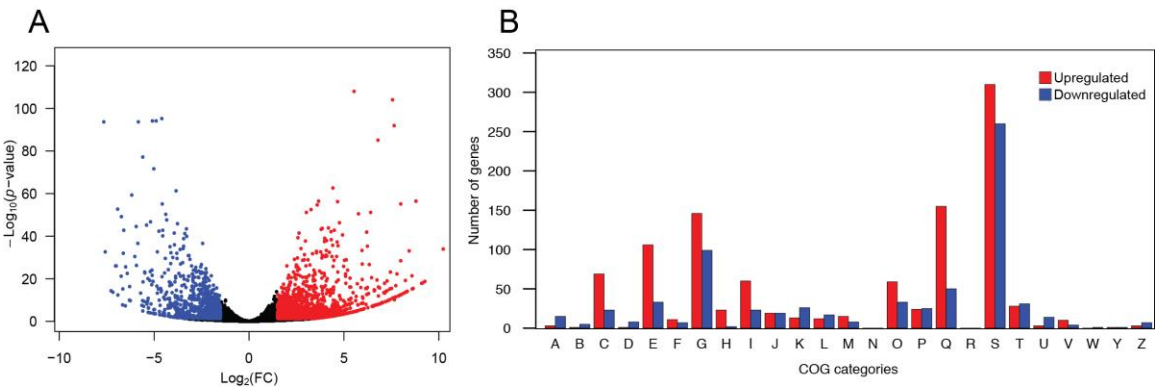

Figure 6. Differentially expressed genes in *P. longicolla* PLH101 compared to the wild type while colonizing soybean seeds. **(A)** Volcano plot of genes expressed during soybean seed colonization. The x-axis shows the $\log_2$ of the fold change in gene expression compared to the wild type, and the y-axis shows $-\log_{10}$ of the adjusted *P*-value. Red and blue dots represent genes up- and downregulated, respectively, with threshold of $|\log_2 FC| > 1.5$ and adjusted *P*-value < 0.05. Parameters obtained from DESeq2 package implemented in R. **(B)** Number of genes differentially expressed classified in different clusters of orthologous groups (COG) categories. A: RNA processing and modification; B: Chromatin structure and dynamics; C: Energy production and conversion; D: Cell cycle control, cell division, and chromosome partitioning; E: Amino acid transport and metabolism; F: Nucleotide transport and metabolism; G: Carbohydrate transport and metabolism; H: Coenzyme transport and metabolism; I: Lipid transport and metabolism; J: Translation, ribosomal structure and biogenesis; K: Transcription; L: Replication, recombination and repair; M: Cell wall/membrane/envelope biogenesis; N: Cell motility; O: Post-translational modification, protein turnover, and chaperones; P: Inorganic ion transport and metabolism; Q: Secondary metabolites biosynthesis, transport, and catabolism; R: General function prediction only; S: Function unknown; T: Signal transduction mechanisms; U: Intracellular trafficking, secretion, and vesicular transport; V: Defense mechanisms; W: Extracellular structures; Y: Nuclear structure; Z: Cytoskeleton.

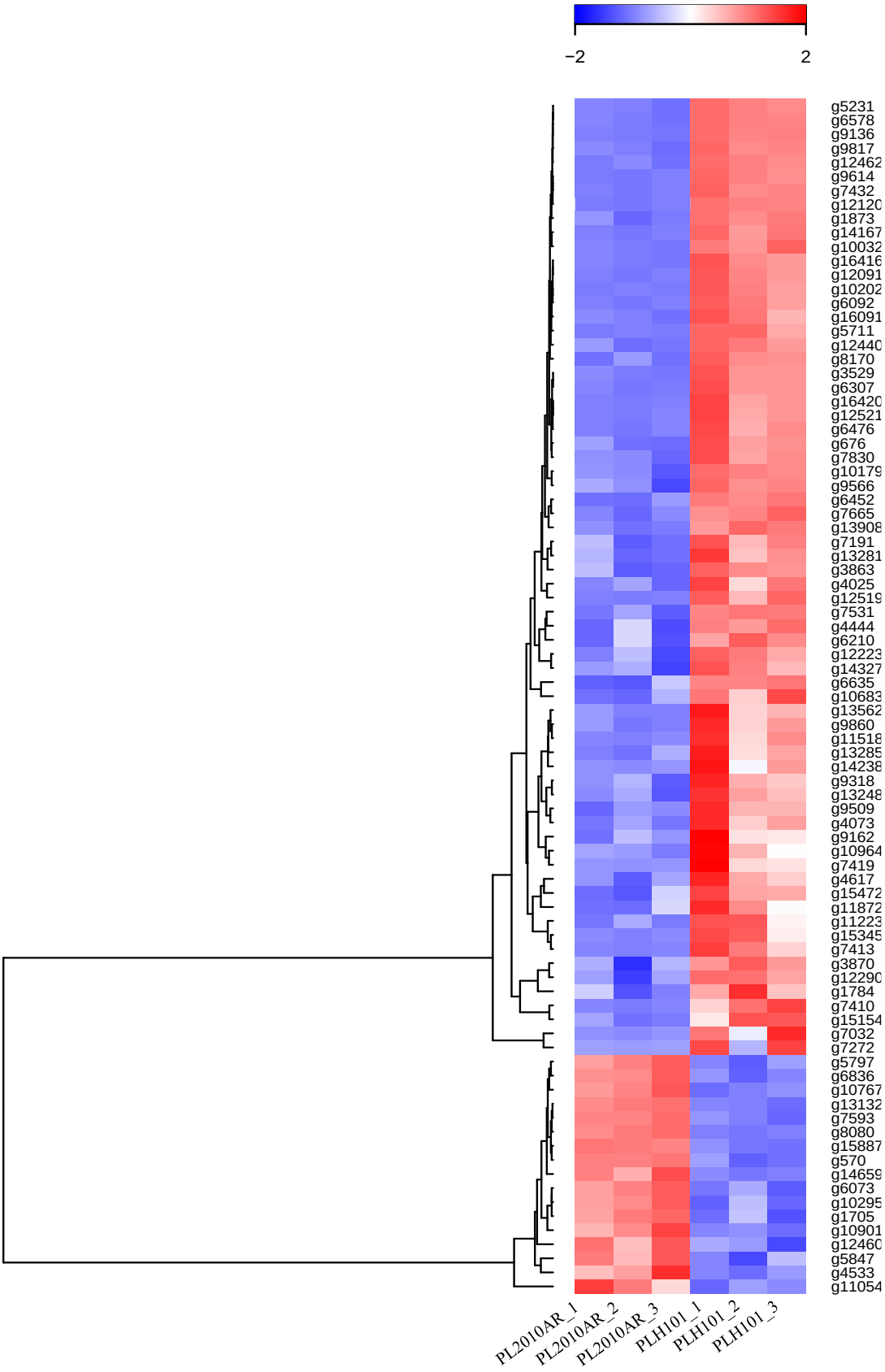
−2
2
g5231
g6578
g9136
g9817
g12462
g9614
g7432
g12120
g1873
g14167
g10032
g16416
g12091
g10202
g6092
g16091
g5711
g12440
g8170
g3529
g6307
g16420
g12521
g6476
g676
g7830
g10179
g9566
g6452
g7665
g13908
g7191
g13281
g3863
g4025
g12519
g7531
g4444
g6210
g12223
g14327
g6635
g10683
g13562
g9860
g11518
g13285
g14238
g9318
g13248
g9509
g4073
g9162
g10964
g7419
g4617
g15472
g11872
g11223
g15345
g7413
g3870
g12290
g1784
g7410
g15154
g7032
g7272
g5797
g6836
g10767
g13132
g7593
g8080
g15887
g570
g14659
g6073
g10295
g1705
g10901
g12460
g5847
g4533
g11054
PL2010AR_1
PL2010AR_2
PL2010AR_3
PLH101_1
PLH101_2
PLH101_3

Figure 7. Candidate effector genes differentially expressed in *Phomopsis longicolla strain* PLH101. The heat map shows the expression values of genes encoding candidate effectors in *P. longicolla* PLH101 compared with the wild type during soybean seed colonization.

Figure 8. Multiple sequence alignment of *Phytophthora sojae* necrosis-inducing protein (PsojNIP) and its homologs in *Phomopsis longicolla* that were upregulated in PLH101 strain during soybean seed colonization. Amino acids in red correspond to predicted signal peptide. Amino acids highlighted in blue were described to be conserved in PsojNIP and its homologs in 10 other species.

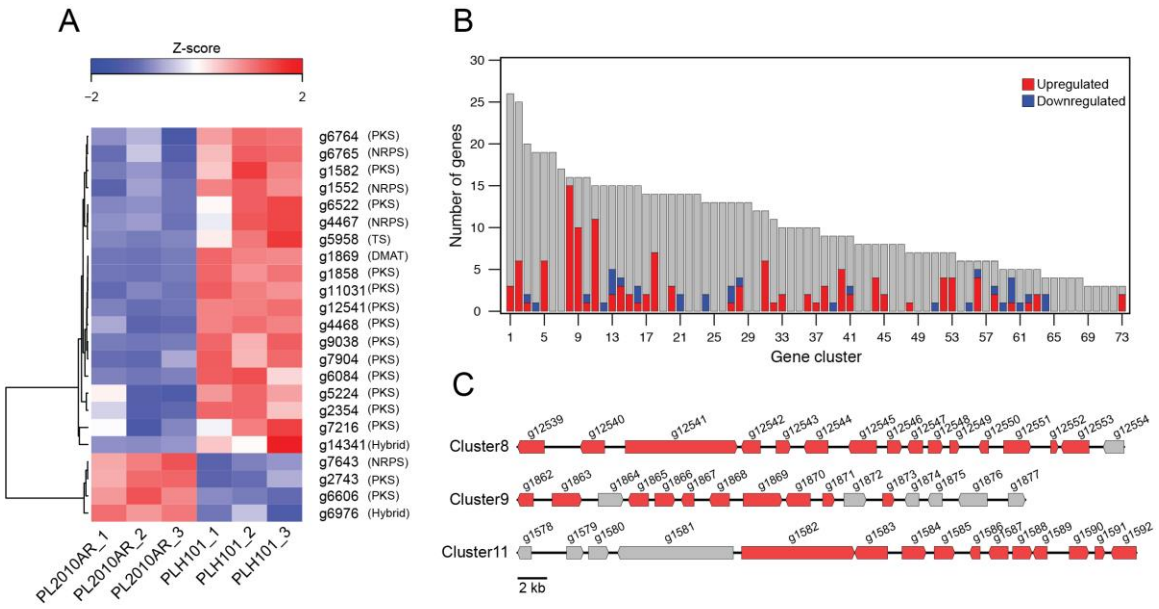

Figure 9. Secondary metabolism genes differentially expressed in *P. longicolla* PLH101. **(A)** Heat map of the expression values of secondary metabolite backbone genes. **(B)** Bar graph showing the size of predicted secondary metabolite gene clusters and the number of genes considered overexpressed (Up) and under expressed (Down) in PLH101. **(C)** Secondary metabolite gene clusters in *P. longicolla* with differentially expressed genes. Genes upregulated are shown in red.

Chapter VII: Conclusion

In this dissertation, studies on the pathogenesis of *Macrophomina phaseolina* on soybean reviewed a complicated relationship. Although this study shows that drought stress does indeed increase charcoal rot severity, the disease was more pronounced when drought followed a period non-drought, from seeding to seed set. To a lesser degree, soil inoculum levels also were shown to affect charcoal rot. Our experiments also showed that there were consistent differences among soybean cultivars for disease severity. In particular, the cultivar 'Hutcheson' consistently displayed higher charcoal rot severity levels than the cultivar 'Osage'. Additionally, the work presented here describes the restriction of soybean root colonization by *M. phaseolina* in the presence of zone lines caused by *P. longicolla*. Zone lines incidence was not affected by irrigation regimes. However, their incidence was significantly affected by cultivar and location. In particular the cultivar Osage had high incidence of zone lines in all field experiments. Thus, indicating this trait might be quantitatively genetically controlled by the host. It remains unclear if zone lines on soybean roots and stems have any effect on crop or disease development.

In more mechanistically investigations, a few candidate genes were identified to be involved in of *P. longicolla* pathogenesis. In particular, the gene *g4307*, a homolog to *CDH2* in *Neurospora crassa*, was shown to be involved in soybean pathogenesis. When disrupted in *P. longicolla*, strains were significantly impaired in infecting and colonizing soybean stems and seeds, while not being affected in vitro. Here we report a new technique developed to economically and effectively used to economically and effectively identify *g4307* disruption in a random mutant. MoNSTR-seq is effective, low cost, and with multiplex applications for high throughput. Importantly, this work illustrated the amenability of *P. longicolla* to forward

genetics and to DNA manipulation techniques. Together, this represents a set of important tools available to scientists to discovery-oriented research in *P. longicolla* pathogenesis and biology.

Here we also report the relevant role of *HAP3* in gene regulation in *P. longicolla* during soybean seed colonization. The targeted disruption of *HAP3* decreased pathogenesis of P. longicolla. Additionally, its disruption was observed to cause thousands of genes to be significantly differentially expressed in *P. longicolla* during pathogenesis when compared to the wild-type strain. This was the first time a gene was targetedly disrupted in *P. longicolla* via reverse genetics. Additionally, the publicly available transcriptomics data reported here represents the first look into gene expression during *P. longicolla* colonization of soybean seeds. All together, the work and resources described here represents a significant advancement in putative molecular mechanisms of Phomopsis seed decay and will aid future studies on this topic.